University of Beira Interior
Engineering

Design and Manufacture of a mini-turbojet

Rui Gonçalo Gonçalves Esteves Pereira

Dissertation for obtaining the Master's Degree in **Aeronautical Engineering** (Integrated study cycle)
(Revised version after discussion)

Advisor: Prof. Dr. Francisco Miguel Ribeiro Proença Brójo

Covilhã, February 2020

Acknowledgements

There are many people without whom this dissertation would not have been possible. First and foremost, my deepest thanks to my family, who supported me throughout these five years. Their help and encouragement certainly made it easier to carry out this project.

Secondly, my gratitude goes to my supervisor, Professor Francisco Brójo, who was al ways available to help and ensure the entire project was on the right track. Furthermore, the patience the Professor demonstrated throughout this project, with several unexpected challenges, was immensely appreciated, because without it, I would not have been able to fulfill the objectives predetermined for this project. Professor, my most sincere thanks for allowing me to develop such a project.

I would also like to thank Mr.Rui Paulo and Mr.João Correia for the help given during the experimental phase. Without their support, this experiment would certainly have been more difficult.

Finally, I am thankful for all the support and unforgettable moments in the company of my friends, especially, José and João, during my academic years.

Summary

The development and production of small jet propulsion engines is relatively recent, considering that this type of gas turbine began to be studied and developed much earlier. However, with the passage of time, gas turbines have become an increasingly difficult challenge to develop and improve. This type of engine requires an intense study of the various areas related to its operation, demanding more and more knowledge and expertise to improve even a small detail. Although the detail may be small, the effect on overall performance is considerable.

Until recently, these small engines were developed without a significant role in the aeronautical industry, being used only for model aircraft. However, due to advance ments in science, these engines are beginning to be studied and prepared to integrate Unmanned Aerial Vehicles, UAV, as their propulsion system [1].

This project involves the development of a turbojet, adhering to the dimensions of two previously obtained components, the compressor and the turbine, from the IHI RHB31 VZ21 turbo model. To understand how to execute the design with appropriate sizing, the study of every component present in a turbojet was pursued, alongside the fundamental areas related to the operation of the turbojet, such as thermodynamic cycles. After a general study of the turbojet, the author proceeded to the design phase, where the sizi ng process begins based on the information contained in various sources found in the bibliography. The sizing was carried out using a scale factor. This scale factor was obtained by a ratio of compressor diameters. Briefly, in Mr. Thomas Kamps' book, the author advises the novice to divide the size of their compressor by that of the c ompressor used for Mr. Thomas Kamps' engine. The diameter ratio, or scale factor, was applied to the remaining components produced by Mr. Thomas Kamps, allowing for the determination of the measurements for this gas turbine, adhering to the recommended guidelines. The dimensions of the compressor cover, inlet flange, diffuser, shaft, shaft coupling tunnel, combustion chamber, fuel distribution ring, nozzle before the turbine with flow guide vanes, exhaust gas nozzle, and finally, the external casing, were o btained. The next step was the design process of the mentioned components, in relation to the designs observed in the studied literature, using the three-dimensional software CATIA V5R18. Design is an empirical process, which makes it extremely difficult to consider a design as absolute.

The manufacturing process of the turbojet was carried out once the design process was completed. The next step was to obtain the necessary materials for the production of the parts, primarily cast aluminum and stainless steel. The aluminum used was cast aluminum, which was then machined to acquire the required shapes according to the established design. Most of the components were produced from stainless steel sheets, from which the parts were cut according to their dimensions and shape in flat geometry. The chapter describing the manufacturing process, as well as the design process, is explained to allow for future reproduction of the completed work or adaptation for a different compressor/turbine set.

Unfortunate However, the manufacture of the diffuser and compressor cover was not possible, as they e

had extremely small dimensions to be produced on a five-axis CNC vertical milling machine. Furthermore, the welding applied to the produced parts was not executed with the required quality, even after increasing the thickness of the parts to facilitate the process, as explained in chapter 4.3. Therefore, one of the objectives was not achieved due to insufficient means that prevented the manufacture of the jet engine parts.

Keywords

Turbojet Model, Mini-turbojet, Thermodynamic cycles, Design, Sizing, CATIA V5R18, Manufacturing process.

Abstract

The development and production of small engines with a jet propulsion system is relatively recent, considering that this type of gas turbine began to be studied and developed many years before the first construction of these small turbojets. However, as time progressed, gas turbines became a greater challenge, becoming increasingly difficult to develop and improve. The gas turbine requires an intense study of the various areas related to its functioning, demanding additional knowledge and skill to improve even a small detail. Although the detail might be small, the effect on overall perfor mance would be considerable.

Until recently, these small engines were developed without playing a significant role in the aviation industry, being used only for model jet engines. However, with the advancement of science, these engines are now being studied and prepared to be integrated into Unmanned Aerial Vehicles, UAVs, as their propulsion system [1].

This dissertation involves the development of a small-scale turbojet, adhering to the dimensions of two previously obtained components, the compressor and turbine, from the model turbo IHI RHB31 VZ21. To understand how to execute a design with appropriate dimensions, a study of every component present in a turbojet was conducted, alongside fundamental areas concerning the functioning of a turbojet, such as thermodynamic cycles. After a general study of the turbojet, the author proceeded to the design phase, where the dimensioning process begins based on information from various sources found in the bibliography. The dimensioning was carried out using a scale factor, obtained by the ratio of the compressor's diameters. In short, in Mr. Tho mas Kamps' book, the author advises beginners to divide their compressor diameter by the compressor used for Mr. Kamps's engine. The diameters ratio, or scale factor, was applied to the remaining components produced by Mr. Thomas Kamps to achieve the measurements for this gas turbine, adhering to the recommended dimensions. The dimensions of the compressor shroud, inlet flange, diffuser, shaft, shaft housing, combustion chamber, fuel distribution ring, nozzle guide vanes, exhaust nozzle, and finally, the outer casing were obtained. The next step was the design process of these components, based on the observed designs found in the studied literature, using the three-dimensional design software CATIA V5R18. The design is an empirical process, which makes it extremely difficult to consider one design as absolute.

The manufacturing process of the Turbojet was carried out once the design process was completed. The next step was to acquire the necessary materials for producing the parts, primarily aluminum and stainless steel. The aluminum used was cast aluminum, which was then worked to achieve the desired shape according to the established design. Most components were manufactured using stainless steel sheets, with the pieces cut according to their dimensions and shape in planar geometry. The chapter detailing the manufacturing process, as well as the design process, is explained to facilitate future reproduction of the completed work or adaptation for a different compressor/turbine s et.

Unfortunately, the fabrication of the diffuser and compressor shroud was not possible, as their extre mely small dimensions could not be accommodated by the 5-axis vertical machining center. Moreover, the welding applied to the manufactured pieces was not executed with the required qual-

ity, even after increasing the material thickness to facilitate the process, as explained in chapter 4.3. Therefore, one of the main objectives was not accomplished due to the insufficient means that prevented the manufacture of the jet engine’s parts.

Keywords

Model Jet Engine, Mini-Turbojet, Thermodynamic cycles, Design, Dimensioning, CATIA V5R18, Manufacturing Process.

Contents

List of Figures

List of Tables

Nomenclature

A Cross-section area $m^2 a$ Speed of Sound m/s
c Specific Heat $kJ/kgKE$ Total Power WF
Thrust $NF/\dot{m}$ Specific Thrust $Ns/kgFHV$ Fuel Heating Value
J/kgf Fuel to Air Ratio$h$ Specific Enthalpy
$J/kgKke$ Kinetic Energy JM Mach Number$m$
Mass $kg\dot{m}$ Mass Flow Rate kg/spe Potential Energy J
P Pressure PaQ Heat Rate WR Real Gas
Constant $kJ/kgKS$ Specific Fuel Consumption mg/NsT
Temperature KVVelocity m/sW Work Rate W
η_p Propulsive Efficiencyγ Heat Capacity Ratio
π Pressure RatioρDensity $kg/m^3\tau$
Temperature Ratioτ_λ Maximum Stagnation
Enthalpy Ratioθ Flowing Fluid Energy J

Subscripts

a Air$b$
Burner$c$ Compressor
cc Combustion
Chamber$f$ Fuel
in Input$m$
Mechanical$o$ Overall
out Output$p$
Constant Pressure$r$
Free stream conditions
t Turbineth
Thermal$v$ Constant
volume0 Total1
Initial state2 Final state

List of Acronyms

CAD Computer Aided Design CATIA Computer Aided Three-Dimensional Interactive Application CC Combustion Chamber CNC Numerical Control FABLAB Fabrication Laboratory NGV Nozzle Guide Vanes RC Radio Controlled TSFC Thrust Specific Fuel Consumption UAV Unmanned Aerial Vehicle UBI University of Beira Interior

Chapter 1

Motivation and Objectives

1.1 Motivation

The dream of humans to fly has intrigued us and occupied our thoughts for a long time. We began with observing birds in flight, leading to the invention of the kite, Leonardo da Vinci's ornithopter, the first hot air balloon known as the Montgolfier's Balloon, the glider, the aerodrome, and finally, the Wright Brothers Glider [2].

In addition to studying sustainable wings for generating lift, research into propulsion systems was also underway, as we understood that sustainable flight required a power source. Steam engines were the first to be developed, followed by the internal combustion engine and then the gas turbine. Our dream finally came true when the Wright Brothers achieved the first flight.

We began developing new aircraft wings, materials, structures, and propulsion systems. Each of these underwent intense study and investigation until we achieved modern aircraft, and still, we continue to seek further improvements. The development of modern aircraft has allowed us to cross continents and interact with different cultures. Moreover, to reach another continent in a matter of hours, the aircraft must be extre mely well-designed, built, and equipped. The aircraft's engines provide a significant amount of thrust, enabling the aircraft to achieve the necessary speed for the intended operation. Depending on the aircraft's purpose, such as military long-range operations, commercial flights, or combat situations, they are developed and refined to the smallest detail. For instance, in combat situations, aircraft are built to fly at astonishing speeds t hat exceed the speed of sound, 343 m/s [3]. With technological and scientific advancements, gas turbine engines are no longer out of reach for those interested in building one. Fortunately, today, there are mini-turbojet engines that one can build and enhance.

The hand-fitted jet engines have appeared recently and are known as mini-turbojets or model jet engines. These small machines have begun to find their place in the industry, where they are being developed and produced by companies for potential application in UAVs[1]. These gas turbines can be applied to a Radio Controlled (RC) model jet engine.

The challenge of building a mini-turbojet is inherently appealing to someone interested in propulsion systems. Additionally, knowing the potential to contribute to future work led to embracing this challenge. Therefore, through the study of gas turbine design and manufacture, a mini-turbojet prototype was designed, and some parts were built. With effort, the remaining parts will soon be fabricated, and the final engine will undergo experimental analysis.

1.2 Objectives

The primary objective of this thesis focuses on the design and construction of a small-dimension turbojet. Initially, a three-dimensional design of the small jet engine was conducted using Computer Assisted Design (CAD) software, specifically CATIA. The design was carried out according to the dimensional values obtained through the study of small-scale jet engine design.

The dimensioning criteria found in the available literature were adopted by the author. This method relies on empirical data, specifically, designs developed by this time. This was a major aid i n obtaining the appropriate measurements for the major components, providing the means to dimension the remaining pieces. The dimensioning approach is duly explained in chapter 3.

The final and main goal of this work is to describe the series of steps taken to produce a small model jet engine for practical applications, in a transparent way, to help the reader produce their small-scale jet engine.

1.3 Document Structure

The entire document is organized into five chapters, where each chapter focuses on several parts, in accordance with the custom format of the master's degree thesis.

The first, and current, chapter reveals the author's motivation that preceded the development of this thesis. Additionally, the objectives and document organization are presented logically, making it easier to understand what is proposed for this thesis.

The second chapter presents a literature review, introducing the gas turbine and describing its types, particularly the turbojet. This is followed by a general description of the components that make up the jet engine, along with the thermodynamic concepts that help us understand the overall functioning of the jet engine.

The third chapter reports on how the dimensioning process was carried out, justifying t he choices for the components' measurements.

The fourth chapter outlines the procedures taken to design and manufacture the required components, completed by their assembly, along with further modifications made throughout the process.

The fifth and final chapter reveals the conclusions drawn from the practical procedure, the obstacles encountered during the development of this thesis, and suggestions for future work.

Chapter 2

Bibliographic Review

2.1 Gas Turbines Historical Review

The initial concept emerged during the Roman-Egypt era, created by Hero, also known as Hero of Alexandria. The aeolipile, the name of Hero’s invention, is a radial steam turbine that combines two nozzles on opposite sides. Steam exits through these nozzles due to the vapor formed by boiling water inside a sphere, causing the sphere's center to spin and generate torque. An example of the steam engine is shown in figure 2.1.

Figure 2.1: *Aeolipile* [5]

The physical principle of reaction was put into practice in the thirteenth century by the Chinese people using fireworks [6]. Three centuries later, in 1687, Sir Isaac Newton made a crucial advance by formulating the three laws of motion:

1. Inertia: An object moving in a straight line will continue in uniform motion unless an external force is applied to it, changing its state [7]. 2. $Force = m \times g$, the change in velocity, g, depends on the mass, m, of the object when an external force, F, is applied [7]. 3. Action-Reaction Law: for example, a stone exerts a force on the earth as the earth applies an equal force to the stone [7].

These laws enabled us to make significant progress towards gas turbines over time. The first step was taken in 1791 by John Barber, an Englishman who was granted a patent for the gas turbine thermodynamic cycle, known as the Brayton Cycle, which is the same cycle used in modern gas turbines. Using this cycle, Hans Holzwarth developed the electrical ignition of the mixture in the combustion chamber, with controlled valves in 1908 [6].

In 1913, an engine using the jet propulsion system was patented by René Lorin. It was the first subsonic ramjet; however, it was not possible to realize the project due to the quality of the materials at that time. The materials could not withstand the heat, and the development of the jet propulsion system was in its early stages, affecting the aircraft's efficiencies [8].

Jet propulsion engines were realized in 1930 when Sir Frank Whittle patented the design of a centrifugal gas turbine for jet propulsion. Later, in 1937, he conducted the first static test in the history of the jet engine. Although Whittle conducted the first static test, it was Hans Joachin Pabst von Ohain, working for the Heinkel aircraft company, who created a turbojet engine powered by gaseous hydrogen, similar to Whittle's design, which was used as the propulsion engine for the He-178 aircraft, achieving the first turbojet flight worldwide in 1939. Three years later, Frank Whittle's engine was used for the first time as the propulsor of an aircraft [6].

The first axial-flow turbojet flight took place in Germany in the same year as Whittle's engine flight. The axial turbojet, Jumo 004A, was the propulsion system for the Me-262 aircraft. The leader of this project, chosen by the Junkers company, was Anselm Franz [6]. Although Frank Whittle's engine could not be built so quickly, he laid the foundation for the modern gas turbine [8].

The jet propulsion system has been and continues to be extensively studied to seek improvements, with the aim of future successful applications in this type of engine. Only years later, when the turbojet engine was applied to an aircraft, did the idea of reproducing the same engine on a small scale begin to emerge. The history of the miniature-turbojet is difficult to date, but it is believed to have been initiated by Kurt Schreckling, a German technician and amateur astronomer. Kurt was the first to replicate a turbojet on a small scale, paving the way for small or miniature model jet engines [9]. In his book, Gas Turbine Engines for Model Aircraft, he explains how he built the engine, the FD 3/64, which became a starting point for future miniature turbojets. This allowed others to improve Kurt's turbojet and develop new small-scale gas turbines based on his engine, such as the KJ66 [10].

2.1.1 Types of Gas Turbines

Gas turbine history records show us the enormous and rapid development of this engine. It is a product of a combination of various fields like thermodynamics, mechanics, aerodynamics, and others, which are still being thoroughly studied for improvements. Only after understanding these fields is the utility of a gas turbine considered, and then designed, depending on whether it is used for a space mission, aviation transport, or air combat situations. Teams of scientists, engineers, and technicians have created gas turbines with different methods of converting and supplying power, according to their purposes, such as jet propulsion engines: rocket, athodyd, also known as a ramjet, the pulse jet, and the turbo-jet, or propeller jet engines: turboprop engine, turbofan, and turboshaft [8].

The ramjet, figure 2.2, consists of a divergent inlet and a convergent or convergent-divergent exhaust. This engine requires forward motion to produce thrust. With no rotating parts, the air is forced into the divergent duct, followed by combustion with fuel, where the gases will accelerate through the exhaust section to the atmosphere [8].

Another relative of the jet propulsion engine, the pulse jet, as shown in figure 2.3, uses a similar duct to the ramjet but is more robust due to the higher pressures involved. The air passes through open valves at the inlet and moves to the combustion chamber, where fuel combustion occurs, causing the gas to expand, thus increasing the pressure. As a result of this increase, the valves close, and the gas is ejected through the rear. Its high fuel consumption and uneven performance compared to the current gas turbine make this engine unsuitable for use in aircraft [8].

The rocket engine, figure 2.4, is distinguished from the other engines by not utilizing the oxygen from atmospheric air for combustion but, instead, using a specific fuel, c hemically decomposed with oxygen [8].

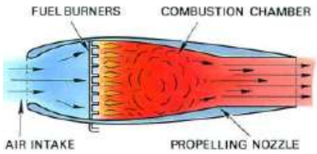

Figure 2.2: Ramjet [8]

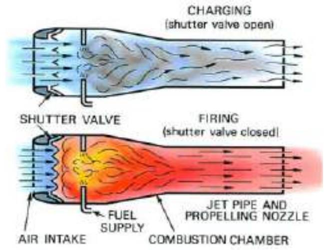

Figure 2.3: Pulsejet [8]

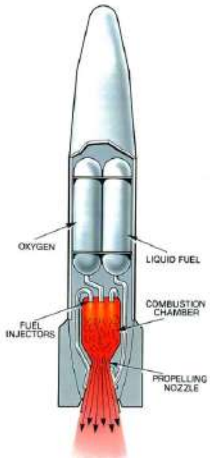

Figure 2.4: Rocket Engine [8]

The Turbojet, shown in figure 2.5, is the junction of a Compressor, Combustion Cha mber, and Turbine, called the gas generator, with an inlet and Exhaust Nozzle. The added Exhaust Nozzle will convert most of the energy of the airflow into velocity.

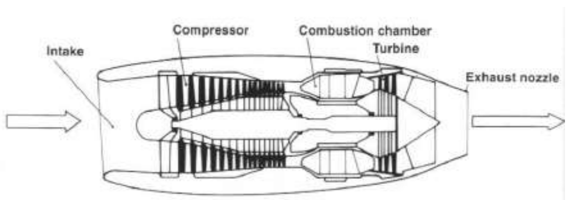

Figure 2.5: Turbojet [6]

With the propeller/turbine combination comes the ducted fan, prop fans, and bypass engines. In the turboprop engine, shown in figure 2.6, the two turbines function to sustain the compressor work demand and make the propeller run. In a similar engine, the turboshaft, shown in figure 2.7, the turbine drives the compressor and the second turbine will drive the

Shaft, which in turn, is connected to a transmission system that rotates the helicopter blades[6].

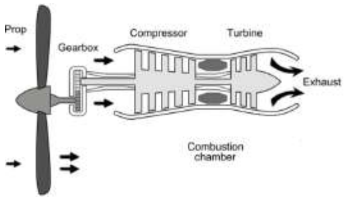

Figure 2.6: Turbopropeller [11]

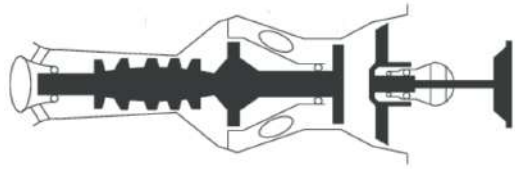

Figure 2.7: Turboshaft [12]

The turbofan, illustrated in figure 2.8, also has two turbines. One absorbs the energy f rom the hot airflow, while the other uses the excess shaft work to drive a low-pressure compressor, a fan. It has lower propulsive efficiency compared to the turboprop when operated at the same cruise speed and lower velocities. However, at higher velocities, the turbofan has an advantage. Engines like the turbofan began to be widely used and continue to be due to their high propulsive efficiency values compared to a turbojet. These values are explained by the bypassed airflow[6].

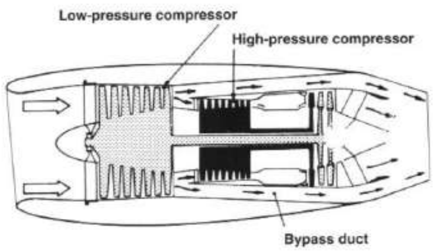

Figure 2.8: Turbofan [6]

Bypassed airflow engines are categorized into two types: low bypass-ratio and high-bypass ratio. The bypass-ratio refers to the amount of air bypassed in relation to the air passing through the engine's core. The engine consists of a high and low-pressure compressor and the corresponding turbines, which are driven by two coaxial shafts. The low-pressure compressor, or fan, draws in air and divides it into two flows. Most of the air is directed around the engine's core, while a small portion is used for combustion. The two airflows are then combined at the exhaust section. This design results in lower fuel consumption compared to earlier engines with similar thrust that lacked this technology, enabling efficient performance during high altitude flights. The prevalent use of this technology, particularly high-bypass ratio engines, in the propulsion systems of civil aviation and long-range military missions is justified by the low fuel consumption, which i s considered the most important performance parameter [6]. An example of a high-bypass engine is shown in figure 2.9.

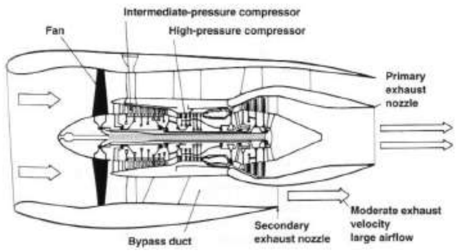

Figure 2.9: High-Bypass Engine, Rolls Royce RB.211 [6]

The turbojet is a simpler form of a turbofan, meaning it does not have a bypassed airflow. This results in lower efficiency, but it compensates with speed. These engines can reach supersonic speeds, which is one of the reasons for their use in military aircraft [6].

2.2 Cycle Review

The literature reviewed contains extensive and detailed information about thermodynamic cycles and their properties. Therefore, only a summary will be presented to avoid an extensive and deep analysis. For more detailed information about thermodynamic cycles and the corresponding gas turbines, the author recommends the reader to consult the following books, where more information can be found in the books *Thermodynamics: An Engineering Approach by Çengel, YunusA. and Boles, Michael A.* and *Aerothermodynamics of Gas Turbines and RocketPropulsion byOates, George C.*, chapters 5.3, 7.4, 9.8, and chapter 2, respectively. Nonetheless, other literature was not disregarded.

In summary, the overall functioning of the gas turbine will be presented, followed by the ideal thermodynamic cycle along with the ideal behavior analysis of the turbojet components. Subsequently, jet performance equations are demonstrated to complete t he analysis of a turbojet engine cycle.

2.2.1 Working Cycle

The working cycle subchapter aims to explain the functioning of an engine with a jet propulsive system, describing its thermodynamic cycle along with properties related to it.

The working cycle begins with the intake of air into the compressor, which is responsible for increasing the pressure through mechanical shaft power [6]. This pressure increase has a diminishing effect on the volume of the airflow, subsequently raising the air temperature [8]. The pressurized air is then discharged into the combustion chamber, where fuel is added and burned, raising the temperature to extremely high levels. As the gas burns, both the volume and temperature increase due to the open structure of the combustion chamber, maintaining constant pressure [8]. The combustion process elevates the energy state of the molecules to high levels, allowing the turbine to effectively harness the necessary amount of energy [6]. As a result of the work extracted from the gas, the turbine begins to rotate, converting the surplus gas energy into mechanical power by generating motion. This spinning motion forces the compressor wheel to rotate due to the work provided by the turbine, which is transferred by the rotation of the shaft to the compressor at the other end of the spool[6]. At this stage, the gas variables, pressure, and temperature decrease, while the volume increases. Finally, the gas flow reaches the final stage at the exhaust nozzle, where the gas is expelled into the environment at high velocities, producing thrust [8].

There are three main conditions to maintain in the engine cycle:

- During compression, pressure increases, leading to a decrease in volume and a rise in temperature [8].
- In the Combustion Chamber, the temperature increases while the pressure remains constant and the volume increases [8].

- During the expansion, the volume increases while the pressure and temperature decrease [8].

The working cycle of a gas turbine is generally compared to that of a four-stroke piston engine, considering the four similar stages of each engine. Both engines start their cycle with the induction phase, followed by compression, combustion, and expansion. However, all the stages of the piston engine occur inside a cylinder, whereas in a jet engine, each component is assigned its specific function, resulting in continuous action rather than intermittent. Additionally, combustion in a jet engine occurs at constant pressure, unlike in a reciprocating engine, where the combustion process takes place in a closed space. Therefore, the jet engine can operate with large masses of air using lightweight components. In the final stage, the exhaust phase, the gases expanded by t he turbine exit through the nozzle, generating a propulsive force essential to this engine. In contrast, the exhaust gases of the piston engine do not have the same significant effects [6]. Considering these differences, the gas turbine engine eliminates three idle strokes, allowing more fuel to be burnt in a shorter time. Since the turbojet engine is a heat engine, burning more fuel increases the temperature of the combustion chamber, leading to substantial gas expansion. Furthermore, a greater amount of power is produced for a given size[8]. For a piston engine to generate the same amount of power, i t would need to be extremely large and heavy, making its manufacture a serious challenge [6].

As the gas is discharged from the nozzle, it will gradually disperse to ambient conditions, returning to its original state. The gas reverting to its original condition implies that the state variables also return to their original conditions, which is termed a reversible process. For a process to be considered reversible, it must combine both internal and external reversibility. If the gas states could be restored in reverse order while a system undergoes a process with minor pressure and temperature gradients, the process is defined as internally reversible. Meanwhile, for a process to be considered externally reversible, the atmospheric changes accompanying the process must be reversible in sequence. However, achieving a reversible process is impossible due to irreversible factors such as temperature, pressure, and velocity gradients caused by heat transfer, friction, chemical reactions, and work applied to the system. Despite the irreversibility of real processes, the reversible process is standardized to estimate the success of real processes by considering the losses and to enable the derivation of thermodynamic relations to estimate reality [13].

2.2.2 Thermodynamic Cycle

2.2.2.1 Theoretical Notions

Further notions are presented to be acknowledged in order to understand the conditions and properties behind the ideal thermodynamic cycle that encompasses all gas turbines, particularly the turbojet engine.

- Steady-Flow Process

  Gas turbines are generally built for continuous operation, where the conditions they operate under are approximated. Assuming it operates under the same conditions over time, the process is termed a steady-flow process. This means the fluid properties remain consistent throughout the entire process. Within a control volume, the fluid properties can change at different fixed points but remain the same from start to finish. As a result, the mass, m, volume, V, and total energy rate or total power, E, remain constant throughout this process [14].

The conservation of mass principle is applied, stating that, considering a control volu me, the total rate of mass entering equals the total rate of mass leaving it [14]. Since there is no increase or decrease in mass, the mass flow rate, $\dot{m}$, remains constant from the beginning to the end of the process [14]. It is expressed in the form of,

$$\sum_{in} \dot{m} = \sum_{out} \dot{m} \quad [14] \quad (2.1)$$

Considering it for a uniform single stream, denoting the inlet and exit states as 1 and 2, respectively, the mass balance becomes,

$$\dot{m}_1 = \dot{m}_2 \rightarrow \rho_1 V_1 A_1 = \rho_2 V_2 A_2 \quad [14] \quad (2.2)$$

Where ρ, V, and A represent density, flow velocity, and cross-sectional area.

In the context of the total energy rate, the energy remains constant within a control volume, indicating no changes in the total power. This simplifies the energy balance to[14],

$$\dot{E}_{in} = \dot{E}_{out} \quad [14] \quad (2.3)$$

Remembering that the energy transfers occur in the form of mass, $\dot{m}$, work, W, and heat, Q, the energy balance is represented as,

$$Q_{in} + W_{in} + \sum_{in} \dot{m}\theta = Q_{out} + W_{out} + \sum_{out} \dot{m}\theta \quad [14] \quad (2.4)$$

Where the energy of a flowing fluid, θ, is described as,

$$\theta = h + ke + pe \quad [14] \quad (2.5)$$

Where h, ke, and pe are defined as enthalpy or internal energy, kinetic energy, and potential energy.

Heat and work interaction is defined by a heat transfer into the system, known as heat input, and the work produced by the system, known as work output [14]. Assuming there are no changes in kinetic and potential energy, the energy balance is expressed as follows,

$$Q - W = h_2 - h_1 \quad [14] \quad (2.6)$$

- Stagnation Properties

In control volume analysis, it is common to combine internal energy and fluid energy into a single variable known as specific enthalpy, h. In most cases, kinetic and potential energy are ignored, defining enthalpy as the total energy of the fluid. However, when kinetic energy is considered, it is generally appropriate to convert kinetic energy into the fluid's enthalpy, combining them into a single term defined as stagnation or total specific enthalpy, as shown in equation 2.7 [14].

$$h_o = h + \frac{V^2}{2} \quad [14] \quad (2.7)$$

In equation 2.7, enthalpy is categorized into two types: static and stagnation enthalpy, h and h_0, respectively.

As a result of converting kinetic energy to enthalpy, the temperature and pressure increase. These fluid properties are known as stagnation properties or isentropic stagnation properties. In an isentropic stagnation state, the enthalpy and stagnation temperature are the same as the actual state, assuming the fluid is an ideal gas. The actual stagnation pressure differs from the isentropic stagnation pressure because entropy increases due to fluid friction [14]. Assuming the fluid is an ideal gas, enthalpy can be replaced by the constant specific heat times the temperature, as shown in equation 2.9.

$$c_p T_o = c_p T + \frac{V^2}{2} \quad [14] \quad (2.8)$$

Becoming,

$$T_o = T + \frac{V^2}{2c_p} \quad [14] \quad (2.9)$$

Where T_0 indicates the stagnation or total temperature, meaning the temperature that the ideal gas reaches when brought to rest in an adiabatic process, and the term $\frac{V^2}{2c_p}$ represents the temperature increase throughout the process known as dynamic temperature [14].

The relationship between temperature and pressure is demonstrated in equation 2.10.

$$\frac{P_0}{P} = \frac{T_0}{T}^{\frac{\gamma}{\gamma-1}} \quad [14] \quad (2.10)$$

Where P_0 and γ are referred to as stagnation pressure and specific heat ratio.

2.2.2.2 Brayton Cycle

It is an idealized thermodynamic cycle present in all gas turbines equipped with the fundamental components, such as the compressor, combustion chamber, and turbine[15]. The cycle is divided into two types: open cycle and closed cycle. The former consists of air at atmospheric conditions, drawn into the compressor, which increases the temperature and pressure of the air. The pressurized air then moves to the combustion chamber, where it is mixed with fuel, followed by combustion at constant pressure. Once the combustion process is complete, the gas exits to the turbine at extremely high temperatures, where the gas expands [14]. At this stage, the interaction of the gas with the turbine is used to drive the compressor. The remaining energy of the gas is used to accelerate the fluid directed by the exhaust nozzle to the exterior [16]. Because the gas is expanded to the exterior, the cycle is classified as an open cycle. Conversely, if the gas were recirculated, the cycle would be considered closed. Figures 2.10 and 2.11 describe an open and closed cycle [14].

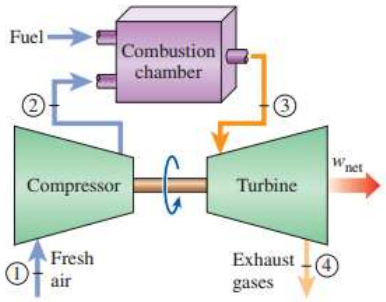

Figure 2.10: Open cycle [14]

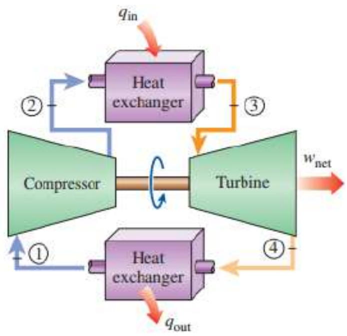

Figure 2.11: Closed cycle [14]

In the closed cycle, it is noted that the combustion process was replaced by a constant pressure additional heat, and the exhaust process was substituted by a heat rejection process at constant pressure to the exterior [14].

The working cycle of the turbojet engine corresponds to an open Brayton cycle, which is the typical cycle for gas turbines [14]. Figure 2.12 illustrates the components of a jet propulsion device with the corresponding Brayton cycle.

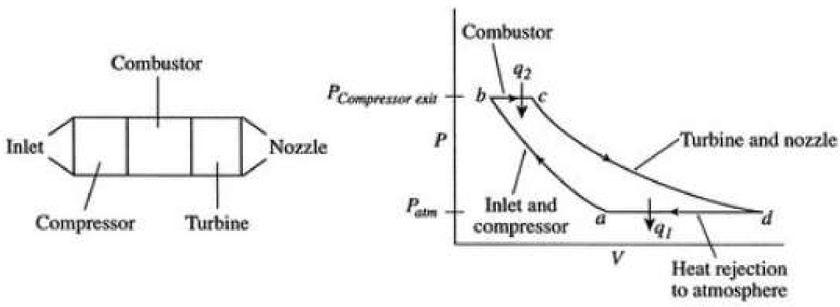

Figure 2.12: Jet Engine Components and analogous thermodynamic states [16]

The thermodynamic states observed in figure 2.12 are distinguished in four processes. The legend of this cycle is formulated in the following manner:

- a-b: Compression at the inlet and compressor, in an isentropic process [16].
- b-c: Combustion of fuel at constant pressure [16].
- c-d: During the expansion, the volume increases along with a decrease in pressure and temperature[16].
- d-a: Air cooling at constant pressure [16].

2.2.2.3 CycleBehavior Analysis

Cycle analysis is a process to obtain estimates for performance parameters such as t hrust or specific fuel consumption, calculated after assuming certain conditions and design specifications, presented below [17].

Conditions

- The working fluid is considered an ideal gas with constant heat capacity and specific heat ratio[17].
- Isentropic Compression/ Expansion [17].
- The external source of heat for combustion and fuel mass is disregarded [17].

Design

- Atmospheric pressure and temperature values [17].
- Compression ratio [17].
- Inlet Mach Number [17].

In this subsection, the ideal and actual behavior of the components are presented, indicating the temperature and pressure for each station. The stations will be distinguished by a number for easier referencing, as demonstrated in Figure 2.13. The actual turbojet cycle analysis is presented in Appendix D.

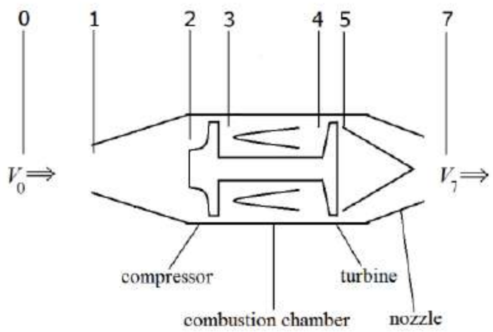

Figure 2.13: Turbojet station numbering [16]

Stations descriptions

- 0: Free stream
- 1: Inlet Entry
- 2: Compressor Entry
- 3: Compressor Exit
- 4 : Turbine Entry
- 5 : Turbine Exit
- 6: Nozzle Entry
- 7: Nozzle Exit

Ideal Behavior Component Analysis

- Inlet(i)

For the ideal case, when the flow passes through the inlet, it is considered isentropic. This makes the induction a process with constant enthalpy. The ratios summarizing the ideal behavior of the inlet are presented in equation 2.11 and equation 2.12, [19].

$$\pi_i = \frac{\text{Pressure at Inlet Entry}}{\text{Free stream Air Pressure}} = \frac{P_{02}}{P_{0r}} = 1 \quad [19] \quad (2.11)$$

$$\tau_i = \frac{\text{Temperature at Inlet Entry}}{\text{Free Stream Air Temperature}} = \frac{T_{02}}{T_{0r}} = 1 \quad [19] \quad (2.12)$$

- Compressor (c)

At this stage, the compressor will add energy to the flow in the form of work, thereby increasing its temperature and pressure. The equation 2.13 expressing the compressor work is demonstrated below [20].

$$W_c = \dot{m}_a c_p (T_{03} - T_{02}) \quad [20] \quad (2.13)$$

The temperature at the Compressor Exit can be obtained using the temperature and pressure relation found in equation 2.14.

$$\tau_c = \pi_c^{\frac{\gamma_c - 1}{\gamma_c}} \quad [20] \quad (2.14)$$

Being the pressure ratio, equation 2.15, and the temperature ratio, equation 2.16

$$\pi_c = \frac{\text{Pressure at Compressor Exit}}{\text{Pressure at Compressor Entry}} = \frac{P_{03}}{P_{02}} \quad [20] \quad (2.15)$$

$$\tau_c = \frac{\text{Temperature at Compressor Exit}}{\text{Temperature at Compressor Entry}} = \frac{T_{03}}{T_{02}} \quad [20] \quad (2.16)$$

- Burner/Combustor (b)

As previously explained in the working cycle, the combustion process is carried out at constant pressure. In the ideal case, the pressure ratio, equation 2.17, and the temperature ratio, equation 2.18, are,

$$\pi_b = \frac{\text{Pressure at Turbine Entry}}{\text{Pressure at Compressor Exit}} = \frac{P_{04}}{P_{03}} \quad [21] \quad (2.17)$$

$$\tau_b = \frac{\text{Temperature at Turbine Entry}}{\text{Temperature at Compressor Exit}} = \frac{T_{04}}{T_{03}} \quad [21] \quad (2.18)$$

Remembering that this is an adiabatic and constant pressure process with co mplete combustion, the combustion efficiency, η_b, is equal to one. Additionally, the enthalpy is the product of the specific heat coefficient at constant pressure and temperature [21]. Therefore, the energy equation 2.19 is,

$$(1+f)c_{pt}T_{04} = c_{pc}T_{03} + fFHV \quad [21] \quad (2.19)$$

Where FHV and f refer to the fuel heating value and fuel to air ratio. Utilizing equation 2.19, it can be related to the temperature ratio, equation 2.20.

$$\tau_b = \frac{T_{04}}{T_{03}} = \frac{1 + fFHV/c_pT_{03}}{1+f} \quad [21] \quad (2.20)$$

Where,

$$f = \frac{\dot{m}_f}{\dot{m}_a} \quad [22] \quad (2.21)$$

- Turbine (t)

The heated flow passing through the turbine experiences a decrease in pressure and temperature. As previously explained, the turbine exploits the energized flow t o perform work. Equation 2.22 illustrates the turbine work per mass of the airflow.

$$\Delta W_m = c_{pt}T_{04}(1-\tau_t) \quad [17] \quad (2.22)$$

Assuming the cycle is ideal, the expansion stage is considered an isentropic process. Thus, the turbine experiences no losses, fully utilizing the energy surplus from the combustion stage, resulting in an efficiency value of one [17]. The relationship between the temperature and pressure ratio of the turbine is described in equation 2.23.

$$\tau_t = \pi_t^{\frac{\gamma_t}{\gamma_t - 1}} \quad [23] \quad (2.23)$$

Where,

$$\pi_t = \frac{\text{Pressure at Turbine Exit}}{\text{Pressure at Turbine Entry}} = \frac{P_{05}}{P_{04}} \quad [23] \quad (2.24)$$

And,

$$\tau_t = \frac{\text{Temperature at Turbine Exit}}{\text{Temperature at Turbine Entry}} = \frac{T_{05}}{T_{04}} \quad [21] \quad (2.25)$$

- Nozzle (n)

The behavior of the nozzle compared to the inlet behavior is the same, meaning the flow is isentropic while passing through the specified stage [17]. Given these conditions, the total pressure and temperature, as per equation 2.26, of the nozzle are,

$$\pi_n = \frac{P_{07}}{P_{05}} = \tau_n = \left(\frac{T_{07}}{T_{05}}\right)^{\frac{\gamma}{\gamma-1}} = 1 \quad [24] \quad (2.26)$$

Jet Engine Performance

This section includes the main metrics for evaluating turbojet performance in an ideal scenario. Assuming the gas is calorically perfect throughout the cycle, the pressure at the turbojet's exit is equal to the ambient pressure, and the fuel-to-air ratio is much less than one [17].

$$\tau_r = 1 + \frac{\gamma-1}{2}M_0 = \frac{T_{0r}}{T_r} \quad [17] \quad (2.27)$$

$$\pi_r = (1 + \frac{\gamma-1}{2}M_0)^{\frac{\gamma}{\gamma-1}} = \frac{P_{0r}}{P_r} \quad [17] \quad (2.28)$$

However, it is common to limit the design concerning the maximum allowable turbine inlet stagnation temperature, hence the term established in equation 2.29 [17].

$$\tau_\lambda \equiv \frac{c_{pt}T_{04}}{c_{pc}T_{0r}} \quad [17] \quad (2.29)$$

The thrust (F), equation 2.30, and specific thrust ($\frac{F}{\dot{m}}$), equation 2.31, can now be determined.

$$F = \dot{m}(V_7 - V_0)[17] \quad (2.30)$$

$$\frac{F}{\dot{m}} = a_0\left(\left[\frac{2\tau_r}{\gamma-1}(\frac{\tau_\lambda}{\tau_r\tau_c} - 1)(\tau_c - 1) + \frac{\tau_\lambda}{\tau_r\tau_c}M_0^2\right]^{\frac{1}{2}} - M_0\right)[17] \quad (2.31)$$

Where the Speed of Sound is found in equation 2.32.

$$a = \sqrt{\gamma RT} \quad [17] \quad (2.32)$$

Finally, the specific fuel consumption, S can be obtained by equation 2.33.

$$S = \frac{f}{\frac{F}{\dot{m}}}[17] \quad (2.33)$$

Actual Behavior Component Analysis

The actual, or nonideal, cycle analysis presents the equations for analyzing the components and the engine’s performance, ignoring the gas velocities throughout the gas generator. The only velocities considered are at the inlet, intake, and outlet nozzle, exhaust. Additionally, the components are considered irreversible but adiabatic. Therefore, isentropic efficiencies are assumed for the inlet, compressor, turbine, and nozzle [11].

- Inlet

At the inlet, when the air is directed to the compressor, there is a reduction in total pressure from the free stream pressure due to friction during intake. As a result, t he temperature increases beyond the ideal case, which is influenced by the inlet efficiency, η_i. The equations 2.34 and 2.35 below determine the pressure and temperature at the inlet, where the outlet temperature is calculated as in the ideal cycle [11].

$$P_{02} = P_{0r}\left(1 + \eta_i \frac{\gamma_c - 1}{2} M_r^2\right)^{\frac{\gamma_c}{\gamma_c - 1}} \quad [11] \quad (2.34)$$

$$T_{02} = T_{0r}\left(1 + \frac{\gamma_c - 1}{2} M_r^2\right) \quad [11] \quad (2.35)$$

The pressure ratio, equation 2.36 is,

$$\pi_i = \frac{P_{02}}{P_{0r}} \quad [11] \quad (2.36)$$

- Compressor

At this stage, the compression occurs in an irreversible adiabatic process. Thus, it is associated with the compressor's isentropic efficiency, η_c [11]. Since this is an actual cycle, the compression of the air suffers losses along the way due to friction, turbulence, and many other unfavorable factors, which will cause the temperature to rise. This rise is related to the compressor efficiency, η_c [11]. So, the exit conditions, pressure, equation 2.37, and temperature, equation 2.38, at the compressor exit are,

$$P_{03} = P_{02}\pi_c \quad [11] \quad (2.37)$$

$$T_{03} = T_{02}\left[1 + \frac{\pi_c^{\frac{\gamma_c - 1}{\gamma_c}} - 1}{\eta_c}\right] \quad [11] \quad (2.38)$$

- Burner

During the combustion, there are losses derived from defective combustion, for example, conduction and radiation, which are accounted for by introducing the burner efficiency, η_b [11]. As a result, the pressure at the burner exit, equation 2.39, is,

$$P_{04} = P_{03}(1 - \Delta P_{cc}\%) \quad [11] \quad (2.39)$$

The temperature at the turbine outlet is predetermined to adhere to material li mitations. Therefore, the fuel-to-air ratio, as per equation 2.40, can be calculated by,

$$f = \frac{c_{pt}T_{04} - c_{pc}T_{03}}{\eta_b FHV - c_{pt}T_{04}} \quad [11] \quad (2.40)$$

- Turbine

In this process, the available power of the turbine is less than in the ideal process. Therefore, the turbine efficiency is related to the expansion, where the expression for the turbine pressure ratio, equation 2.41, becomes,

$$\pi_t = \left(1 - \frac{(c_{pc}/c_{pt})T_{02}}{\lambda(1+f)\eta_c \eta t T_{04}} \left[\left(\frac{P_{03}}{P_{02}}\right)^{\frac{\gamma_c - 1}{\gamma_c}} - 1\right]\right)^{\frac{\gamma_t}{\gamma_t - 1}} \quad [11] \quad (2.41)$$

Where, λ represents the ratio between the power required to drive the compressor and the available power generated by the turbine. The values of this parameter range from 75$\%$ to 85$\%$ [11].

The latter equation can be associated with equation 2.42 to obtain the exit temperature[11].

$$\frac{P_{05}}{P_{04}} = \left[1 - \frac{1}{\eta_t}\left(1 - \frac{T_{05}}{T_{04}}\right)\right]^{\frac{\gamma_t}{\gamma_t - 1}} \quad [11] \quad (2.42)$$

- Nozzle

At this stage, a critical pressure is introduced to verify whether the nozzle is choked or not. Therefore, the critical pressure is obtained by equation 2.43 [11].

$$\frac{P_{06}}{P_{crit.}} = \frac{1}{\left[1 - \frac{1}{\eta_n}\left(\frac{\gamma_t - 1}{\gamma_t + 1}\right)\right]^{\frac{\gamma_t}{\gamma_t - 1}}} \quad [11] \quad (2.43)$$

If $\frac{P_{06}}{P_{crit.}} > \frac{P_{06}}{P_{0r}}$, the nozzle is unchoked. The exhaust velocity is calculated from equation 2.44.

$$V_7 = \sqrt{\frac{2\gamma_t \eta_n R T_{06}}{(\gamma_t - 1)}\left[1 - (P_{0r}/P_{06})^{\frac{(\gamma_t - 1)}{\gamma_t}}\right]} \quad [11] \quad (2.44)$$

From the equation above, the exhaust temperature is obtained from equation 2.45.

$$T_{07} = T_{06} - \frac{V_{07}^2}{2c_{pt}} \quad [11] \quad (2.45)$$

If $\frac{P_{06}}{P_{crit.}} < \frac{P_{06}}{P_{0r}}$, the nozzle is choked, altering the exhaust temperature equation, 2.46, to,

$$\frac{T_{06}}{T_{07}} = \frac{\gamma_t + 1}{2} \quad [11] \quad (2.46)$$

Transforming the exhaust velocity equation, 2.47, into,

$$V_{07} = \sqrt{\gamma_t R T_{07}} \quad [11] \quad (2.47)$$

Jet Engine Performance Parameters

Specific Thrust, equation 2.48, is now expressed as,

$$\frac{F}{\dot{m}_a} = [(1+f)V_{07} - V] + \frac{A_7}{\dot{m}_a}(P_{07} - P_{0r}) \quad [11] \quad (2.48)$$

And, the thrust specific fuel consumption equation, TSFC equation 2.49, can be demonstrated as,

$$TSFC = \frac{\dot{m}_f}{F} \quad [11] \quad (2.49)$$

2.3 Components

In this section, background information on each component is provided, along with the different types and their functionalities.

2.3.1 Inlet Nozzle

The Inlet Nozzle functions like an air filter for the Compressor. In other words, when air is being directed to the Compressor, the Inlet Nozzle is responsible for allocating and c ontrolling the airflow, providing the required amount of airflow to the engine. Before the airflow enters the Compressor smoothly, the Inlet Nozzle performs its task by providing a uniform, stable, and high-quality airflow to the Compressor. The inlet is indirectly responsible for generating thrust, being considered one of the major components of a Turbojet [6].

The development of the Inlet Nozzle involves an extensive study and application of fluid dynamics laws to control airflow at subsonic or supersonic flight speeds. The distinction of the flight regime is made according to the Mach Number at which the intake is operating. For a Mach Number lower than 1.0, it operates in a subsonic condition, and if the Mach Number is higher than 1.0, the flight speed is supersonic [25]. The Mach Number is shown in equation 2.50.

$$M = \frac{V}{a} \quad (2.50)$$

Considering the flow of air entering the compressor uniformly is an idealized assu mption because, in reality, components like the engine pylon, wing, and fuselage deviate from the ideal, affecting the airflow and undermining the performance of the inlet nozzle. Cross-wind and vortex are examples of factors that undermine intake performance. In a cross-wind scenario, the stronger it is, the riskier it becomes, because the velocity at the lip might exceed the speed of sound in that area, jeopardizing the blades due to the consequent increase in flow speed added by the windward side of the air intake. An example of a vortex is the ground vortex.

It can develop as a result of the engine placement under the wings being next imbibed by the intake, which could have a negative impact on the intake performance [6].

The intake design for a subsonic airflow features a well-rounded lip, as shown in figure 2.14, to prevent flow separation, resulting in a thicker lip compared to a sharp lip for a supersonic airflow. Regarding the inlet cross-section, for subsonic speed, they have a round or elliptical shape, whereas for supersonic speed inlets, they have a central cone to significantly reduce the flow to subsonic speeds or a rectangular shape intake, as shown in figures 2.15 and 2.16 [26].

Figure 2.14: Subsonic Inlet [26]

Figure 2.15: Axisymmetric Supersonic Inlet [26]

Figure 2.16: Rectangular Supersonic Inlet [26]

2.3.2 Compressor

The compression of the air is crucial for gas turbines, and the compressor is responsible for ensuring this. Its principle is to convert mechanical energy, supplied by the turbine in the form of work, into pressure energy. Therefore, the better the conversion, the better the overall functioning of the gas turbine. To enhance this, there are three important parameters that characterize compressor performance. The first, compressor efficiency, indicates the energy loss during the conversion; in other words, it shows the energy the compressor needs to increase the pressure energy. The second, compressor pressure ratio, is the ratio of the total pressure at the compressor's release to the pressure at its entrance. The third, airflow rate, refers to the volume of airflow the compressor can process within a unit of time. These three parameters are interrelated and play an important role in the compressor's performance. For example, the compressor pressure ratio is directly connected to thrust, fuel consumption, and engine efficiency [6].

2.3.2.1 Centrifugal

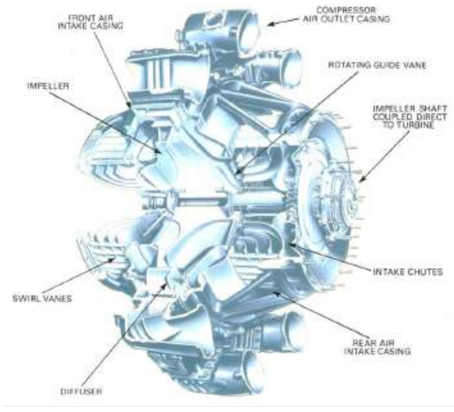

Figure 2.17: Centrifugal Compressor [8]

This compressor, shown in figure 2.17, has a rotating impeller to accelerate the air and a fixed diffuser that produces the required pressure rise. The impeller rotates at high speed, continuously drawing air into its center, generating a radial airflow directed by vanes to the impeller tip, which changes the airflow to a perpendicular direction relative to the rotation axis. The action of the impeller accelerates the airflow, causing the pressure to rise [8]. At the exit of the impeller, the air passes through a vaneless space followed by a vaned diffuser made up of vanes tangent to the impeller, which converts the kinetic energy into pressure energy [27]. When the air leaves the impeller, it depends on the configuration of the impeller, which dictates the airflow direction. The different types of impellers are illustrated in figure 2.18.

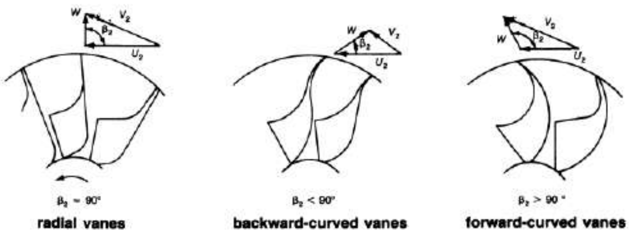

Figure 2.18: Types of impeller [27]

When the air passes through the impeller, there are changes in pressure and velocity. These changes can be observed in Figure 2.19, which traces a graph of pressure and velocity, illustrating the airflow passage through the elements of the compressor.

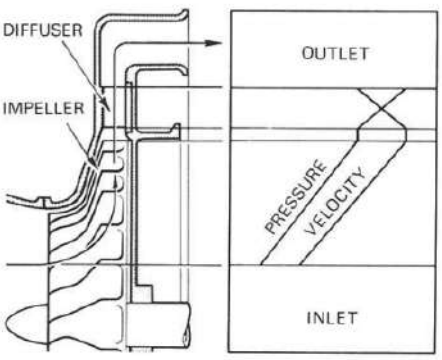

Figure 2.19: Pressure and Velocity evolution throughout the impeller-diffuser system [27]

This compressor is a choice for smaller gas turbines because it is simpler, has low-cost manufacture, and high stability, which means a greater operating range. Radial compressors achieve a high-pressure ratio, like 13:1 in experimental modes and, on average, 5:1 [17]. An overall balance of the positive and negative points about the three impellers can be seen in table 2.1.

Table 2.1: Advantages and disadvantages of the different impellers [27]

Types of Impellers	Advantages	Disadvantages
Radial vanes	1. Reasonable compromise between low energy transfer and high absolute outlet velocity 2. No complex bending stress 3. Easy manufacturing	1. Surge margin is relatively narrow
Backward-curved vanes	1. Low-outlet kinetic energy = low-diffuser inlet mach number 2. Surge margin is wide	1. Low-energy transfer 2. Complex bending stress 3. Hard manufacturing
Forward-curved vanes	1. High-energy transfer	1. High-outlet kinetic energy = High-diffuser inlet mach number. 2. Surge margin is less than radial vanes 3. Complex bending stress 4. Hard manufacturing

2.3.2.2 Axial

The axial compressor, shown in figure 2.20, is the most used in engine designs for current aircraft because it can deliver high-pressure ratios and high mass flow rates simultaneously, allowing for the creation of high-thrust engines. This compressor c onsists of several rotors connected to the central shaft, which increases the kinetic energy and static pressure. Each rotor is accompanied by stators, which are fixed rotors that reduce kinetic energy, thereby increasing static pressure and preventing the flow from spiraling [28]. Acting as air straighteners that remove the swirl, stator vanes achieve this due to their varying angle that corrects the flow from the rotor and directs the flow i n the correct direction for the next rotor [6]. By lowering the angle of attack, the variable stators reduce the tendency to stall [17]. The pressure and velocity throughout the axial compressor are demonstrated in figure 2.21.

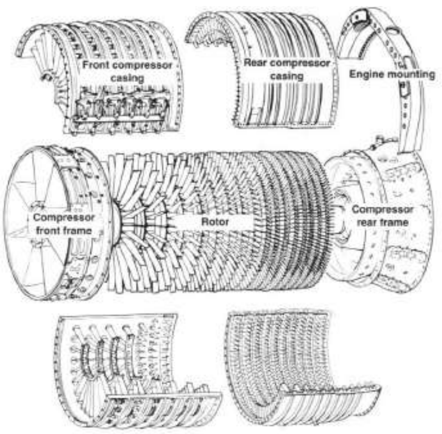

Figure 2.20: Axial Compressor [6]

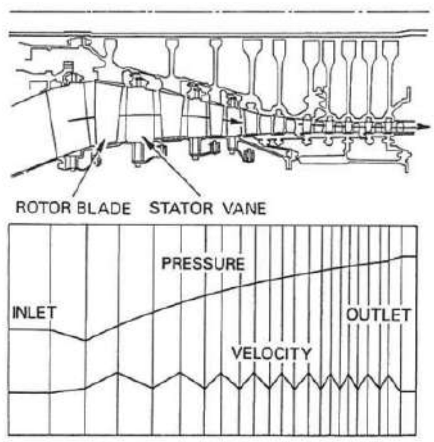

Figure 2.21: Pressure and Velocity changes i n an axial compressor [8]

A row of a rotor, along with a row of stator vanes, is called a stage. Each stage has a low pressure increase. The increase is small due to the deflection angle of the blades, and the rate of diffusion must be limited to prevent air breakaway at the blades, which could lead to blade stall. To suppress this effect, “bleed valves” were created to release part of the air from the blades in the intermediate rows and variable stator. By controlling as much as possible to prevent these losses, the body of the compressor can be constructed to have multiple stages, which, when compared to the centrifugal compressor with the same frontal area, achieves higher pressure ratios, resulting in much more thrust. This is why the axial compressor is chosen for most aircraft engines [6]. Other advantages include reduced aerodynamic drag due to a smaller cross-section and the absence of a need to turn the flow, as the airflow streams uniformly towards the turbine [8].

These engines can consist of more than one spool. The spool is the shaft that connects the compressor and turbine, on which the latter rotates. If there is only one set of compressor and turbine, the propulsion device is classified as a single-spool, as shown in figure 2.22. A multi-spool consists of two or more rotor assemblies, with each rotor being driven by its own turbine [8]. An example of a multi-spool is demonstrated in figure 2.23.

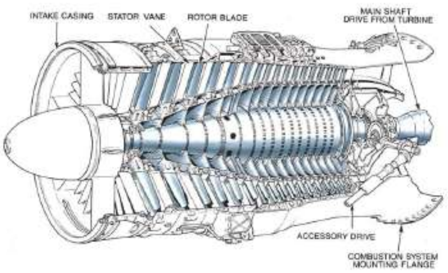

Figure 2.22: Single-spool axial compressor [8]

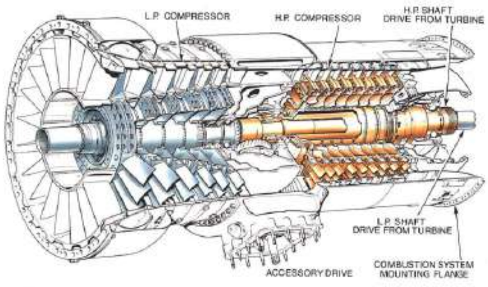

Figure 2.23: Twin-spool axial compressor [8]

If the compressor rotates at an optimum speed, it achieves higher pressure ratios. With high-pressure ratio values, fuel efficiency is improved, but it has limitations. The casing tends to expand and distort, necessitating a heavier compressor casing to support vibration stresses[8].

2.3.3 Diffuser

The Diffuser or stator is a subcomponent of the compressor system, which redirects the high-speed radial airflow coming from the impeller to the Combustion Chamber, converting the residual speed energy into pressure energy [29].

The Diffuser system can be categorized into two types: bladed or non-bladed. The non-bladed or bladeless annular space is easy to produce and can be efficient. Since it lacks blades, the correct blade angle is not a concern, which prevents flow separation. However, the bladeless Diffuser might not be the best choice because the flow duct would widen, increasing the risk of flow separation. According to Bernoulli law, the total energy of the flow remains constant; in other words, if the speed increases, the pressure decreases. Furthermore, since the relationship between speed and the Diffuser dia meter, based on the vortex law, is constant, widening the flow would not achieve the desired effect on pressure conversion, thus, the flow could break down [29].

The bladed diffuser can have guide vanes that curve in the direction of the compressor rotation, curve in the opposite direction, or even blades that widen to form thick wedges that can be drilled. The latter allows for the fixation of bolts without interfering with the gas flow. These types, shown in figure 2.24, are identified as straight diffuser blades, forward curved blades, and wedge-shaped blade diffuser, respectively. Moreover, these diffuser types possess blades that counter the twisting motion of the gases, preventing a drop in gas pressure by eliminating the residual spiral motion [29].

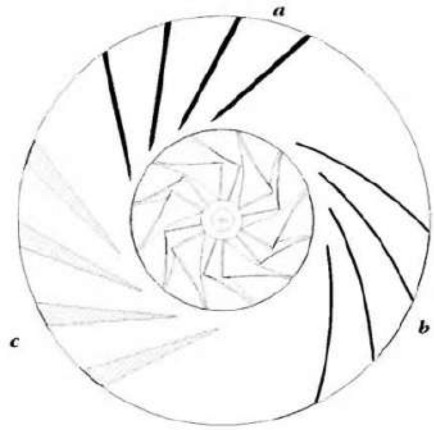

Figure 2.24: Diffuser Types [29]

2.3.4 Combustion Chamber

It is in the Combustion Chamber, see figure 2.25, that most of the internal energy increase occurs, making it one of the most important components for the thrust generated. It is designed to provide efficient combustion while minimizing pressure losses due to its significant role in operating and range costs [17]. This is where the fuel is burned after mixing with the air induced by the Compressor, followed by a release of thermal energy after combustion, where the air will expand and accelerate through a stream [6]. For the air to be uniformly

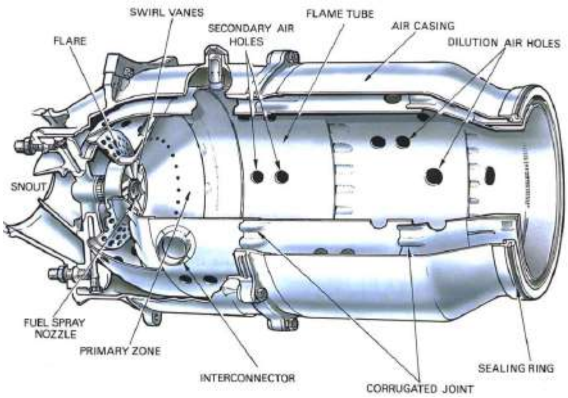

Figure 2.25: Combustion Chamber [8]

heated, there must be temperature control during combustion and suitable materials to withstand extreme temperatures throughout the combustion process. The combustion chamber accommodates heat increases from 650 to 1150 degrees Celsius of pre-heated air, which enters the chamber at 250 to 550 degrees Celsius. However, only 20 percent of the air mass flow passes to the primary zone (where the fuel burning occurs) of the combustion chamber, through swirl vanes to promote recirculation of the hot gas and small orifices of the disk supporting the swirl generator. This recirculation is created by the swirl vanes, which are part of a component called the snout, that reduces the airflow velocity to desired levels to keep the flame continuously lit throughout the range of ongoing operation. Additionally, there is also, another 20 percent that goes through the secondary air holes, joining the hot gas to lower the temperature before it reaches the turbine [8].

In the secondary air holes, the air passes through the external and internal walls of the flame tube, entering after the adjacent flow moves past the primary zone. The merging of these two streams creates low-velocity recirculation, forming a toroidal vortex to achieve a stabilized flame [8].

With such high temperatures, it would be extremely difficult for a material to maintain its performance regardless of how high the temperature is. Therefore, to ensure the material functions properly, the combustion chamber was designed to direct the airflow. This allows for the cooling of both the material and the hot gas. To prevent undesired performance of the chamber, spacing in the flame tube was developed so that the airflo w cools the flame tube walls, preventing overheating. On average, for cooling purposes, 40 percent of the total 60 percent of air is not used for combustion [6]. Then, another 20 percent of air passes through the secondary air holes into the dilution zone, reducing the hot gas temperatures from 1800 to 2000 degrees Celsius before it reaches the turbine [8]. The air distribution inside the burner is demonstrated below in figure 2.26.

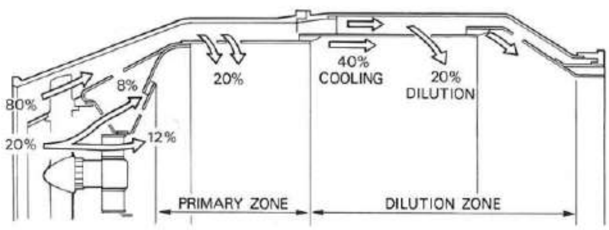

Figure 2.26: Distribution of air inside the burner [8]

Types of combustion chambers

- Multiple combustion chambers or can-type combustion chamber

It consists of multiple single chambers arranged in parallel, forming a circle around the central shaft. Combustion is easily achieved as ignition is required at only one or two combustors. A flame spreads from flame tube to flame tube through a connection link called an interconnector, allowing the burners to operate at equalized pressure [6]. An example of this chamber is shown in figure 2.27.

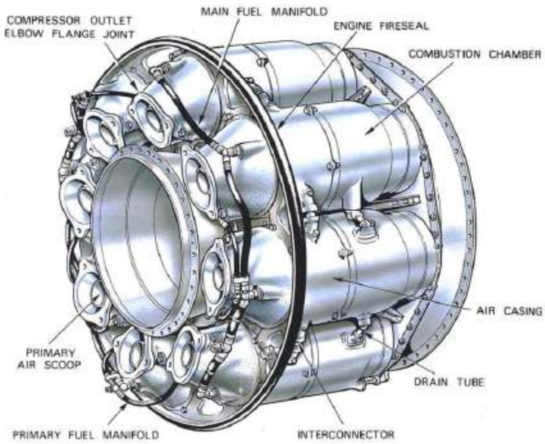

Figure 2.27: Multiple combustion chamber [8]

- Tubo-annular or can-annular combustion chamber

It emerged as an intermediate solution between the can-type and annular chamber, addressing the shortcomings of each while combining their strongest features. This combustion chamber, shown in figure 2.28, differs from the multiple combustion chambers by having an outer casing that surrounds the several chambers for secondary air supply, making it more mechanically stable than before. This improvement allowed for more efficient use of the available space [6].

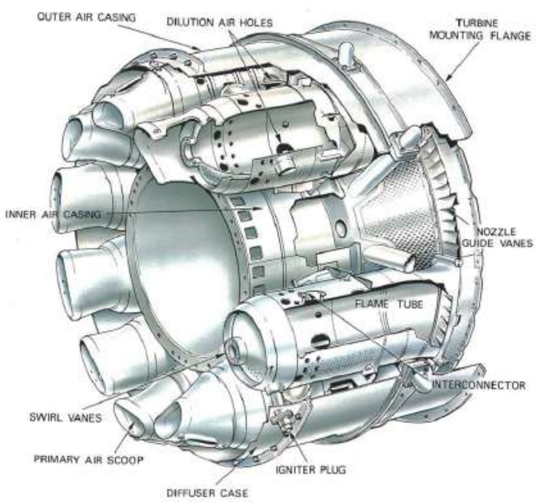

Figure 2.28: Tubo-annular combustion chamber [8]

- Annular combustion chamber

It is a single flame tube, shown in figure 2.29, in an annular form, which uses the volumetric space more efficiently, allowing for an even combustion process. Its simpler design beneficially reduces the overall weight, as the energy expanded through the burners remains the same, with 25 percent less length. Consequently, this impacts the production cost by decreasing it [8].

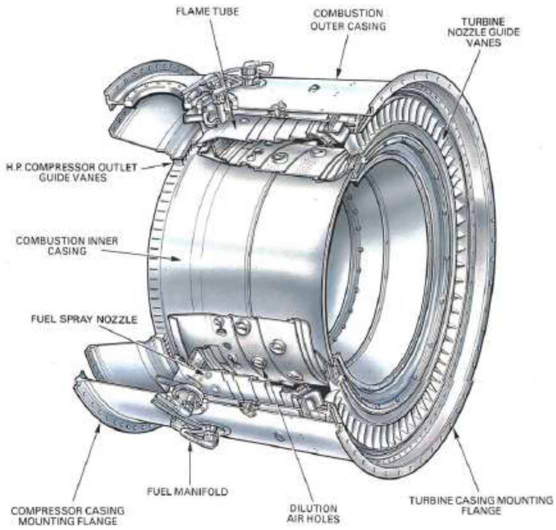

Figure 2.29: Annular combustion chamber [8]

2.3.5 Turbine

The turbine is a primary component of the gas generator that drives the compressor. Its primary function is to extract the energy contained in the hot gas from the combustion process by absorbing the energy when the gas flow impacts the blades. It extracts energy when the hot gas, at high temperatures, reaches the space limit available in the turbine. This cycle, repeated continuously, promotes the high-speed rotation of the turbine, fast enough to drive the compressor in the form of mechanical shaft power, which is achieved by converting kinetic energy into pressure energy and work [8].

2.3.5.1 Axial

Most aircraft engines have axial-flow turbines due to their higher mass flow intake. This type of turbine is characterized by a sequence of one stator followed by one rotor. A stator is a stationary nozzle with guide vanes of an airfoil section that adjusts the flow from the combustion chamber to the turbine by straightening the flow path, accelerating the gas, and creating a nozzle effect, which is the reason for its name. This is followed by a rotating wheel that uses the kinetic energy to create motion [8].

For successful energy extraction, the turbine blades induce a swirl in the gas flow to achieve uniform work across the length of the blades. The design of the blades will affect the flow expelled from the turbine, turning it more into axial flow before entering the exhaust system [6].

To be an efficient turbine, its design and development must align with the engine's specifications. A key specification is the power demand, which will influence the number of stages in a turbine. However, the number of stages to be added depends not only on the power demand but also on the rotational speed, maximum permissible turbine diameter, and the number of compressor spools. For instance, engines with a high compression ratio typically have two shafts to drive the low and high-pressure compressor [6].

The rotational movement causes stress in the turbine disc, which increases with the square of the speed [8].

New materials and cooling techniques were developed to withstand the high temperatures and pressures. One commonly used material in blade speeds is nickel-based superalloys due to their high resistance to creep and high-temperature strength [30]. Despite this, efforts are being made to prevent and manage losses in any part and functioning of the turbine. However, it is extremely difficult to prevent losses such as friction, turning the flow, or tip clearance [6].

The way a turbine converts energy determines its type, distinguishing it into three types: impulse, reaction, and impulse-reaction.

The impulse turbine, shown in figure 2.30, is similar to a water wheel that extracts energy from the gas flow by the impact of the gas on the turbine blades. The gas flows through the nozzle guide vanes, exiting with a higher velocity, which decreases pressure and temperature. In the rotor stage, the accelerated flow impacts the rotor blades, reducing velocity due to the energy transferred from the gas to the blades. This momentum exchange results in wheel rotation[6].

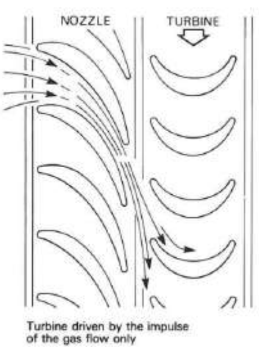

Figure 2.30: Impulse turbine [8]

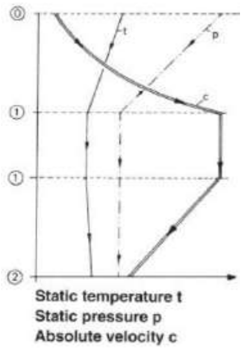

Figure 2.31: Properties variation throughout [8]

Observing Figure 2.31, there are three distinct phases. When the gas enters the nozzle guide vanes, corresponding to phase zero to one, it experiences a decrease in pressure and temperature with an increase in velocity. Subsequently, throughout phase one, as the gas exits the nozzle guide vanes and reaches the rotor blades, the temperature, pressure, and velocity remain constant. It then proceeds to the rotor blades path, phase one to two, where energy is extracted in the form of work, reducing the gas flow speed. A slight temperature rise can be observed as a consequence of friction [8].

The reaction turbine does not differ much from the impulse turbine. The difference lies in the rotor blades. In other words, the rotor blades path, due to the design of the blade, creates a nozzle effect, further accelerating the gas flow. Because of its design, an aerodynamic force is also generated, in addition to the momentum generated from the impact of the gas on the blades, causing the rotor to spin [8].

The constriction in the cross-sections of the flow path causes the previously explained nozzle effect. Additionally, there is a slightly smaller reduction in temperature and pressure than in the impact turbine.

2.3.5.2 Radial

From the first use in a jet engine flight at the end of 1930 to the utility of turbochargers, the radial-inflow turbine is used for various purposes, such as gas liquefaction expanders in the petrochemical industry, small gas turbines that provide power to helicopters, or as generating units [27].

A radial turbine offers significant advantages for work production. This type of turbine delivers more power than two or more stages of an axial-flow turbine. Additionally, the cost of manufacturing it is lower than that of a single or multistage axial turbine. However, in terms of efficiency, this type of turbine is outperformed by the axial type, which is the main reason why the axial type is predominantly used in aircraft engines [27].

The radial-inflow turbine is categorized into two types:

- Cantilever radial-inflow turbine

This turbine, shown in figure 2.32, resembles a low-reaction or impulse turbine because there is no acceleration of the flow across the turbine. It is characterized by not using radial inlet angles and having two-dimensional cantilever blades. Low efficiency values and manufacturing challenges are the reasons for their infrequent use [27].

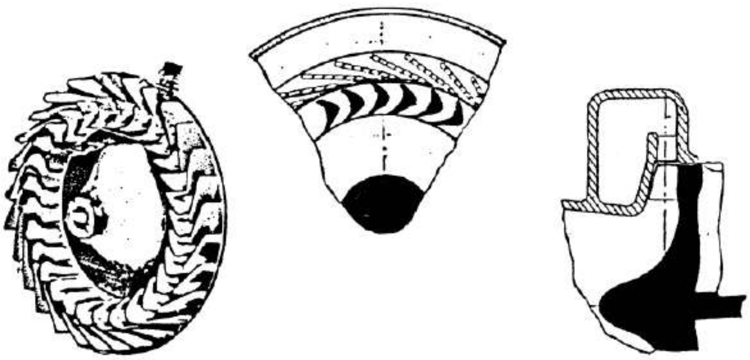

Figure 2.32: Cantilever radial-inflow turbine [27]

- Mixed-flow radial-inflow turbine

This turbine, shown in figure 2.33, is composed firstly of a scroll that collects the fl ow from a single duct to nozzle blades, which are often used as vaneless nozzles, similar to turbochargers where efficiency is not crucial due to the excess energy in the exhaust gases. With a vane design, the flow is directed by the blades, accelerating it. These blades are integrated into the hub or the disc, creating a force normal to the flow guideline. When the flow reaches the curved end section of the blades or exducer, part of the tangential velocity force is removed. Finally, the flow reaches the outlet diffuser, where the high absolute velocity from the exducer is transformed into static pressure [27].

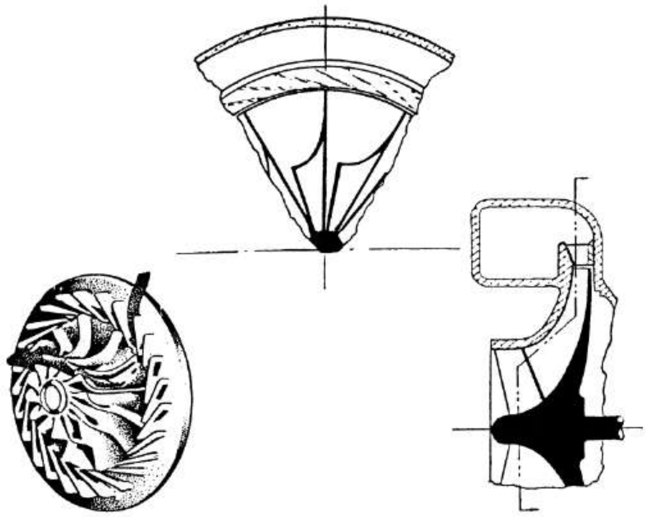

Figure 2.33: Mixed-radial inflow turbine [27]

2.3.6 Exhaust Nozzle

The last component of a turbojet is responsible for generating thrust, distinguishing the turbojet from being merely a gas generator, as mentioned previously. Its method of producing thrust involves converting the remaining enthalpy into exhaust speed [29].

The nozzle is developed according to the required performance and takes various shapes. Regarding the design, three types are distinguished:

- Convergent Nozzle

  The cross-section area of the duct decreases along the streamline direction, ending with a smaller cross-section area, thus accelerating the flow. The acceleration occurs due to a higher pressure at the nozzle entry than the ambient pressure, discharging the flow until it reaches the ambient pressure, where the gas will fully expand. If this nozzle discharges at sonic velocity, where the mass flow rate is maximum, the nozzle is considered to be choked. It is mostly applied in high-subsonic commercial and military aircraft [6].

- Divergent Nozzle

  The cross-section area increases reaching its maximum size at the discharge. This causes the fluid stream to spread across the nozzle, decelerating the flow [31].

- Convergent-Divergent Nozzle

  Characterized by a varying cross-section. At the forward part, the cross-sectional area decreases, followed by a subsequent increase in the cross-sectional area. Controlling the convergent and divergent parts makes the nozzle of variable geometry often used to add more thrust[6]. Figure 2.34 is a sketch of the convergent and divergent nozzle.

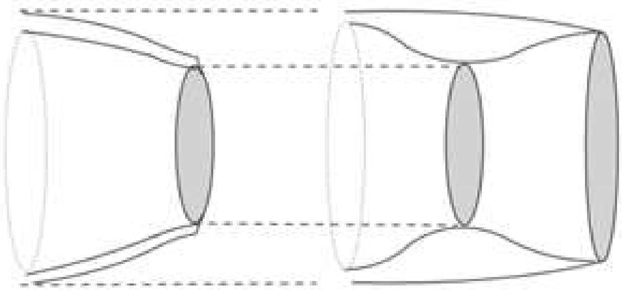

Figure 2.34: Convergent-Divergent Nozzle

2.3.7 Fuel system

2.3.7.1 Fuels

Selecting the appropriate fuel for a small size turbojet engine depends on the maximum available energy per kilogram of fuel [10]. The fuels with a high specific heat of combustion include petrol, kerosene, diesel, JP1 to JP8, which are different types of jet petrol, propane, and butane gas. If possible, the use of jet petrol type four kerosene and petrol are the best options for the combustion process. The heavy presence of volatile hydrocarbons in these two fuels makes them favorites [29]. However, diesel fuel, which is similar to kerosene, has a high energy density, making it preferable for use because it is easily obtained, being found at every gas station [10]. Furthermore, diesel vapor-air mixture has a lower ignition temperature, roughly 300 degrees Celsius, compared to petrol vapor-air mixture, which requires a temperature above 600 degrees Celsius to ignite [10].

The most suitable fuels for small-sized turbojet engines are gaseous fuels, particularly propane or butane. Besides these gases, methanol could be considered, although its low energy density is a disadvantage for its selection. A fuel pump for this type of fuel is unnecessary since the pressurized gas flows through the engine spontaneously [29]. Among the gaseous fuel types mentioned, propane is considered more suitable for static testing or development work [10]. Despite its benefits, this gas requires a pressure tank with twice the volume for the same mass of diesel fuel, due to its low energy density [10]. The differences between the discussed fuels can be seen in the demonstrated table, Table 2.2.

Table 2.2: Fuels [29]

SPECIFICATION OF POSSIBLE MODEL JET ENGINE FUELS

	Diesel	Petrol	JP1/Jet A	JP4	Propane	Methanol
Density [kg/l]	0.85	0.76	0.804	0.76	0.5(1)	0.79
H_{0u} [MJ/kg]	42.8	42.5	43.3	>42.6	46.3	19.5
Boiling Range (°C)	190-334	80-130	160-260	60-240	-42	65
Fuel tank Capacity (ml) (5 Minutes, 30 N Thrust)(2)	880	990	920	990	1,380	2,080
Flammability/Fire Hazard	Low	High	Low	High	Very High	High
Price (£/1)	0.8	1.05	1.2	?	0.7	0.6

(1) Liquid Under Pressure
(2) Sufficient for 5 minutes of powered flight at a thrust of 30 Newtons. (Specific Consumption = 0.3 kg/N/h)

2.3.7.2 Fuel Injection Modes

The air and fuel mixture can be achieved through fuel atomization or vaporization. The former is a common technique used in full-size aircraft, where the quality of combustion heavily depends on the droplet size of the atomized fuel. The complexity of this tec hnique outweighs its benefits for injection in small engines [29].

The fuel vaporization consists of small tubes, known as vaporizers, where the pre-heated gas flows, vaporizing part of the fuel before reaching the primary zone. The fuel is pushed through thin tubes, each connected to a single hooked tube. The beneficial aspect of this system is that the fuel mixes with air before entering the combustion zone. Unfortunately, the effectiveness of this method can only be confirmed through systematic experiments. For example, if the vaporizer is overextended, the temperature tends to rise [29]. The types of fuel injection can be seen in figure 2.35.

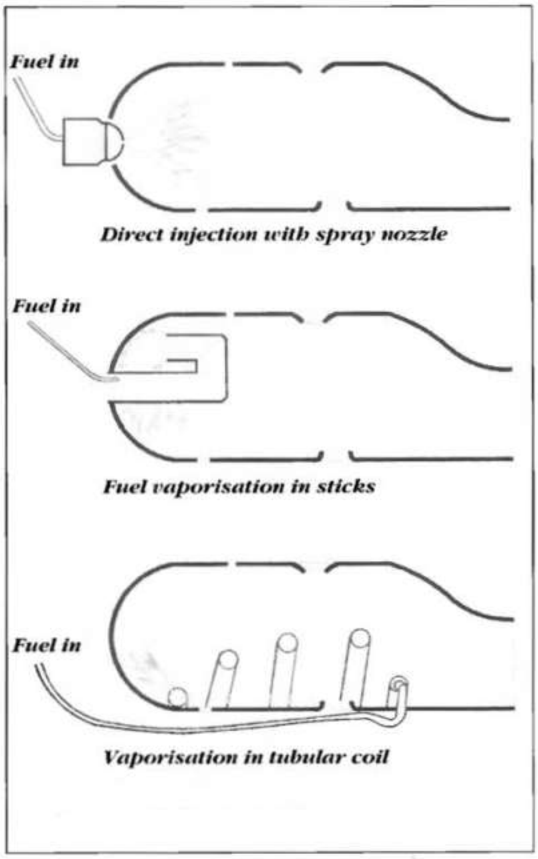

Figure 2.35: Fuel Injection Modes [29]

2.4 Turbocharger Basics

The very beginning of the turbocharger dates back to 1885 when Gottlieb Daimler created and patented the mechanical process of pre-compressing the air entering the engine. However, the person considered the creator of the turbocharger was a Swiss engineer, Alfred Büchi, who patented his invention in 1915, as demonstrated in figure 2.36 [32].

This device is composed of a Compressor and Turbine connected by a common Shaft, forcing th e

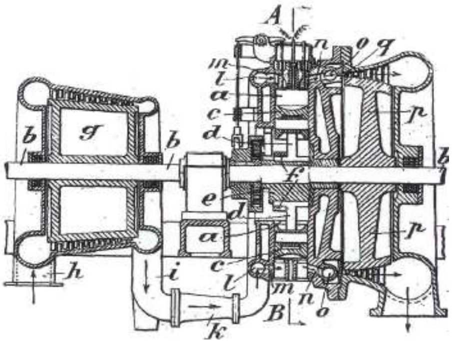

Figure 2.36: Turbocharger, Alfred Büchi’s Patent [32]

induction of air to the Combustion Chamber, of an internal combustion engine. The components of the Turbocharger are illustrated in figure 2.37.

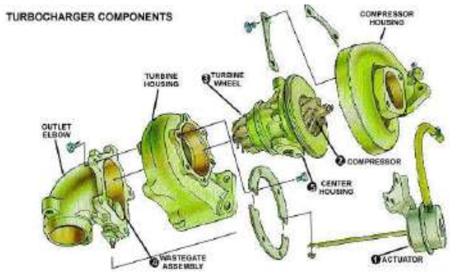

Figure 2.37: Turbocharger Components

The turbine uses the engine's exhaust gases to produce the necessary work, driving it by the shaft, to start the compressor's rotation. The compressor pressurizes the air, supplying it to the combustion chamber. In the combustion chamber, there is an increase in the fuel-air mixture flow, as the amount of fuel is proportionate to the surplus of air [33].

With more fuel burned, the power output increases along with the internal combustion engine efficiency. This cycle is demonstrated in figure 2.38. These outcomes were first discovered by Alfred Büchi in his initial successful application, achieving a power increase of over 40 percent [32]. This boost, both in power and efficiency, made the turbocharger a widely used device in vehicles.

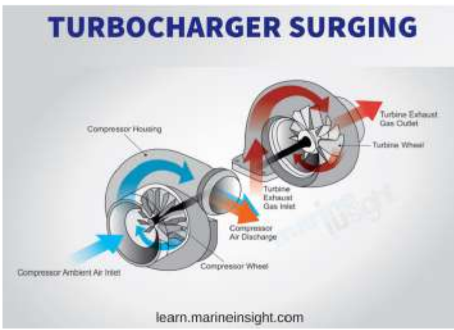

Figure 2.38: Turbocharger Work[35]

The development of a turbocharger involves designing the compressor and turbine blades as well as their housings. The blade designs are analyzed using CFD, Computational Fluid Dynamics, to understand how the air flows. Regarding the housing design, the gap between the rotor must be small enough for the rotor to effectively conduct the airflow. Otherwise, there is a possibility of the flow slipping between the rotor edge and the housing [33].

In general, if more information is needed about a specific turbocharger, the fabricator provides a chart describing the performance of the turbo's compressor, which includes the pressure ratio, mass flow rate, turbo speed, and efficiency regions. This chart, known as the compressor map, offers important details, allowing one to determine the airflow rate for this specific compressor at a given pressure ratio. Figure 2.39 is presented, highlighting the different performance characteristics in the chart. Below is a brief explanation of the observed characteristics [34].

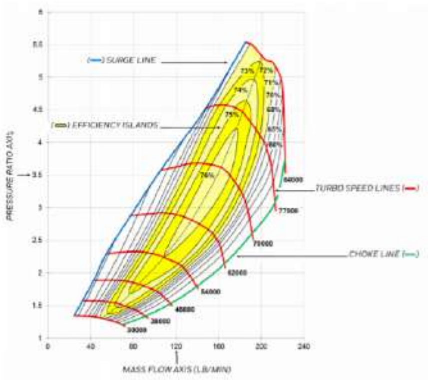

Figure 2.39: Example of a compressor map[34]

- Pressure ratio: ratio of absolute outlet pressure to absolute inlet pressure [34].
- Mass Flow Rate: mass of air passing through the compressor during a given period of time[34].
- Surge line: traces the line that distinguishes stable operation, found on the right si de of the line, from a flow instability region that could lead to a sudden turbo failure caused by large thrust loading [34].
- Choke line: is the line that separates the maximum mass flow rate the compressor can handle, on the left side of the line, from the compressor's inability to process the flow due to sonic speeds reached at the rotor inlet by the flow, preventing an increase in the flow rate [34].
- Efficiency Islands: are concentric regions on the compressor map that correspond t o compressor efficiency, differentiated by the sizes of the regions. The smaller the region, the higher the efficiency [34].

The compressor map obtained for this thesis is shown in figure 2.40. However, it is not the actual graphic of the compressor's performance, which made it challenging to determine an exact mass flow rate for a given pressure ratio. The graphic represents the compressor map of the turbo model, RHB31 VZ21, similar to the IHI RHF turbo 3 [36].

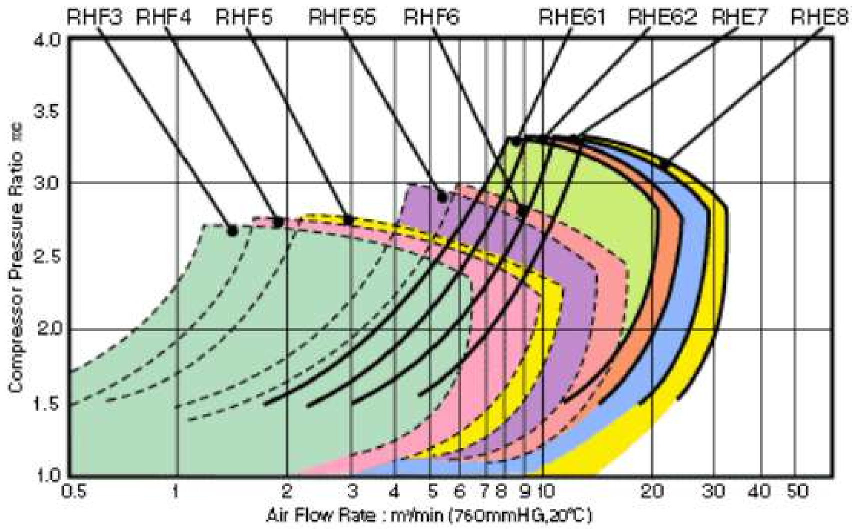

Figure 2.40: RHB31VZ21 Compressor Map [36]

Chapter 3

Methodology

This chapter outlines how the design and manufacturing process of each component of the mini-turbojet was conducted. Each component of the engine is designed, explaining how the dimensions were determined for the design and what materials are used for each component. The second section describes the chosen manufacturing process. A flowchart of the methodology is presented in figure 3.9, located at the end of chapter 3.

3.1 Dimensioning Process

3.1.1 Compressor

The starting point for sizing this engine is the Compressor. The Compressor chosen for this experimental project is from the turbo company IHI, the RHB31 VZ21 model.

From the literature review, the Compressors used in similar projects, such as the Kamps Turbojet or the WPI Turbojet, were Centrifugal because they offer a greater compression ratio and efficiency. Moreover, the turbo or the compressor/turbine set is easily available online and can be purchased at a relatively low cost compared to other turbos. Since it was already purchased, this Compressor was used to develop this thesis.

The design of the Compressor should be done with precise measurements to ensure accuracy. To achieve this, the turbo producers were contacted. However, they were unable to provide these dimensions as it is confidential information. The information obtained through research for the compressor map was found in the ECOTRON technical specifications document [36], shown in figure 2.40.

The basic dimensions such as base thickness, impeller/blade height, and impeller inlet/exit diameter were measured using a caliper. However, only the impeller exit diameter was necessary.

According to Kamps, a model of a Turbojet can be produced using his Turbojet dimensions with a scale factor, derived from the ratio between the compressor diameter, 36.6 millimeters, and Ka mps's compressor diameter, 66 millimeters [29] with a value of approximately 0.55. From this value, the estimated dimensions of the engine pieces were obtained.

3.1.2 Inlet Flange

This piece is the cover of the engine on the compressor side that secures the diffuser to the outer casing. It was designed based on the Worcester Polytechnic Institute project [37], , adapting its size according to the compressor shroud and outer casing dimensions of this engine, to ensure the design fits within the outer casing with very minimal clearance. Additionally, the bolt holes were aligned with the diffuser and outer casing holes for better coupling of both components.

Aluminum was chosen as the material for manufacturing this component. However, it is not possible to specify the type of metal, as this material was sourced from a spare engine block.

3.1.3 Compressor Shroud

This component was designed according to the diameter of the diffuser vanes, to avoid oversizing the shroud and to ensure the screw holes align with the diffuser vane holes. Then, the part accommodating the compressor was addressed. The gap of the inlet surrounding the compressor must not exceed 0.3 millimeters to achieve acceptable efficiencies [29].

However, to successfully design the compressor shroud within the tolerance, a 3D scan of the compressor should have been conducted to determine the curvature of the rotating compressor. Since it was not possible to obtain a 3D scan, the shroud was designed by creating circumferences based on the exducer and inducer diameter of the compressor. Figure 3.1 shows the starting point for this design.

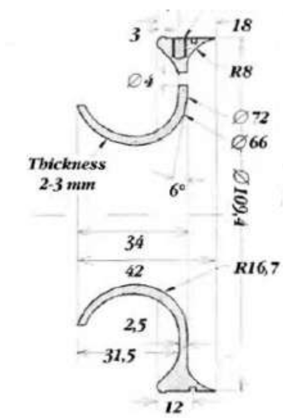

Figure 3.1: Compressor Shroud [29]

In the literature reviewed, aluminum is the recommended material for this part. Therefore, it was decided to construct it using this material. Unfortunately, the specific type of aluminum is unknown, as it was sourced from a spare engine block.

3.1.4 Diffuser

The most challenging piece to design was the diffuser. The first step was to choose the diffuser style: bladeless or bladed, and if bladed, to decide between straight, forward-curved, or wedge-shaped blades. Based on examples from the literature, a wedge-shaped blade diffuser was chosen, considering the fixing bolts that allow the compressor shroud to attach to the diffuser and prevent gas flow leaks [29].

First, the diffuser was dimensioned based on Kamps's diffuser. Thomas Kamps's book, [29] provides the diffuser dimensions and includes the axial blade profile, shown in figures 3.2 and 3.3.

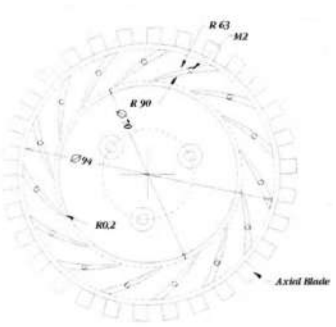

Figure 3.2: Diffuser [29]

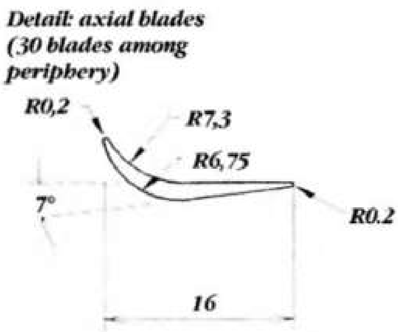

Figure 3.3: Diffuser Blading Profile[29]

3.1.5 Shaft and Shaft Housing

Upon reviewing mini-turbojet shaft designs like the KJ66, AMT Olympus, or Kamps's engine, it was noted that the designs were relatively similar. Therefore, the shaft was dimensioned by scaling down the dimensions of Kamps's shaft as described in figure 3.4.

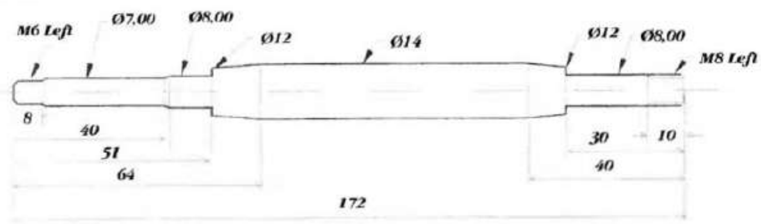

Figure 3.4: Shaft [29]

The Shaft accommodates two bearings, located at the bearing seats, positioning the bearings on both sides of the Shaft. The steps are for tight-fitting of the bearings to prevent them from displacing. To produce this Shaft, a stainless steel rod was chosen as the material to be further machined.

The Shaft Housing was designed, like the Shaft, to accommodate the Shaft with the two bearings inside and to couple the Diffuser, which is fixed with bolts to the housing, along with the Stator Housing, which will also be bolted to the housing. Despite the variety of Shaft Housing designs, the chosen design is simple and straight, widening at both ends of the housing to provide space for the bolts to secure the Diffuser and Stator Housing. The dimensions were determined by adapting the Shaft Housing dimensions shown in Figure 3.5 to our scale.

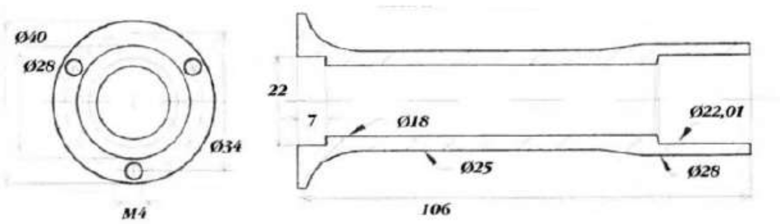

Figure 3.5: Shaft Housing [29]

The aluminum is the material from which the shaft housing is made, but its type is not feasible to determine since it was taken from a spare engine block.

3.1.6 Combustion Chamber

The design for the combustion chamber that was considered optimal was an annular chamber. According to the literature reviewed, it seemed the best choice for its simple design and practicality, meaning it would facilitate the manufacturing process compared to other types. Moreover, combustor design generally comes from empirical data, and since the objective is not to improve a design, choosing a combustion chamber that had successfully performed its role was the wisest choice. Therefore, it was decided to design it based on the combustion chamber of Kamps, adapting its size and holes for this combustion chamber. It consists of a stainless steel sheet of 0.5 mm thickness shaped into a tube with the desired diameter and a series of holes of different diameters. Figures 3.6 and 3.7 below demonstrate the combustion chamber design that was relied on [29]. The combustion chamber

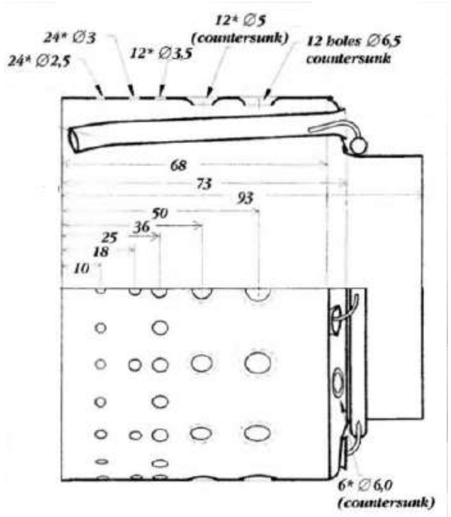

Figure 3.6: Outer Flame Tube [29]

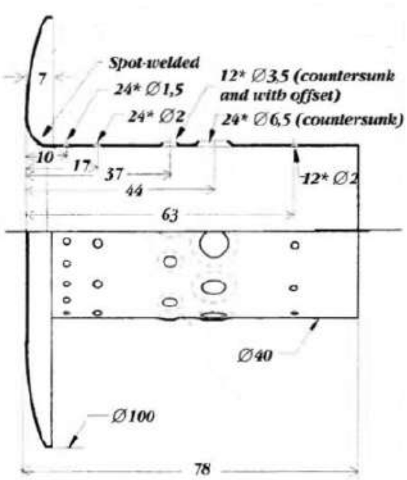

Figure 3.7: Inner Flame Tube[29]

has two tubes, one smaller tube that fits inside the larger one. The diameters of the holes and the distance between them were scaled down to an appropriate size and distance for this mini-turbojet.

3.1.7 Fuel Distributor

The Fuel Distributor, as the name suggests, distributes the fuel to the vaporization tubes of the Combustion Chamber. In the small gas turbines observed, the design is almost identical. Therefore, an injector ring with an appropriate diameter was designed for the Combustion Chamber. The injector ring is positioned on the inner side of the Co mbustion Chamber on the turbine side and has several injectors corresponding to each vaporization tube. The fuel is supplied from an external source connected to a tube that passes through the Outer Casing to the Combustion Chamber, where it is also connected to the injector ring. The Fuel Distributor is made of a stainless steel tube with a diameter of 3 millimeters [29].

3.1.8 Nozzle Guide Vanes System

The guide vanes or stator, fixed to the housing, redirect the flow to the turbine. The housing, in addition to holding the guide vanes, is designed to provide the necessary space for the turbine to rotate, maintaining a constant gap between the two components, so the efficiency is not affected. Most of the nozzle guide vanes system designs were made for axial turbines. However, the nozzle guide vanes system was designed based on other designs using a radial turbine[38].

The dimensioning was considered with respect to the components affected by its design, such as the combustion chamber, fuel distributor, and the shaft housing. The idea was to integrate the outer flame tube with the nozzle guide vanes, where the fuel distributor would be fixed in a flange at the inner flame tube.

3.1.9 Turbine

The turbine, like the compressor, was sourced from the RHB31 VZ21 turbo.

3.1.10 Exhaust Nozzle

This component is responsible for generating thrust. However, the primary objective of this dissertation is not the optimization of the generated thrust, but rather the design and manufacturing of a self-reliant small gas turbine. The nozzle design is a simple, convergent nozzle ensuring straightforward construction, designed based on the dimensioning of this component as informed by the literature review. Figure 3.8 demonstrates the exhaust nozzle dimensions, although it was scaled down and adapted for this jet engine. The recommended material for this component is a stainless steel sheet with a thickness of 0.5 millimeters[29].

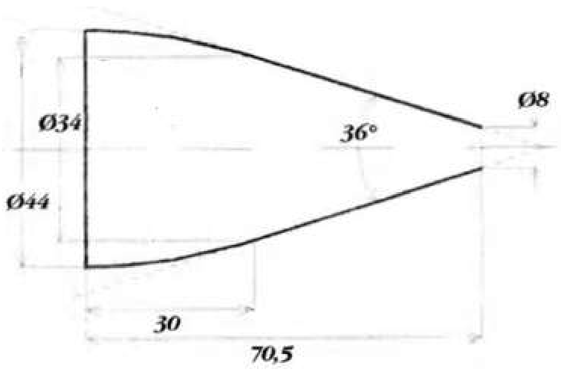

Figure 3.8: Exhaust Nozzle [29]

3.1.11 Bearing, Lubrication, and Fuel Injection

The selection of bearings must consider the purpose of the bearing. For a small gas turbine, the bearing must withstand high temperatures and extreme rotational speeds. With these requirements in mind, manufacturers were sought out for those that offered a set of bearings with the desired dimensions to fit properly in the shaft.

The bearings selected were deep groove ball bearings made of stainless steel from SKF, capable of withstanding up to 120,000 RPM[39] and are resistant to high temperatures because, the higher the RPM, the higher the temperature of the bearing will be [40]. For the bearings to operate properly, a lubrication system is necessary, which should be created by implementing two thin, stainless steel tubes on the shaft housing, connected to an oil pump. Each tube enters on each side of a bearing to transport the lubricant. The tubes pass through the outer casing and then to behind the diffuser, inserted in the shaft housing.

The fuel injection is carried out by a fuel tube that extends from the fuel distribution ring through the turbine side of the casing to the external fuel source. At the distribution ring, the fuel then proceeds to the vaporization tubes. The combustion chamber was designed to allow the engine to operate on different fuels in either a gaseous or liquid state.

3.1.12 Outer Casing

The final part of this engine consists of a stainless steel tube with a thickness of 0.5 millimeters[29]. On the compressor side, holes were made to allow bolts to pass through the casing and reach the diffuser. The bolts were screwed in, securing the outer casing to the diffuser. At the other end, the outer casing is attached to the nozzle guide vanes. Since this component was one of the last to be designed, there was no need to scale it down based on the literature. With the other components already designed, the outer casing must adequately cover the gas generator.

3.2 Manufacturing Process

The construction guidelines for this thesis, based on the literature reviewed and online videos of the model jet engines manufacture, are divided into two subsections, distinguished by the two main materials used to produce the necessary components for the engine. One is aluminum and the other is stainless steel.

The aluminum-based components are the inlet flange, compressor shroud, and the diffuser. These parts were produced with the help of UBI's FABLAB, Fabrication Laboratory, using the 5-axis CNC milling machine. This location was chosen due to the precision of production, which cannot be matched by handmade methods using manual milling machines. For the 5-axis CNC milling machine to produce the desired co mponent, a .stp format file obtained from the design software, in this case, CATIA software, is required. Through this procedure, round blocks of aluminum are t ransformed into the expected shape with an extremely low margin of operating error. However, the shaft housing was created through the manual operation of a lathe machine.

The stainless steel elements were manufactured using a vertical drilling machine, a lathe machine, a roller, and a water jet machine. Initially, the water jet machine was used to cut the pieces designed for each component. These pieces were cut from a stainless steel sheet, so the designed components had to be drawn to their flat shape, which was later worked on to achieve the desired form. The next step was to drill the holes in the flat pieces belonging to the inner and outer flame tube and the combustion chamber. The drilling was done using a vertical drilling machine.

“Flat washers” will later be attached to the respective components, specifically the nozzle guide vane system, the rear end of the combustion chamber, and the casing. The next step was to mold the flat pieces of the combustion chamber, nozzle guide vane system, and casing to the required diameter. Upon completing the molding of the piece, the “flat washers” were welded to form the tubes and flat rings. The last component, the shaft, with the help of a two-dimensional sketch design, was manufactured using a lathe machine.

In general, parts were designed and manufactured using a procedure similar to the one used for the diffuser, as seen in figure 3.9.

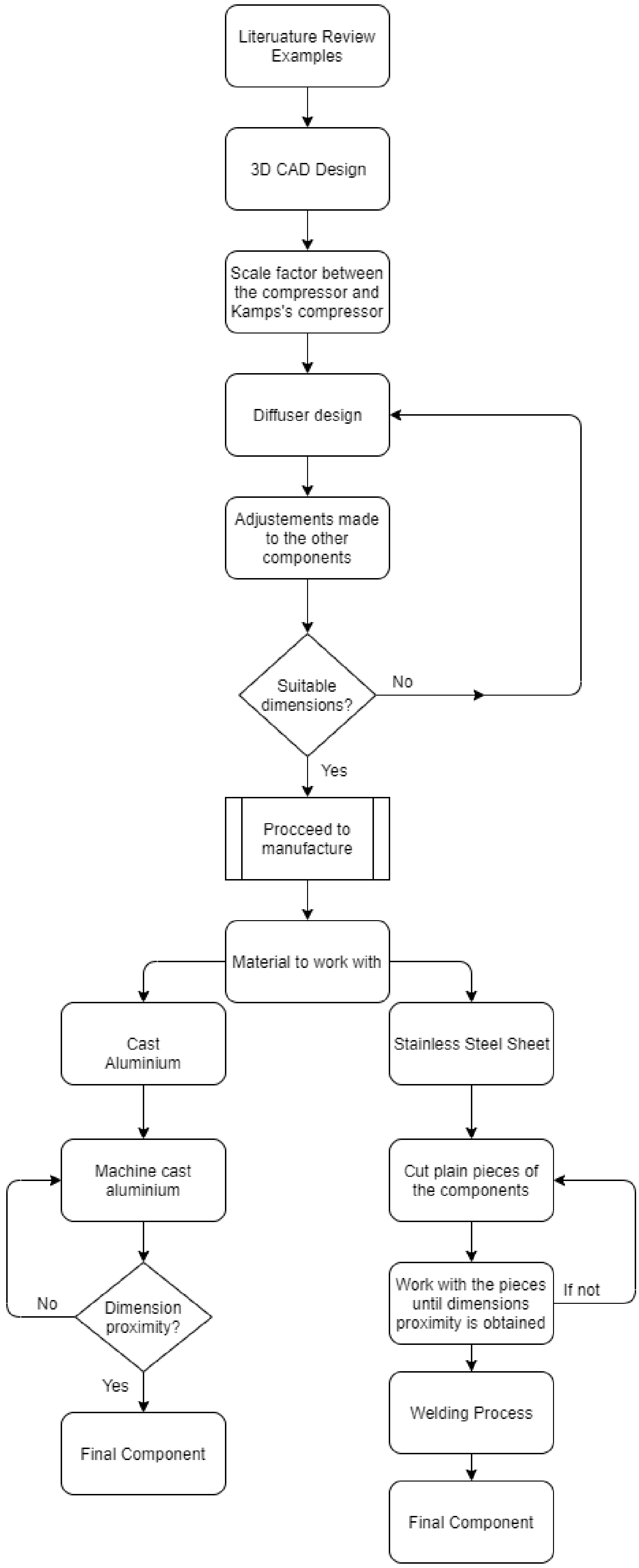

Figure 3.9: Diffuser design procedure

Chapter 4

Practical Case

In this chapter, the results from the dimensioning of the components will be presented, along with their design. The fabrication process followed to obtain the components and how they were machined will also be explained in depth.

4.1 Dimensioning Results

The final dimensions of the mini-turbojet are described along with the assembly design i n Appendix B and C. As previously stated, the dimensioning was executed by comparing empirical data, which was then adapted to this design. Some pieces did not precisely follow the scale factor due to adjustments made during the design of all components. The design was finalized when the parts were assembled to verify if all components were aligned and fit properly.

4.2 Design of the Mini-Turbojet Prototype

The design of the components of this small gas turbine was briefly explained in the previous chapter 3. In this section, the design techniques applied to determine the shape and dimensions of the parts composing the gas turbine will be described. The blueprint will be created using CATIA V5R18 software, owned by Dassault Systèmes.

4.2.1 Compressor

The compressor design was challenging to comprehend, and efforts were made to replicate it in CATIA software, deviating as little as possible from its physical dimensions. Initially, the base of the compressor was drawn as shown in figure 4.1. Following the shaft CAD operation, the profile of the compressor vanes, as seen in figure 4.2, was drawn from a visual perspective. Finally, the multi-section solid was applied to create the solid vanes from the sketch, completing the overall design with a hole through the compressor to accommodate the shaft. The final product is shown in figure 4.3.

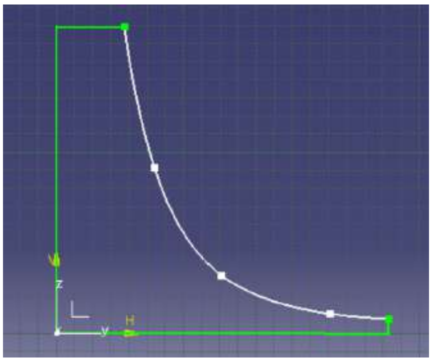

Figure 4.1: Compressor CAD shaft operation

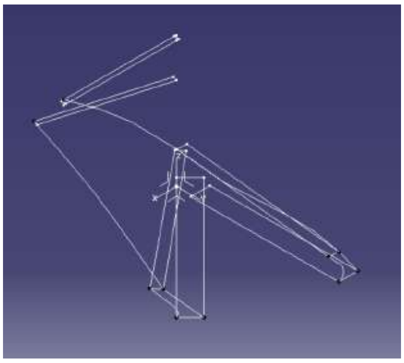

Figure 4.2: Compressor CAD Vanes Sketch

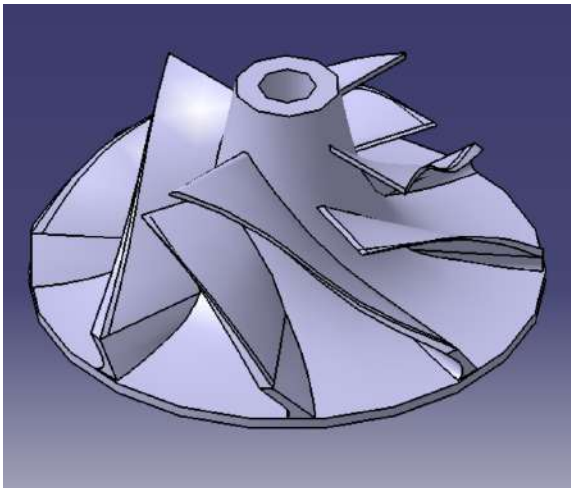

Figure 4.3: Compressor CAD view

4.2.2 Inlet Flange

The design for this component was straightforward and direct. Initially, a sketch was created, adhering to the compressor shroud dimensions to ensure a proper fit. Additionally, sufficient space was provided for the coupling of the diffuser and outer casing. The inlet flange sketch, shown in figure 4.4, was applied in a shaft operation, shaping it into the solid demonstrated in figures 4.5, 4.6, and 4.7, with holes included to secure it to the diffuser (front side) and outer casing (side view). An isometric view of the designed piece is illustrated in figure 4.8.

Figure 4.4: Compressor CAD view

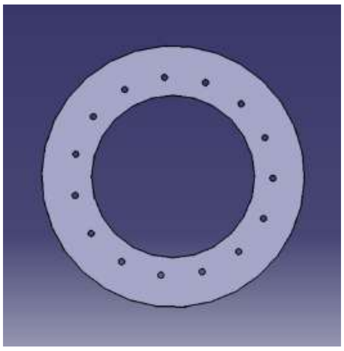

Figure 4.5: Inlet Front View

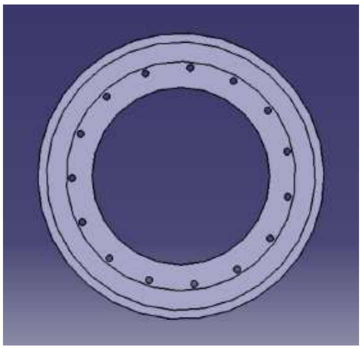

Figure 4.6: Inlet back view

Figure 4.7: Inlet side view

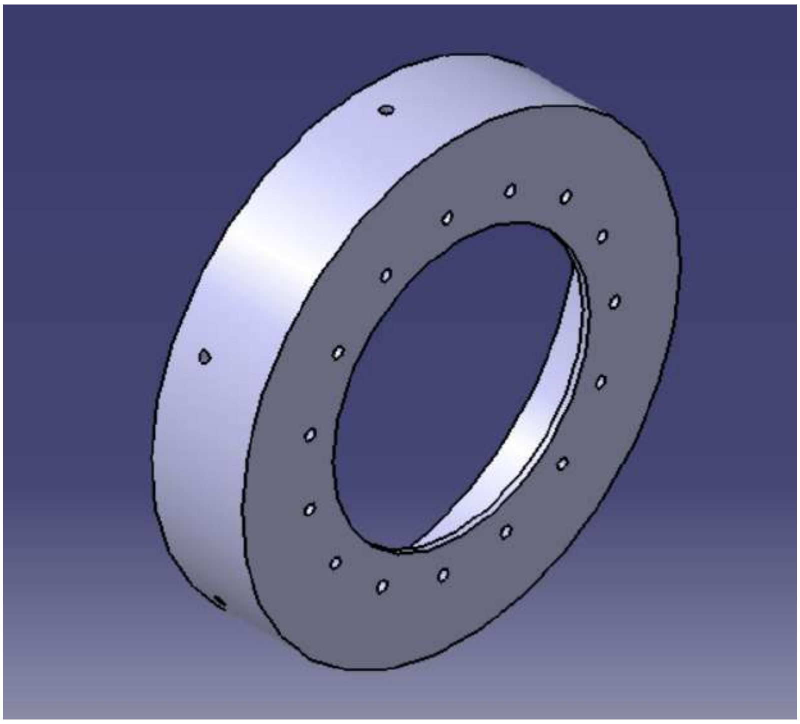

Figure 4.8: Inlet isometric view

4.2.3 Compressor shroud

This design is based on the exducer and inducer diameters of the compressor. It was created using the multi-section solid, utilizing the sketches presented in figure 4.9. The inner circumferences were drawn considering the 0.3 millimeters of tolerance gap between the rotor and the inside walls of the compressor shroud. The outer circumferences were designed, when applying the multi-section solid and removing solid function, to ensure the 2 millimeters of thickness as recommended [29]. The circumferences' height was drawn in relation to the compressor blades' height and the exducer height. Figure 4.10 describes the circumferences sketch with height measurements. Furthermore, the holes were made after the solid product was designed, with the correct diameter for fixing to the diffuser. The design of the compressor shroud is shown in figure 4.13 along with the side view, figure 4.11, and back view, figure 4.12.

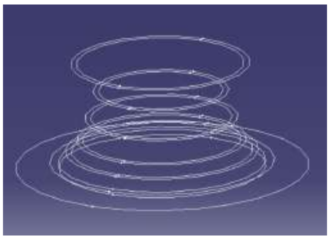

Figure 4.9: Compressor Shroud sketch

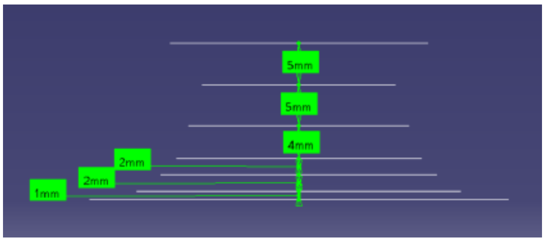

Figure 4.10: Compressor shroud design planes height

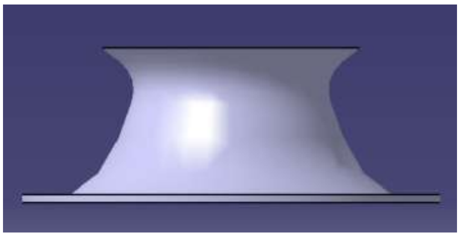

Figure 4.11: Compressor Shroud side view

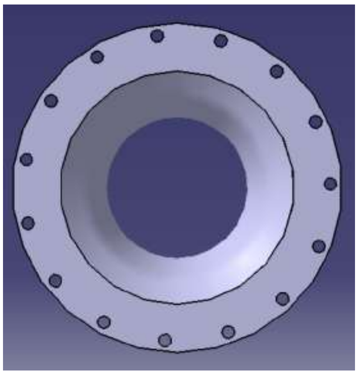

Figure 4.12: Compressor Shroud back view

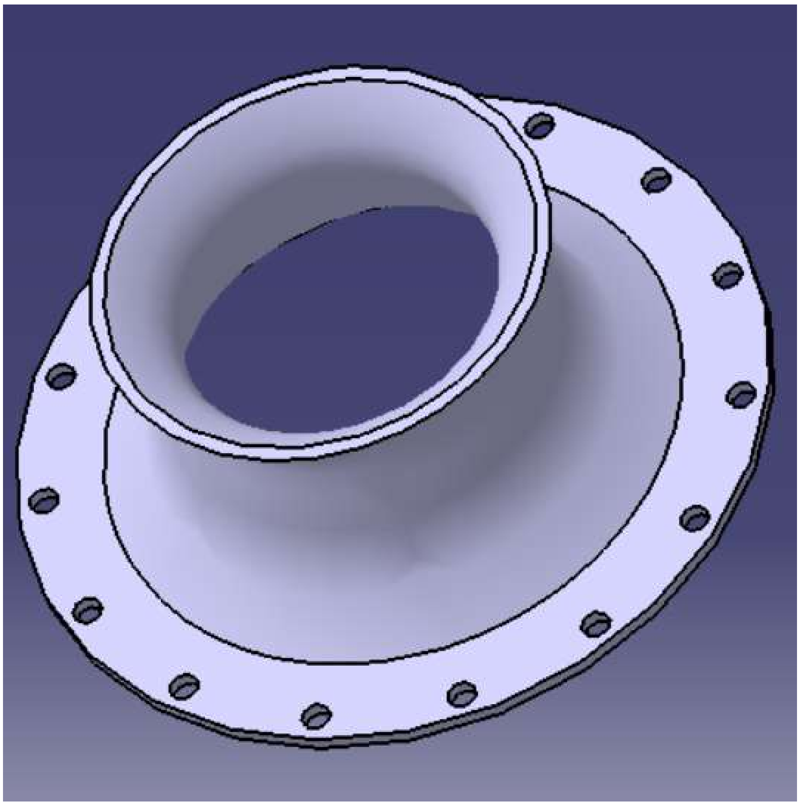

Figure 4.13: Compressor Shroud isometric view

4.2.4 Diffuser

The starting point for this piece is a small cylinder, where the axial and wedged-shape blades are created, adhering to the dimensions and angles recommended in Thomas Kamps's book, chapter 3. The base was designed with space to accommodate the compressor, via shaft operation, followed by the design of the wedged-shape and axial blades, as shown in figure 4.15 and figure 4.16.

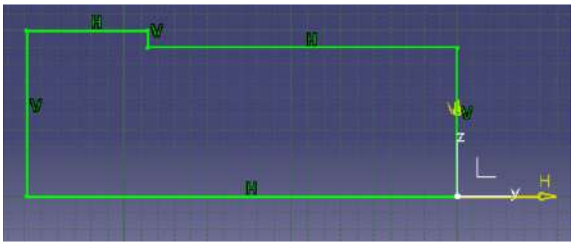

Figure 4.14: Diffuser Base

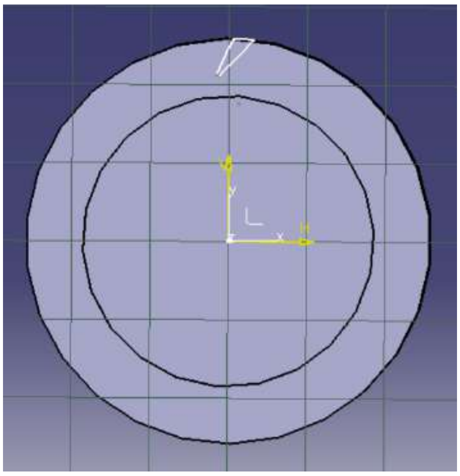

Figure 4.15: Diffuser Wegded-shape blade

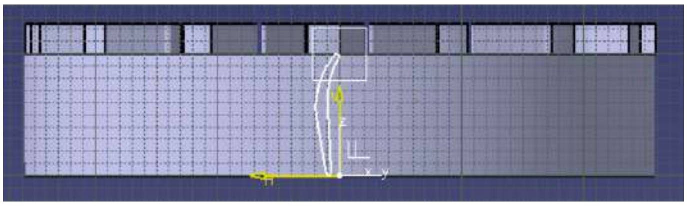

Figure 4.16: Diffuser axial blade airfoil

The wedge-shaped blades, shown in figure 4.15, were given a gap of 1.15 times the compressor wheel diameter [29]. The diffuser, figure 4.17, was finalized by creating the holes to attach it to the shaft housing and outer casing.

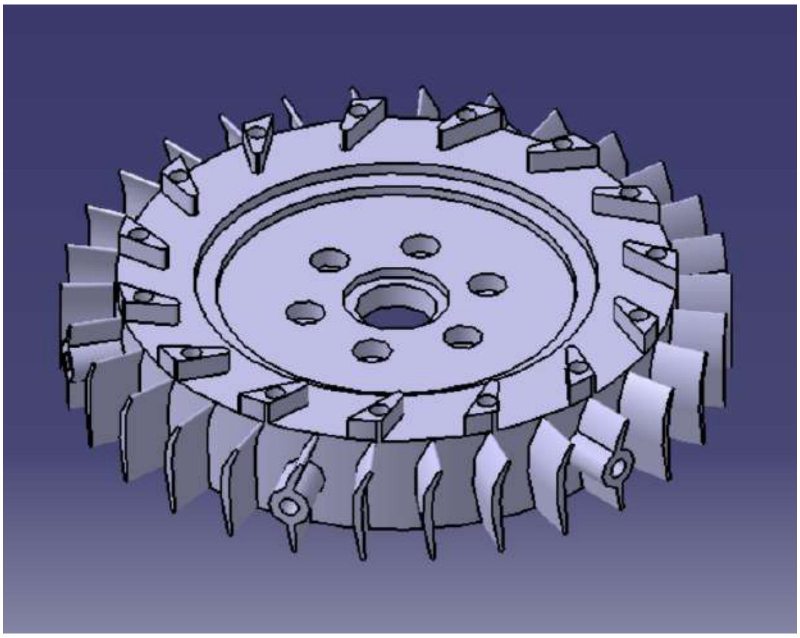

Figure 4.17: Diffuser isometric view

4.2.5 Shaft and Shaft Housing

The shaft housing was the first to be designed following the completed designs of the NGV, Combustion Chamber, and diffuser. The objective was solely to design a rigid structure connecting the NGV with the diffuser, adhering to the general design of other housing structures used for constructing a small-dimension turbojet. Initially, a straighter design was chosen, as it was more convenient for attachment to the diffuser or NGV using screws tightened by nuts as fastening elements. With the design conceptualized, the draft was executed. It consists of two thick rings, joined by a compact rod, designed using shaft operation. This operation was applied to the sketch shown in figure 4.18.

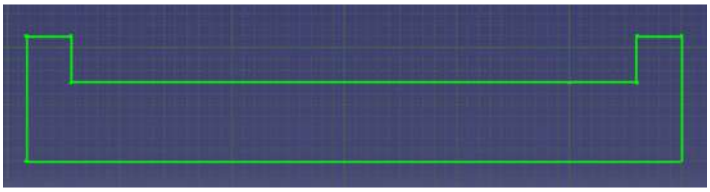

Figure 4.18: Shaft Housing sketch

Subsequently, holes were made to attach the housing to the diffuser and NGV, as well as to provide space for the shaft to pass through with the bearings. The inside of the housing, on the turbine side, was extended to allow space for a string and a sleeve. The second part, the shaft, was also created using the shaft operation, applied to the following sketch, illustrated in figure 4.19.

Figure 4.19: Shaft sketch

The length of the shaft was determined when all the parts traversed by the shaft were designed and assembled in the correct positions. The assembly mode was used, and the necessary length for the shaft was measured. Subsequently, the design of the actual component was completed, as shown in Appendix C.

4.2.6 Combustion Chamber

This part is straightforward to outline, consisting of two tubes with a total of 132 holes: 72 holes are distributed in the primary zone, 48 holes in the intermediate zone, and the remaining 12 holes in the dilution zone. The first step was to determine the diameter and length of the outer flame tube. The same procedure was followed for the inner flame tube, with the addition of a cover for one end of the combustion chamber and support f or the fuel distributor ring. The design was completed using shaft operation, based on their initial sketches, as shown in figure 4.44 and figure 4.43. The support for the fuel ring distributor was further added to the design, with a suitable diameter for later welding, as demonstrated in figure 4.22 with an overview of the outer flame tube, figure 4.23.

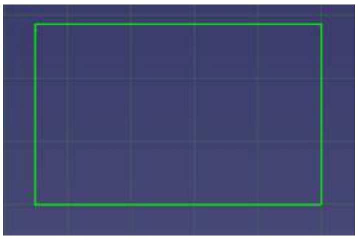

Figure 4.20: Outer Flame tube sketch

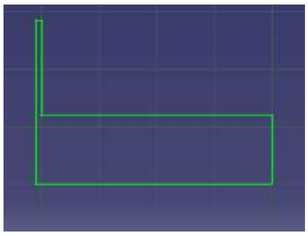

Figure 4.21: Inner Flame tube sketch

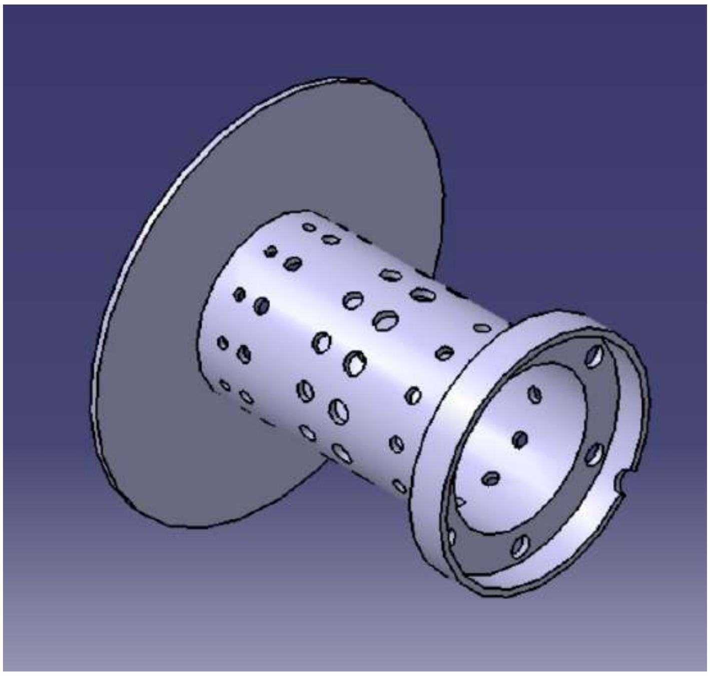

Figure 4.22: Inner Flame tube isometric view

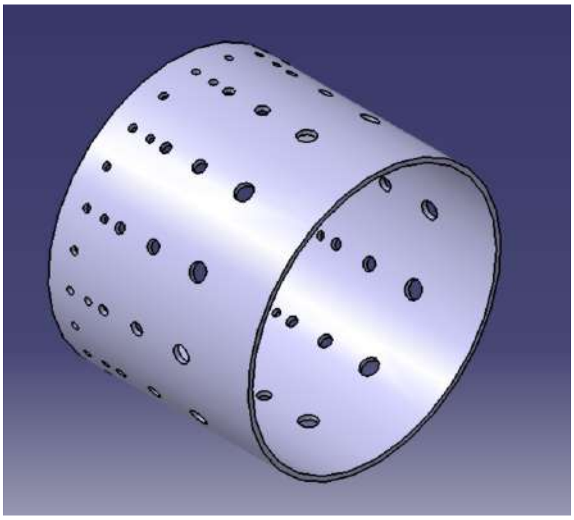

Figure 4.23: Outer Flame tube isometric view

4.2.7 Fuel Distributer

This design began by drawing a tube with a diameter of 3 millimeters. Once the tube was created, 6 needles were made using the pad and pocket function of the CAD software for distributing fuel to the vaporization tubes. The needles are a similar representation of t he real ones, further used for constructing the small turbojet. An image of the fuel ring is presented in figure 4.24.

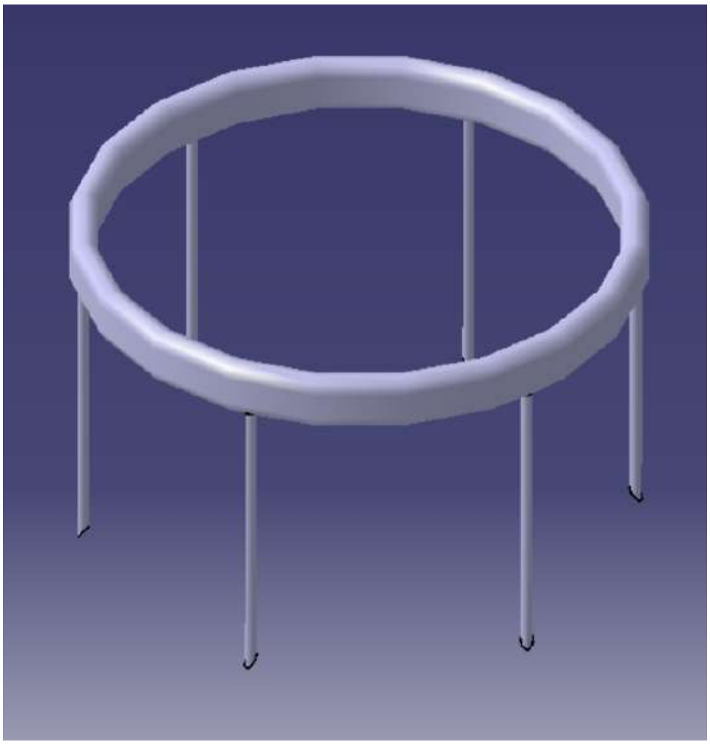

Figure 4.24: Fuel Ring

4.2.8 Nozzle Guide Vane System

This part was designed according to the NGV system observed from an online video [38]. This design was made as a single part rather than in different parts with an assembly. First, the base was created, where one end of the shaft housing will be fixed. The part t hat surrounds the base, and the guide vanes, was created through the use of the multi-section and removing solid function, in the sketch presented in figure 4.25.

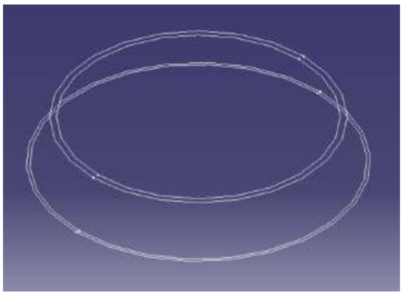

Figure 4.25: NGV system

The design of the turbine blades was similar to the design process of the compressor and turbine blades. The only alteration was in the planned positioning chosen to draw the sketch. There are two sketches: one is connected to the turbine's base, while the second i s connected to a washer. The washer is the final piece designed, positioned to be aligned with the surrounding top part of the NGV system. With the solid design, holes were made to allow the bolts to fix to the shaft housing, as well as the spacer at the turbine side. The end-piece is demonstrated in figure 4.26 and figure 4.27.

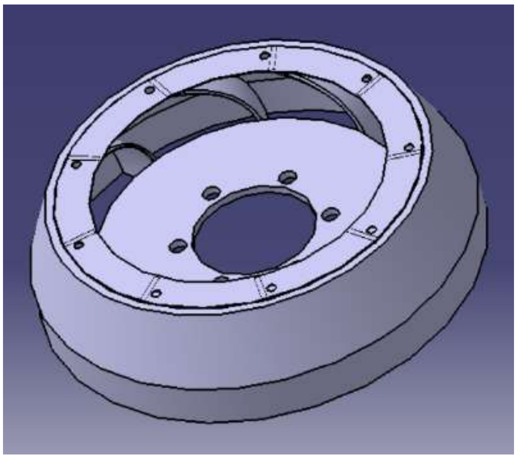

Figure 4.26: Nozzle Guide Vanes system view

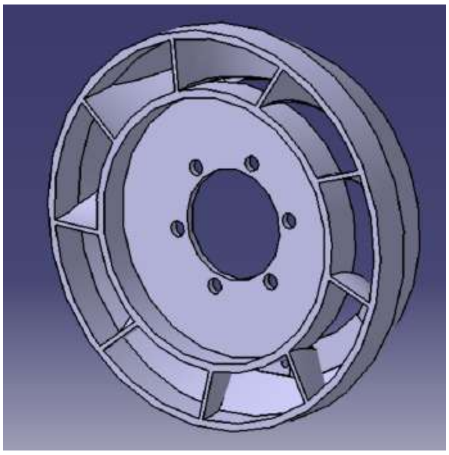

Figure 4.27: Nozzle Guide Vanes system view

4.2.9 Turbine

The procedure to attempt to reproduce the turbine of the turbo RHB31 VZ21 was similar to the compressor design. Firstly, a basis for the turbine vanes was designed, respecting the inducer diameter, as shown in figure 4.28. The second step was to design the sketch of the vanes from a visual perspective. The design of the vanes was divided into two sketches, addressing two different heights: the inducer blade height and exducer blade height, as demonstrated in figure 4.29.

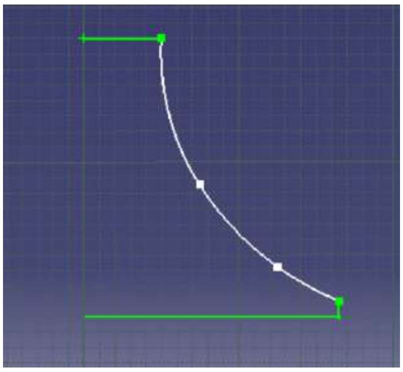

Figure 4.28: Turbine shaft operation sketch

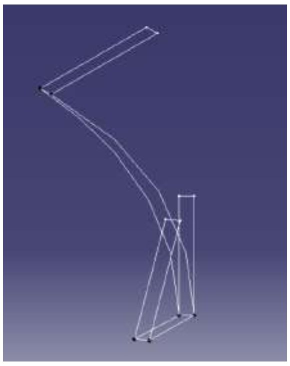

Figure 4.29: Turbine vane sketch

The design was concluded by using the shaft and multi-section solid function, in the respective order. The final product is illustrated in figure 4.30.

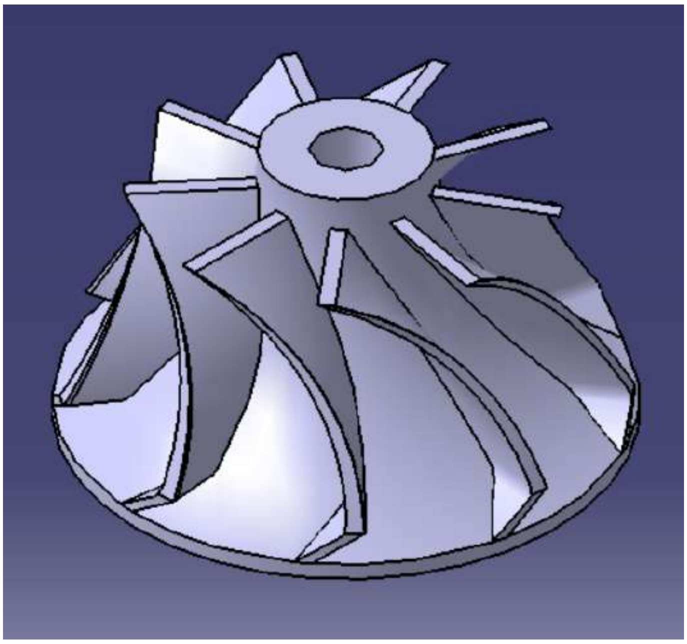

Figure 4.30: Turbine isometric view

4.2.10 Exhaust Nozzle, OuterCasing, and Bearings

The Turbine was measured from the exducer and inducer diameter, as well as the height of the blade, to design an Exhaust Nozzle based on the mentioned diameters and height, starting with sketches of the circumferences. This was followed by using the remove and multi-solid function, applied to the sketches shown in figure 4.31. Additionally, a round piece was added to the base of the Exhaust Nozzle to serve as a connector, allowing the bolts to pass through and secure the NGV system, Exhaust Nozzle, and Outer Casing together. The final product is illustrated in figure 4.32.

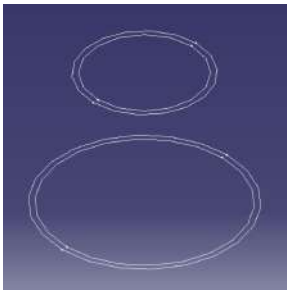

Figure 4.31: Exhaust Nozzle sketch

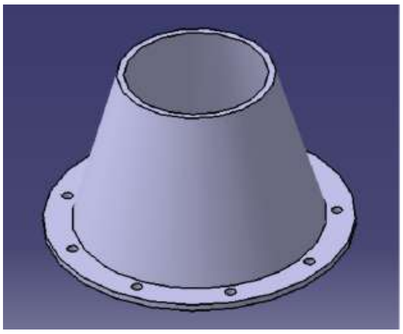

Figure 4.32: Exhaust Nozzle isometric view

The Outer Casing was the easiest component to design since it follows the same design procedure as the Combustion Chamber. It is demonstrated in figure 4.33.

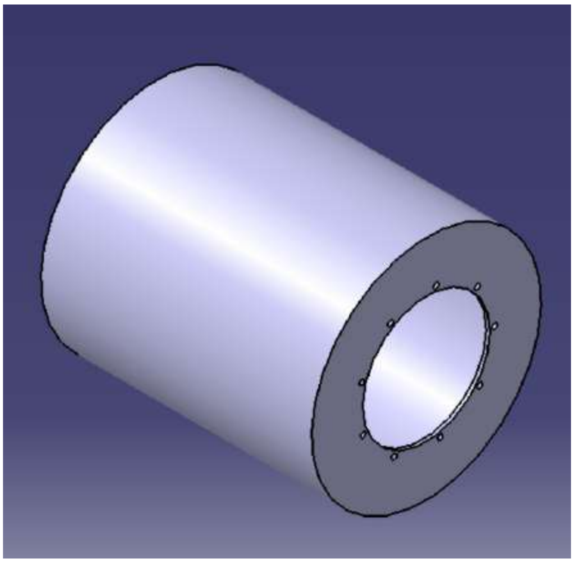

Figure 4.33: Outer casing isometric view

The final component, bearings, was designed according to the dimensions provided by SKF's company site for model 618/5 [39]. The first step was designing the rings surrounding the spheres, using the sketch described in figure 4.34 for a shaft operation. The next and final step was designing the spheres. This was also a design for a shaft operation applied to the sketch in figure 4.35, followed by a circular pattern that multiplies the spheres to nine, correctly positioned. The reproduction of Bearing 618/5 is displayed in figure 4.36.

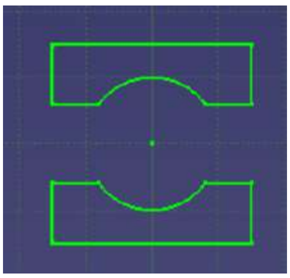

Figure 4.34: Bearing casing sketch

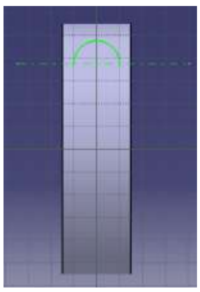

Figure 4.35: Bearing spheres sketch

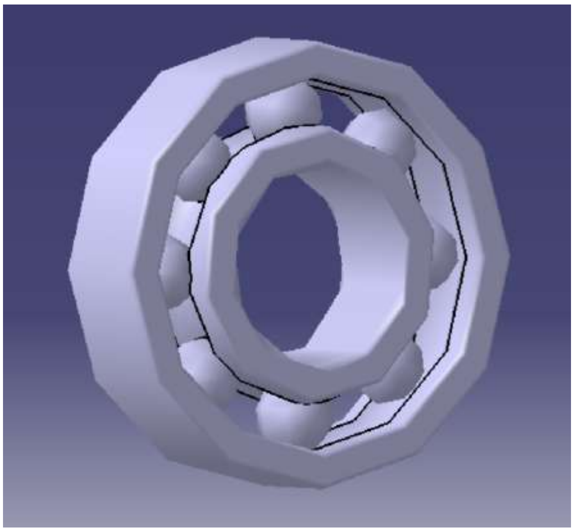

Figure 4.36: Bearing 618/5 example

4.3 Components Manufacturing

At this stage, with the concept design of the various components completed, the manufacturing process was initiated. This process involves a series of different machines and steps to produce the desired pieces. The raw material chosen for the majority of the components was stainless steel in sheet form, due to its physical properties such as resistance to corrosion, extreme temperatures, and high strength [41]. Additionally, the use of this material was frequently found in the reviewed literature as the material for certain components of small-scale turbojets. Another raw material chosen was cast aluminum, known for its lightweight, high strength-to-weight ratio, corrosion resistance, robustness, and ease of fabrication and assembly [42].

The production phase began by casting aluminum from the remains of an engine block that was available for use. The first step was to cut off enough aluminum for the casting process. Some pieces of steel scraps were cut and welded to make a cup for melting the aluminum, as well as to create molds and fill them after the aluminum forging was completed. For the forging, the furnace was heated as shown in figure 4.37, with a torch placed in the bottom hole. To achieve the lowest possible amount of impurities while the aluminum was being melted, sodium carbonate was applied. This chemical substance, when mixed with the aluminum in its liquid phase, pushes most of the material i mpurities to the top of the casting cup. However, this purification method is not completely efficient. Afterward, the cast aluminum was poured into the previously obtained steel molds. The molds were relatively simple to produce, consisting of thick, large, tubular steel with a base underneath. The molds were chosen with large dia meters to allow for the machining process. Once the aluminum cooled, it was extracted by cutting the molds with a grinding wheel. The cast aluminum is shown below in figure 4.38.

Figure 4.37: Furnace

Figure 4.38: Cast aluminum

The manufacturing process is organized into different sections, each categorized by the machining procedure used to manufacture the components, explaining how and what pieces were manufactured through the use of the corresponding process.

4.3.1 Shaping Process

The stainless steel was acquired from a metalwork shop in the form of a sheet with a thickness of one millimeter. The first attempt at working with the stainless steel sheet was with a thickness of 0.5mm, as recommended [29]. However, the sheet's thickness was insufficient for the necessary manufacturing methods to be applied, hence the choice of the one-millimeter sheet.

Firstly, the pieces were designed in their planar shape according to the dimensions, using CATIA V5. The draft or blueprint was created using a saving option that specifies the file format, .dxf. The .dxf file format is necessary for the software of the water jet cutter to read the delineated cuts to be made in the stainless steel sheet. A sample of pieces is shown below in figure 4.39.

Figure 4.39: Samples of the pieces cut with the water jet

The next step involved drilling the holes for the Combustion Chamber, followed by covering the two rectangular-shaped pieces at the left end of figure 4.39 with paper glue tape.

Lines and points were drawn on the paper glue tape using a ruler and set square. Once the positions for the drilling holes were marked, the holes were drilled with a vertical drilling machine, using borers with the following diameters in millimeters: 0.75, 1, 1.5, 2, 2.5, 3, 3.5. In the first attempt with the 0.5-millimeter sheet, it was possible to drill the holes, but the borers were too fragile due to their reduced thickness. Consequently, during the drilling process, the thinner borers broke, despite using appropriate techniques such as marking the holes on the sheet with a puncture for more stable and precise drilling. When the borer encountered resistance while drilling, oil was applied to assist the process. Even with careful drilling, due to the increased thickness to one millimeter, the diameter of the holes was changed to 2, 2.5, 3, and 3.5 millimeters. Figure 4.40 and 4.41 illustrate the method used to drill the two small sheets and the completed drills.

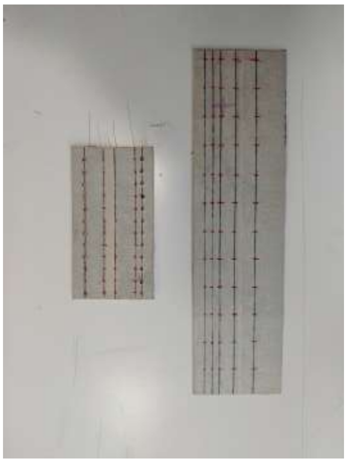

Figure 4.40: Holes pointed in the plain flame tubes

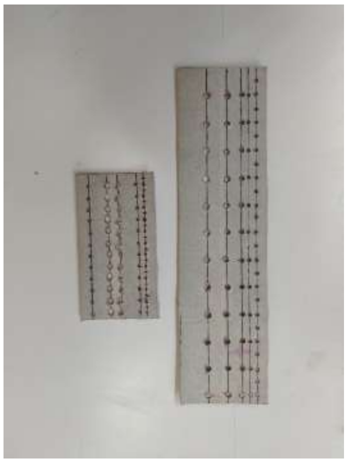

Figure 4.41: Plain flame tubes drilled

The parts made of stainless steel were molded using a wooden tapping block, which was wider than the pieces being worked on. This is necessary to ensure the piece forms evenly without folding. The pieces must be molded around a tube that is strong enough not to bend under the taps. The tube's diameter should be slightly smaller than the desired diameter; however, this technique is not entirely precise, which caused the pieces' diameters to differ from the designed component measurements. Before using a tapping block, a roller was used to form the pieces, but unfortunately, it was not possible to make the pieces round due to the sheet's thickness, which did not fit between the rollers. Below, the hand-shaped parts are demonstrated.

Figure 4.42: Exhaust Nozzle

Figure 4.43: Inner Flame

Figure 4.44: Outer Flame

Figure 4.45: Outer Casing Tube

4.3.2 Milling Process

Turbine

The next step was to dismantle the core of the turbocharger used for this thesis by detaching the compressor and the turbine from the shaft. The compressor was easily removed as it was only secured by a nut. On the other side of the shaft, the turbine was friction-welded to the shaft, which was removed along with the top nut from the turbine using a grinding wheel. Subsequently, the center of the turbine was drilled using a milling machine to achieve a well-executed drill to fit the designed shaft. Since the t urbine material is hardened, a drill bit was used to pierce the turbine from one end to the other, as illustrated in figure 4.46. However, due to ineffective methods chosen to drill t he turbine, the drill was not centered with the turbine, rendering future use of this turbine impossible, as using it at high speeds would turn the small gap into a large one, leading to a serious accident and compromising the safety of those around the turbine. The optimal drilling method would be to preserve the shaft attached to the turbine and fi x it in the correct placement on a lathe machine, ensuring the drill will be centered.

Figure 4.46: Turbine drilled

Nozzle Guide Vane system

The nozzle guide vane system was based on the procedure of an experienced person in making small model turbojets, found online at [38]. The surrounding parts of the NGV were cut and welded. However, to complete this system, blades were cut from another turbine, using a grinding wheel to individually separate the blades from the rotor. Later, some width of the blades was removed to fit between the surrounding parts and the turbine's base. The blades taken from the other turbine are shown in figure 4.47.

Figure 4.47: Blades of the nozzle guide vane system

The final step to fabricate this component was to weld the blades between the two metal pieces, as demonstrated in figure 4.48 and figure 4.49. Unfortunately, it was not possible to fix the blades in this component due to the welding technique, which released too much heat considering the size and thickness of the component.

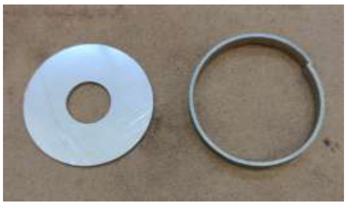

Figure 4.48: Turbine's base

Figure 4.49: Surrounding and upper part of the nozzle guide vane system

The washer in figure 4.48 is the turbine's base, which, along with the rectangular piece next to it, forms the inner part of the nozzle guide vane system, where a segment of the blades would be welded. Figure 4.49 illustrates the three external parts of the system: a lower part that surrounds the blades, a conic piece placed on top of the lower piece, and then the washer welded on the upper base of the conic piece.

4.3.3 Lathe Process

Aluminum

The aluminum components were processed differently from the other components. This material was machined using a lathe machine. The blueprints of the aluminum components were printed, and only then was the cast material machined. The blocks were placed in the lathe machine, where they were secured in the appropriate setting. Subsequently, the cast aluminum was machined, removing the necessary material to achieve the design with the correct shape and dimensions. However, it is extremely difficult to work the pieces and obtain an exact physical copy of the design, because it is not possible to know if the lathe machine is removing the right amount of material, even with the utmost caution while working with it. The components worked on with the lathe machine were the shaft housing and the inlet flange, as indicated in figure 4.50 and figure 4.51, respectively. The compressor shroud and diffuser were intended to be made in the vertical machining center at UBI's FABLAB. Unfortunately, it was not possible to produce these two pieces due to their small-scale dimensions, which require extremely precise machinery.

Figure 4.50: Shaft Housing

 

Figure 4.51: Inlet Flange

Stainless steel

Another piece worked on with the lathe machine was the shaft. This component is made from a stainless-steel solid cylinder, which was machined according to the dimensions obtained for the shaft manufacture. However, the recommended material is a steel scre w with a tensile grade of 12.9 or 10.6 because this component must withstand immense tension when the turbine and compressor are operating [29]. Figure 4.52 represents the shaft obtained after the described manufacturing process.

Figure 4.52: Shaft

4.3.4 Brazing Process

The ring support was drilled six times, with the positions of the holes marked using a transfer and a puncture. Subsequently, a three-millimeter drill was used so the vaporization tubes could fit within the holes. These tubes were cut from stainless steel with a diameter of three millimeters. The small tubes were brazed to the fuel ring s upport for the subsequent placement of the fuel ring distributor, as shown in figure 4.53. The distributor is made from the same tube as the vaporization tubes, which had to be shaped into a small circle to fit in the ring support. A steel wire was inserted along the entire length of the tube to prevent it from creasing, which would compromise an even distribution of fuel. The methods used to shape the tube were applied with extreme caution to avoid creasing. Despite the caution taken while working with the tube, it could not be molded to the appropriate dimensions, as shown in figure 4.54.

 

Figure 4.53: Fuel ring support

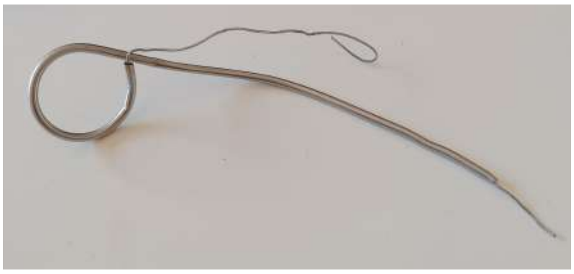

Figure 4.54: Fuel ring

4.3.5 Welding Process

Both ends of the molded pieces were welded, and during this process, only some were shaped into their final form. The type of welding used was Gas Tungsten Arc Welding or TIG. The welding process was one of the reasons for choosing a thicker stainless-steel sheet. There was a risk that the heat from the welding could melt parts of the pieces, which was more likely with a thinner sheet. However, even with increased thickness, it was only possible to weld the components shown in the figures below. The remaining components could not be welded because both ends of the pieces had to be joined without any air gaps. Sandpaper was used on the ends of the pieces to wear down uneven parts and prevent air gaps when joining the ends. Nonetheless, it was not f easible to weld all the pieces, as demonstrated.

Welded pieces:

Figure 4.55: Exhaust Nozzle

Figure 4.56: Outer Casing

Figure 4.57: Inner Flame Tube Front View

Figure 4.58: Inner Flame Tube Back View

Figure 4.59: Outer Flame Tube

Figure 4.60: Nozzle Guide Vane external parts

Figure 4.61: Internal part of the nozzle guide vane system

Chapter 5

Conclusion

This thesis primarily aimed to build a small turbojet engine, beginning with a study of the turbojet's components and working cycle. Studying the jet engine was already a c hallenge due to the vast amount of information available, making it difficult to deter mine the most important concepts one should understand before developing a turbojet.

This dissertation provided the author with the opportunity to learn part of the science behind this engine, as well as the practical knowledge of how to build a turbojet, which is not something learned every day and certainly not possible to learn in a classroom. This dissertation achieved one of the two proposed objectives. The design was completed, with an explanation provided so that future work could be based on the steps taken. Unfortunately, the construction of this engine was not accomplished due to a lack of means to proceed with adequate manufacturing.

5.1 Drawbacks

The design of this project was primarily based on Thomas Kamps' book [29] , and the author is grateful for its existence. Information on how to build a turbojet, especially with a radial compressor/turbine set, was not available except in the books by Kurt Shreckling and the aforementioned author. However, their engines did not involve a radial turbine, but an axial one. These two books provide detailed descriptions of the manufacturing process of a turbojet engine, with all procedures explicitly outlined. Since this engine is based on empirical data, the dimensions are not definitive, and one cannot be certain if the engine has the proper dimensions for the given compressor. Only with experience in modeling jet engines and testing them can one ensure that the dimensions of the components allow the engine to operate without issues.

Throughout the experimental phase, many obstacles were encountered in the attempt to build this turbojet. The first was the increased thickness of the stainless steel sheet. This had a significant impact on the manufacturing of the pieces, as it made it more difficult t o hand-shape them, making it impossible to adjust them to the appropriate dimensions of the designed components. As a consequence of the sheet's thickness, a roller could not be used. This would have been extremely helpful due to the more accurate process of rolling the pieces, as well as facilitating the welding, since using a roller would result in consistent, aligned pieces.

Regarding the welding process, the most critical obstacle could not be adequately addressed because the technique previously mentioned in chapter 4.3 did not allow the pieces to be positioned as desired, preventing the achievement of the main goal of this thesis. Despite the technique, the size of the pieces required extraordinary manufacturing precision, which was really difficult for a beginner in experimental tasks to achieve.

5.2 Futureworks and recommendations

Further work based on this dissertation can be developed due to the wide range of themes the turbojet involves. Since the manufacture of this engine was not completed, the first possible task could be the finalization of this project. If possible, a stereolithographic file of the compressor should be generated for an accurate design of the compressor shroud, respecting the compressor's curvature, which is an important factor for efficient air induction, and thus, compression and engine functioning.

For the testing of the engine, the author recommends a shaft calibration, if possible. Additionally, an axial turbine should be developed for this type of engine. It would facilitate the manufacturing process, such as the production of the nozzle guide vanes system.

The future works following this dissertation could be:

- Finish the development of this engine with the appropriate techniques.
- Study and fabrication of an axial turbine to match the compressor.
- Conduct a computational fluid dynamics study of the jet engine's airflow and i dentify potential improvements in the designed components.
- Develop a testing workbench.

Bibliography

[1] Turkay Mehmet, Gurgen Selim, Keskin Goksel, Durmus Seyhun, Kushan Melih Ce- mal. Research on applications of mini-turbojet and turbojet engined military UAVS. In: The 21st Edition of the International Conference AFASES; 2019 May; Basov, Romania. v, vii, 1

[2] ”History of Flight” [Online]. Available at: https://www.grc.nasa.gov/WWW/K-12/UEET/StudentSite/historyofflight.html (accessed in 2019-03). 1

[3] ”Speed of Sound” [Online]. Available at: https://www.grc.nasa.gov/www/k-12/airplane/sound.html (accessed on 2019-03). 1

[4] “Hero of Alexandria Invented the Steam Engine” [Online]. Available at: https://www.greekboston.com/culture/inventions/steam-engine/ (accessed at 2019-03).

[5] ”Aeolipile” [Online]. Available at: https://en.wikipedia.org/wiki/Aeolipile (accessed at 2019-03). xi, 3[6] Hünecke Klause,*Jet Engines: Fundamentals of Theory*,*DesignandOperation*, 6th Edition, Motorbooks International, 2003. xi, 3, 4, 5, 6, 7, 8, 18, 19, 21, 22, 23, 24, 25, 26, 27, 29[7] ”Newton’s Laws of Motion” [Online]. Available at: https://www.grc.nasa.gov/www/k-12/airplane/newton.ht ml (accessed at 2019-03). 3[8] Rolls Royce plc, *The Jet Engine*, 5th Edition, Rolls Royce plc, 1996. xi, 4, 5, 7, 8, 19, 20, 21, 22, 23, 24, 25, 26, 27[9] ”Kurt Shreckling” [Online]. Available at: https://en.wikipedia.org/wiki/Kurt_Schreckling (accessed at 2019-03). 4[10] Shreckling Kurt, *Gas TurbinesFor Model Aircraft*, 5th Edition, Traplet Publications, 2003. 4, 30[11] El-Sayed Ahmed F., *Fundamentalsof Aircraft and Rocket Propulsion*, Springer, pp 531-588, 2016. xi, 6, 15, 16, 17, 18[12] Chen Min, Zhang Kun, Tang Hai-Long, A Probabilistic Design Methodology for a Turboshaft Engine Overall Performance Analysis, Advances in Mechanical Engineering, 2014;1(12), doi: 10.1155/2014/976853, May 2014. xi, 6[13] C. Weston Kenneth, *Energy Conversion*, Electronic Edition, 2000. 8[14] Çengel Yunus A., Boles, Michael A., *Thermodynamics*, *An Engineering Approach*, 8th Edition, McGraw-Hill Education, 2015. xi, 9, 10, 11[15] ”Ideal Brayton Cycle” [Online]. Available at: https://www.grc.nasa.gov/www/k-12/airplane/brayton.html. (accessed at 2019-03). 10

[16] ”Brayton Cycle” [Online]. Available at: https://web.mit.edu/16.unified/www/FALL/thermodynamics/notes/node28.htm l.

(accessed at 2019-03). xi, 11, 12[17] C. Oates Gordon, *Aerothermodynamics of Gas Turbinesand Rocket Propulsion*, 3rd Edition, American Institute of Aeronautics and Astronautics, Inc., Seattle, Washington, 1998. 12, 14, 15, 20, 21, 23[18] Fahlstrom Simon, Pihl-Roos Rikard, *DesignandConstructionof a simple turbojetengine* [MSc Thesis],Uppsala University, 2016.[19] ”Inlet Performance”. Available at: https://www.grc.nasa.gov/WWW/K-12/airplane/inleth.html. (accessed at 2019-04). 13[20] ”Compressor Thermodynamics” [Online]. Available at: https://www.grc.nasa.gov/WWW/K-12/airplane/compth.html. (accessed at 2019-04). 13[21] ”Burner Thermodynamics” [Online]. Available at: https://www.grc.nasa.gov/WWW/K-12/airplane/burnth.html. (accessed at 2019-04). 13, 14

[22] “Fuel Mass Flow Rate” [Online]. Available at: https://www.grc.nasa.gov/WWW/K-12/airplane/fuelfl.html. (accessed in 2019-04). 14

[23] ”TurbineThermodynamics” [Online]. Available at: https://www.grc.nasa.gov/WWW/K-12/airplane/powtrbth.html. (accessed at 2019-04). 14

[24] ”Nozzle Performance” [Online]. Available at: https://www.grc.nasa.gov/WWW/K-12/airplane/nozzleh.html. (accessed at 2019-04). 15

[25] “Mach Number” [Online]. Available at: https://www.grc.nasa.gov/www/k-12/airplane/mach.html. (accessed in 2019-04). 18[26] “Inlets” [Online]. Available at: https://www.grc.nasa.gov/www/k-12/airplane/inlet.html. (accessed in 2019-04). xi, 19[27] Boyce Meherwan P., *Gas TurbineEngineering Handbook*, 2nd Edition, Gulf Professional Publishing, 2002. xi, xv, 20, 21, 28, 29[28] “Axial Compressor” [Online]. Available at: https://www.grc.nasa.gov/www/k-12/airplane/caxial.html. (accessed in 2019-04). 21[29] Kamps Thomas, *Model Jet Engines*, 3rd Edition, Traplet Publications, 2005. xi, xii, xv, 22, 23, 29, 30, 31, 35, 36, 37, 38, 39, 40, 45, 47, 55, 59, 63, 88

[30] Lin Jiangui, Balint Daniel, Pietrzyk Maciej, editors, Micostructure Evolution in Metal Forming Processes, Woodhead Publishing, pp.384-394 2012. Available from: Sciencdirect. 27[31] C.Lyons William, J.Plisgam Gary, D.Lorenz Michael, editors, Standard Handbook of Petroleum and Natural Gas Engineering, 3rd Edition, 2016. 29[32] "History of the exhaust gas driven turbocharger" [Online]. Available at: https://en.turbolader.net/Technology/History.aspx. (accessed in 2019-05). xi, 31, 32[33] Tsei Lauren, Design and Performance of a Gas-Turbine Engine from an Automobile Turbocharger [BEng], Massachusetts Institute of Technology, May-2004. 32, 33[34] "Turbo Tech 103| Expert: Compressor Mapping" [Online]. Available at: https://www.garrettmotion.com/wp-content/uploads/2019/10/GAM_Turbo-Tech-103_ Expert-1.pdf. (accessed in 2019-05). xi, 33[35] "Turbo Tech 103| Expert: Compressor Mapping" [Online]. Available at: https://www.marineinsight.com/main-engine/what-is-turbocharger-surging/. (accessed in 2019-05). xi, 32[36] "Turbocharger Technical Spec" [Online]. Available at: https://www.ecotrons.com/files/ECOTRONS%20Turbo%20VZ21%20-technical%20specl.pdf. (accessed in 2019-05). xi, xv, 33, 34, 35, 87[37] Alonzo Daniel, Crocker Alex, James Eric, Kingston III John, Design and Manufacturing of a Miniature Turbojet Engine [BSc], Worcester Polytechnics Institute, 2018-03. 35[38] " From the construction of the Turbo Jet engine to the flight - just one step"[Online]. Available at: https://www.youtube.com/watch?v=dYFYZ-g7fzA. (accessed in 2019-06). 39, 51, 57[39] "Deepgroove Ball Bearings SKF 618/5" [Online]. Available at:
https://www.skf.com/pt/products/bearings-units-housings/ball-bearings/deep-groove-ball-bearings/deep-groove-ball-bearings/index.html?designation=618/5. (accessed in 2019-10). 39, 53[40] Rolling Bearings for Industrial Machinery, NSK Motion & Control, 2016 39[41] "Stainless Steels - Specifications, Grades and Propertie" [Online]. Available at: https://www.azom.com/article.aspx?ArticleID=2874. (accessed in 2020-01). 54[42] "Aluminum and Aluminum Alloys - Characteristic Advantages and Beneficial Properties of Aluminum Extrusions" [Online]. Available at: https://www.azom.com/article.aspx?ArticleID=4192. (accessed in 2020-01). 54

Appendixes

Appendix A - Part List

Table 1: Part List

Part No.	Description	No. Off	Material/Type	Blank Dimensions/Notes
1	Compressor Shroud	0	Aluminium	
2	Compressor Wheel	1	Cast Aluminium	Possible alloys: Al-Si-Cu-Mg
3	Diffuser	0	Aluminium	
4	Spacer Disk	2	Stainless Steel/Aluminium	
5	Bearing	2	618/5	Deep groove ball bearings
6	Engine shaft	1	Stainless Steel	Turned
7	Shaft Tunnel	1	ALuminium	Turned
8	Combustion Camber	1	Stainless Steel	TIG Welding
8.1	Outer section	1	Stainless Steel	Sheet, 1mm thick
8.2	Inner section	1	Stainless Steel	Sheet, 1mm thick
8.3	Front Section	1	Stainless Steel	Sheet, 1mm thick
8.4	Rear Section	1	Stainless Steel	Sheet, 1mm thick
8.5	Fuel Ring Support	1	Stainless Steel	Sheet, 1mm thick
8.6	Vaporization Tubes	6	Stainless Steel	ø3 mm tube
9	Injector Ring	1	Stainless Steel	Soldered
9.1	Injector Ring	1	Stainless Steel	ø3 mm tube
9.2	Injector Needle	6	Syring needle	ø0,8 mm
10	Turbine NGV	1	Stainless Steel, Cast Aluminium	Possible alloys: Al-Si-Cu-Mg
10.1	Turbine's base	1	Stainless Steel	Sheet, 1mm thick
10.2	Blades	9	Cast Aluminium	Possible alloys: Al-Si-Cu-Mg
10.3	Blade jacket	1	Stainless Steel	Sheet, 1mm thick
10.4	Turbine jacket	1	Stainless Steel	Sheet, 1mm thick
11	Turbine	1	Cast Alumium	Possible alloys: Al-Si-Cu-Mg
12	Exhaust Nozzle	1	Stainless Steel	Sheet, 1mm thick
12.1	Washer	1	Stainless Steel	Sheet, 1mm thick
13	Casing	1	Stainless Steel	Sheet, 1mm thick
13.1	Casing Rear Section	1	Stainless Steel	Sheet, 1mm thick
14	Inlet Flange	1	Aluminium	Turned
16	Pre-Load Spring	1	Steel	
17	Sleeve	1	Stainless Steel	Sheet, 1mm thick, welded

Appendix B - 2D Draws of the turbojet’s components

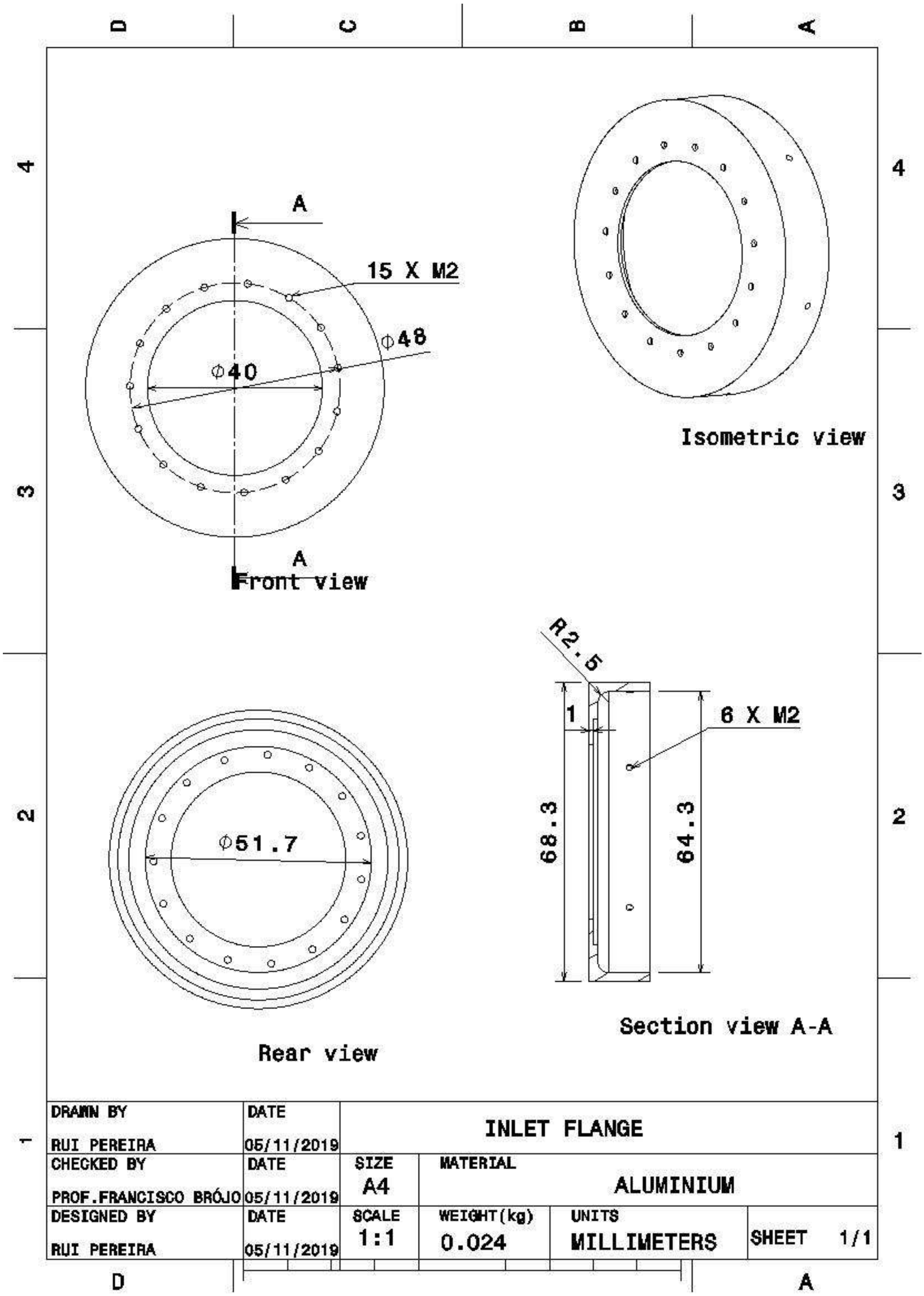

Figure B.1: Inlet Flange

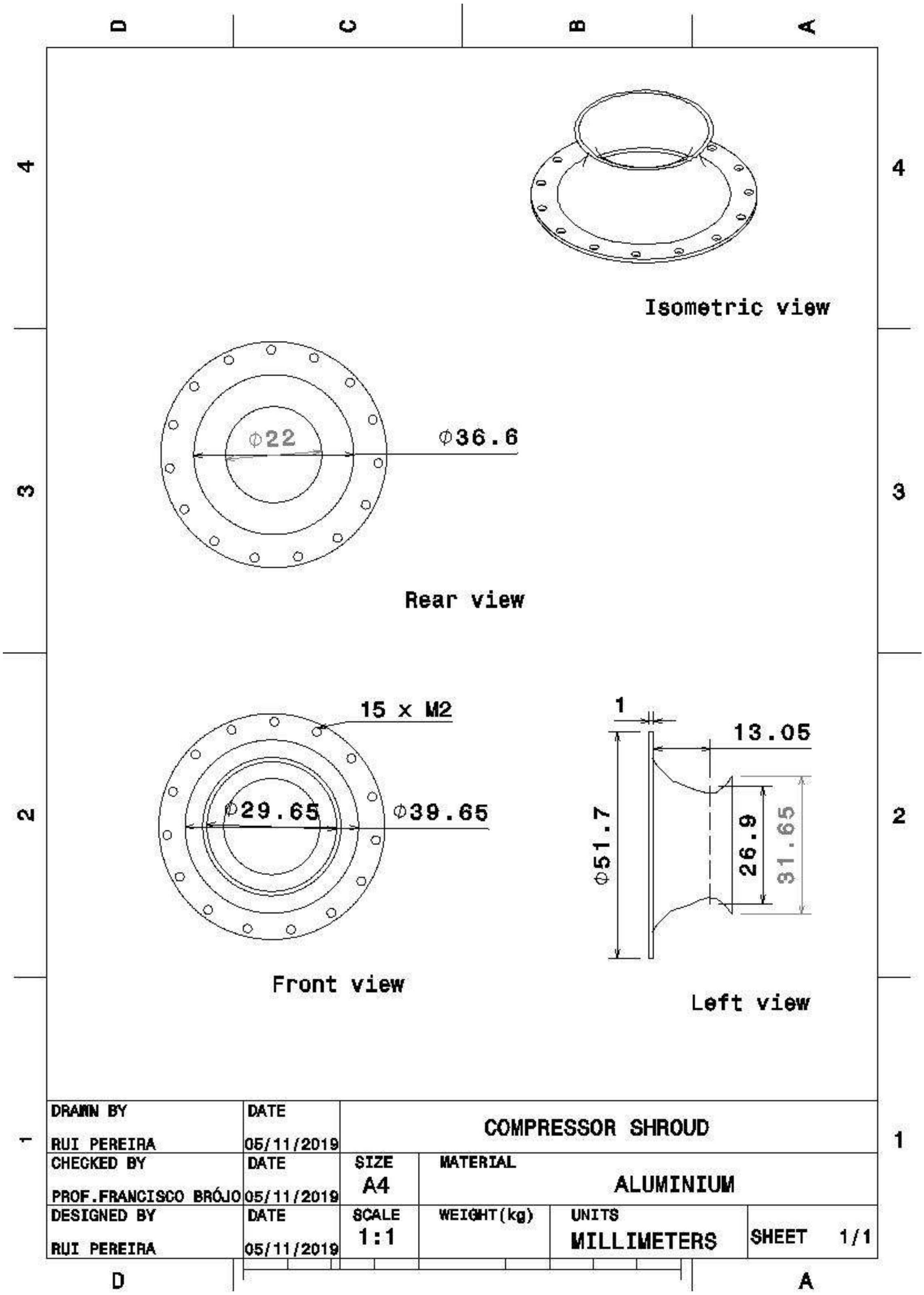

Figure B.2: Compressor Shroud

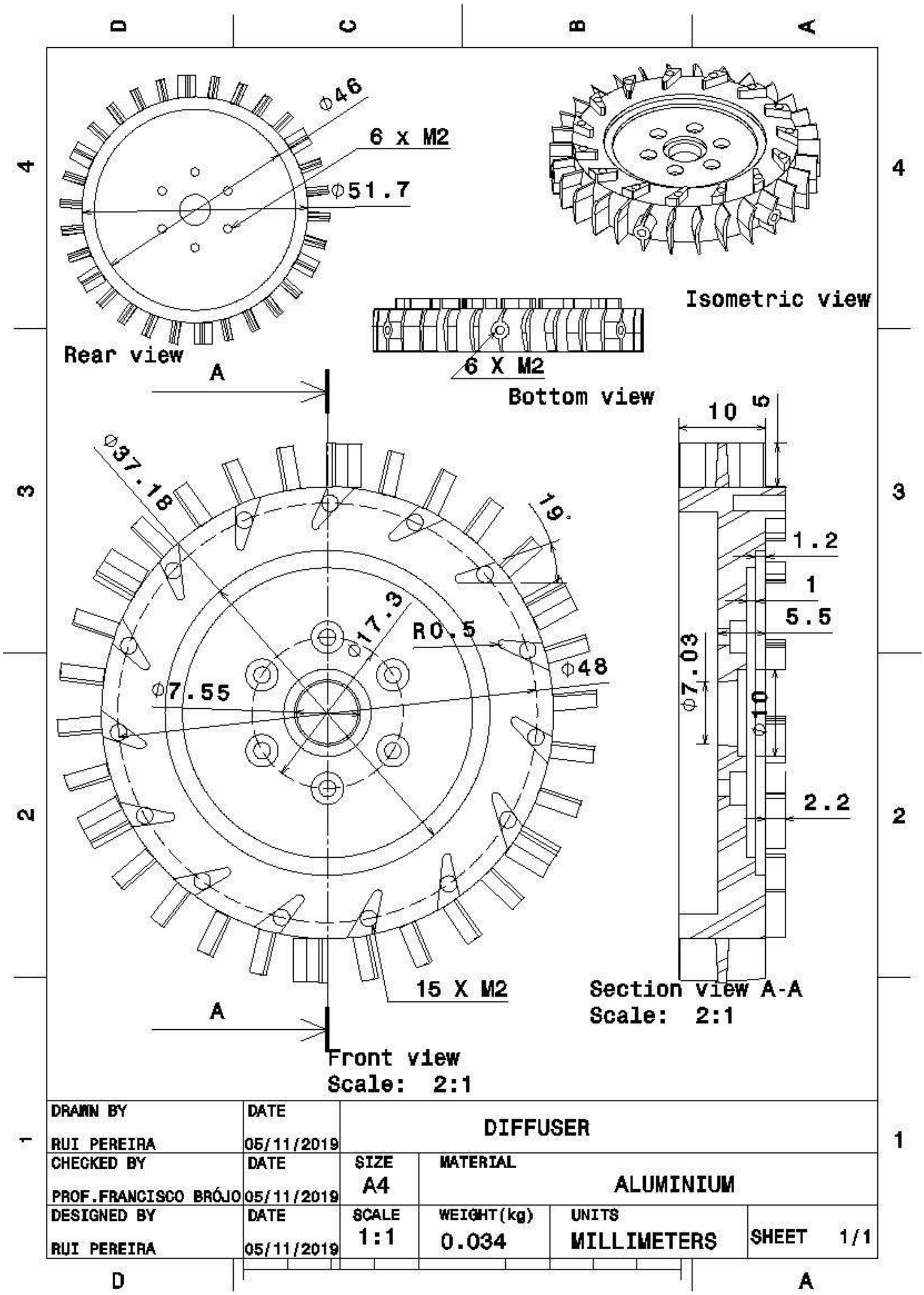

Figure B.3: Diffuser

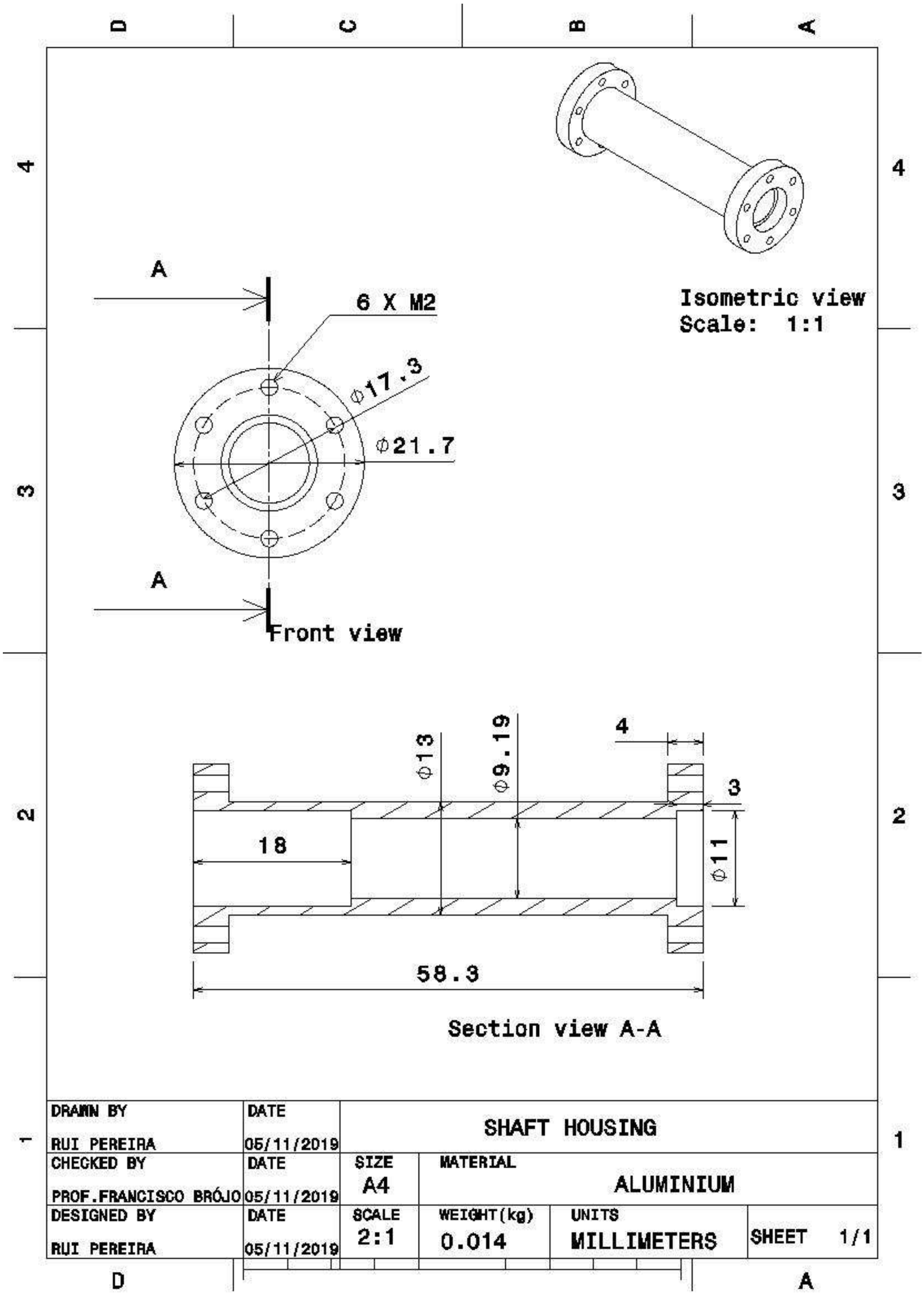

Figure B.4: Shaft Housing

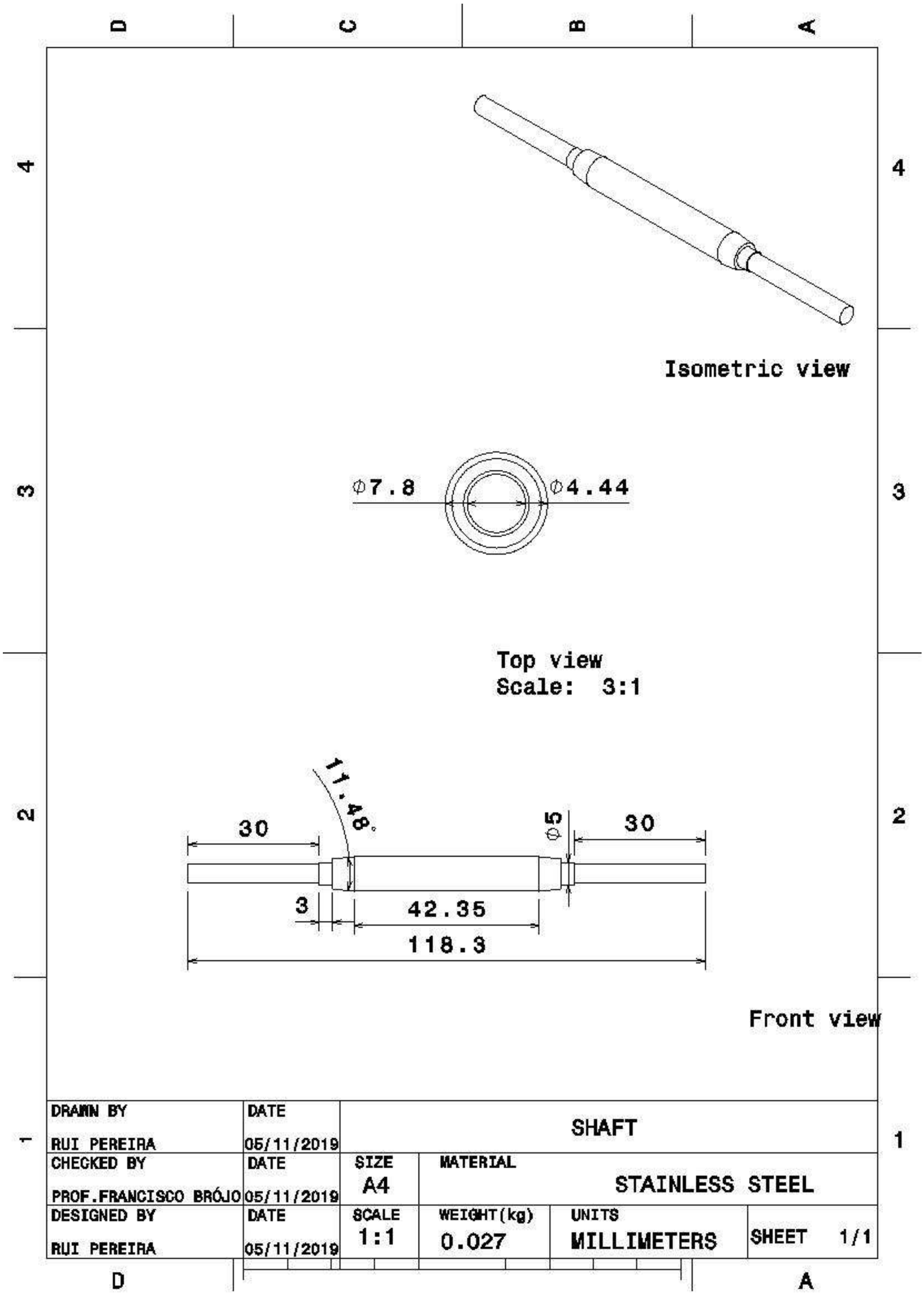

Figure B.5: Shaft

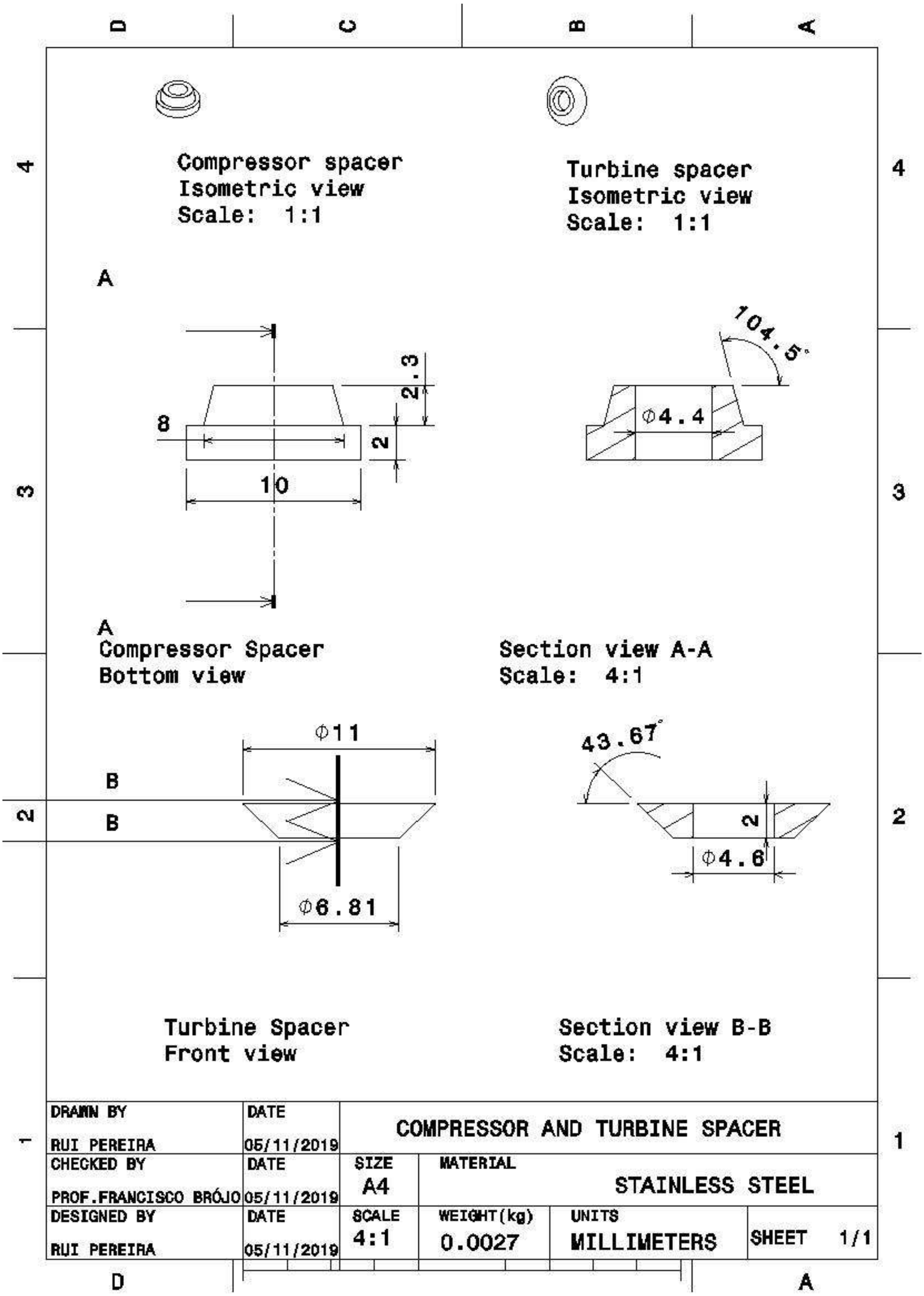

Figure B.6: Spacers

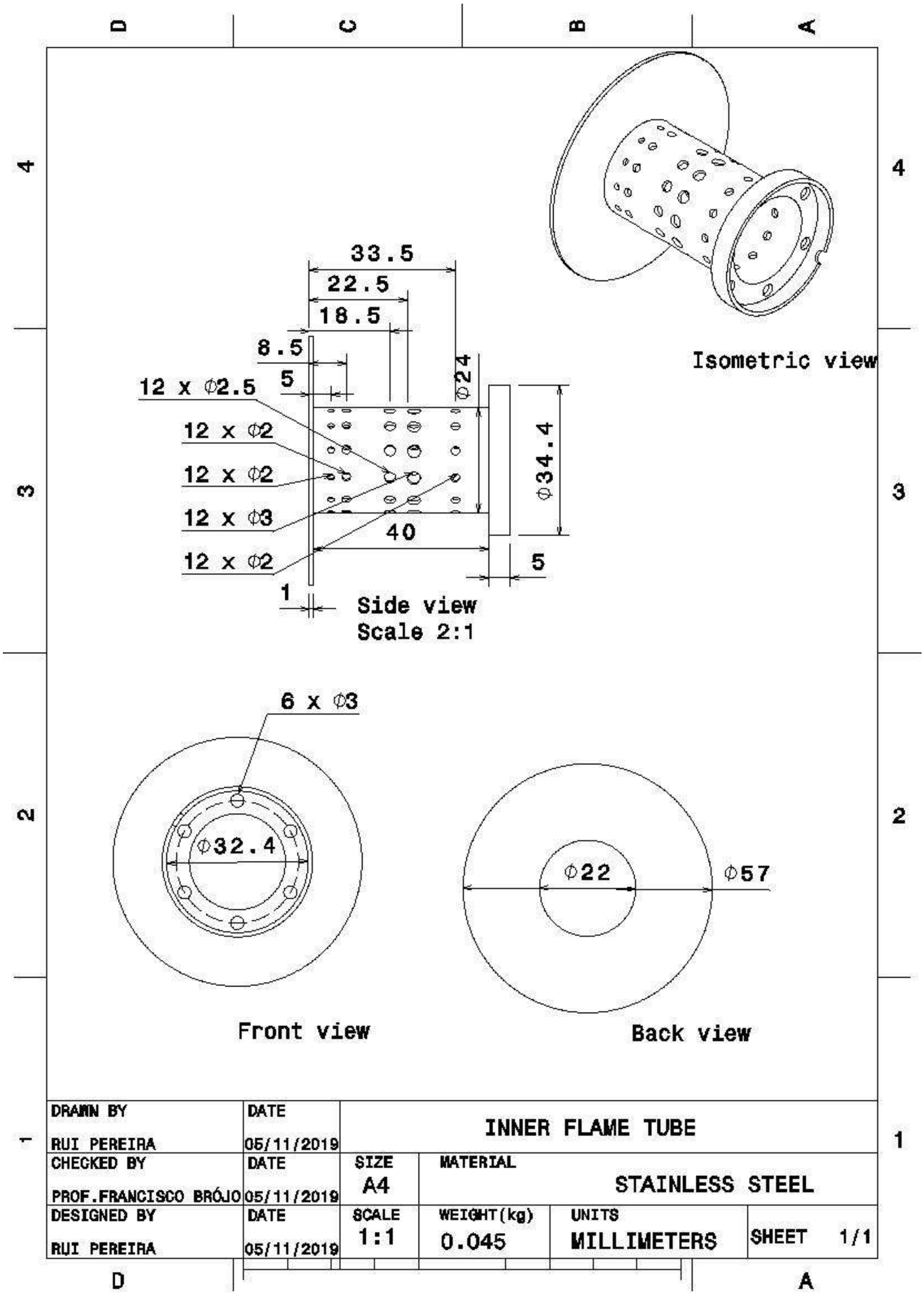

Figure B.7: Inner Flame Tube with fuel ring support

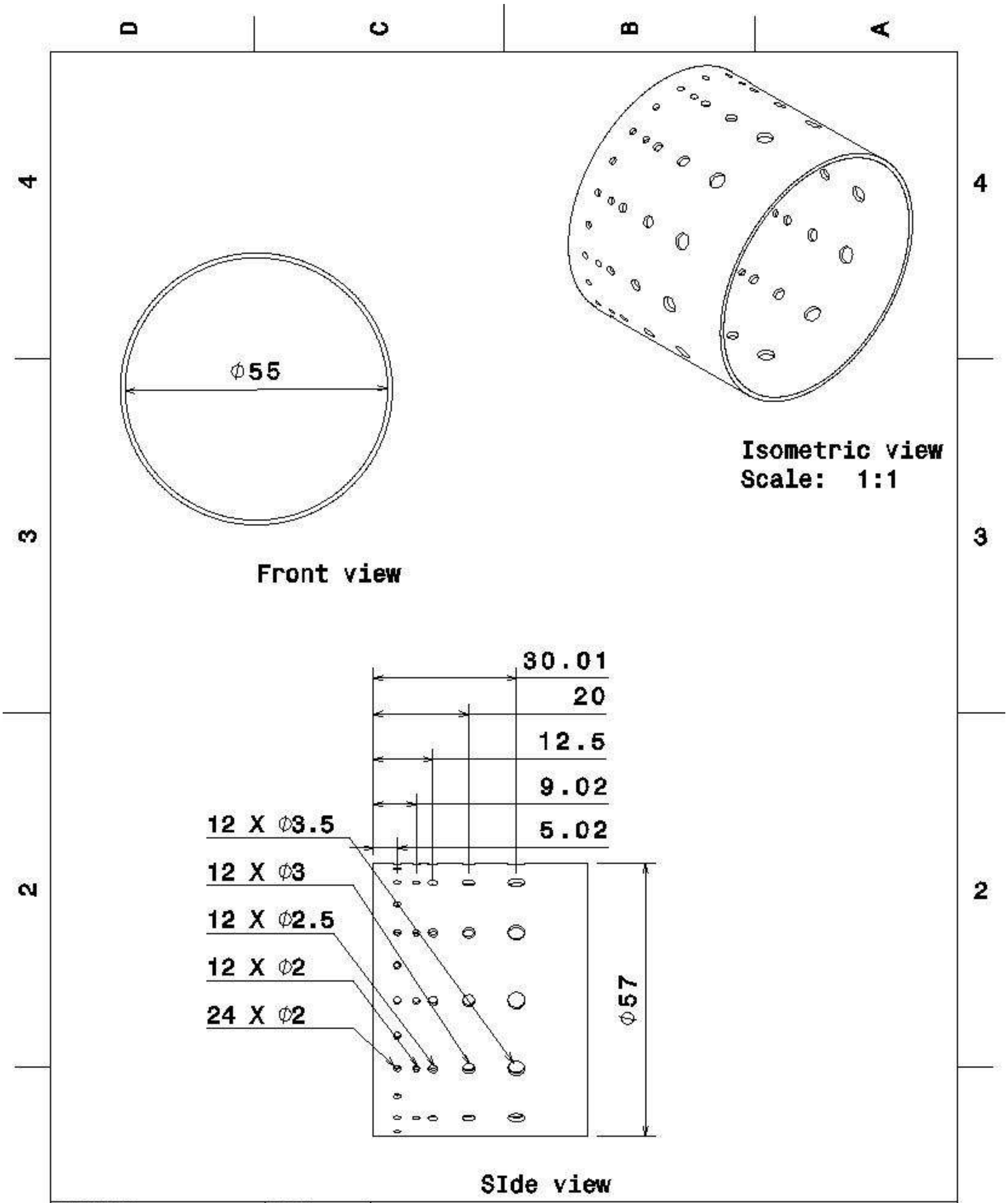

DRAWN BY RUI PEREIRA	DATE 05/11/2019	OUTER FLAME TUBE			
CHECKED BY PROF.FRANCISCO BRÓJO	DATE 05/11/2019	SIZE A4	MATERIAL STAINLESS STEEL		
DESIGNED BY RUI PEREIRA	DATE 05/11/2019	SCALE 1:1	WEIGHT(kg) 0.06	UNITS MILLIMETERS	SHEET 1/1

Figure B.8: Outer Flame Tube

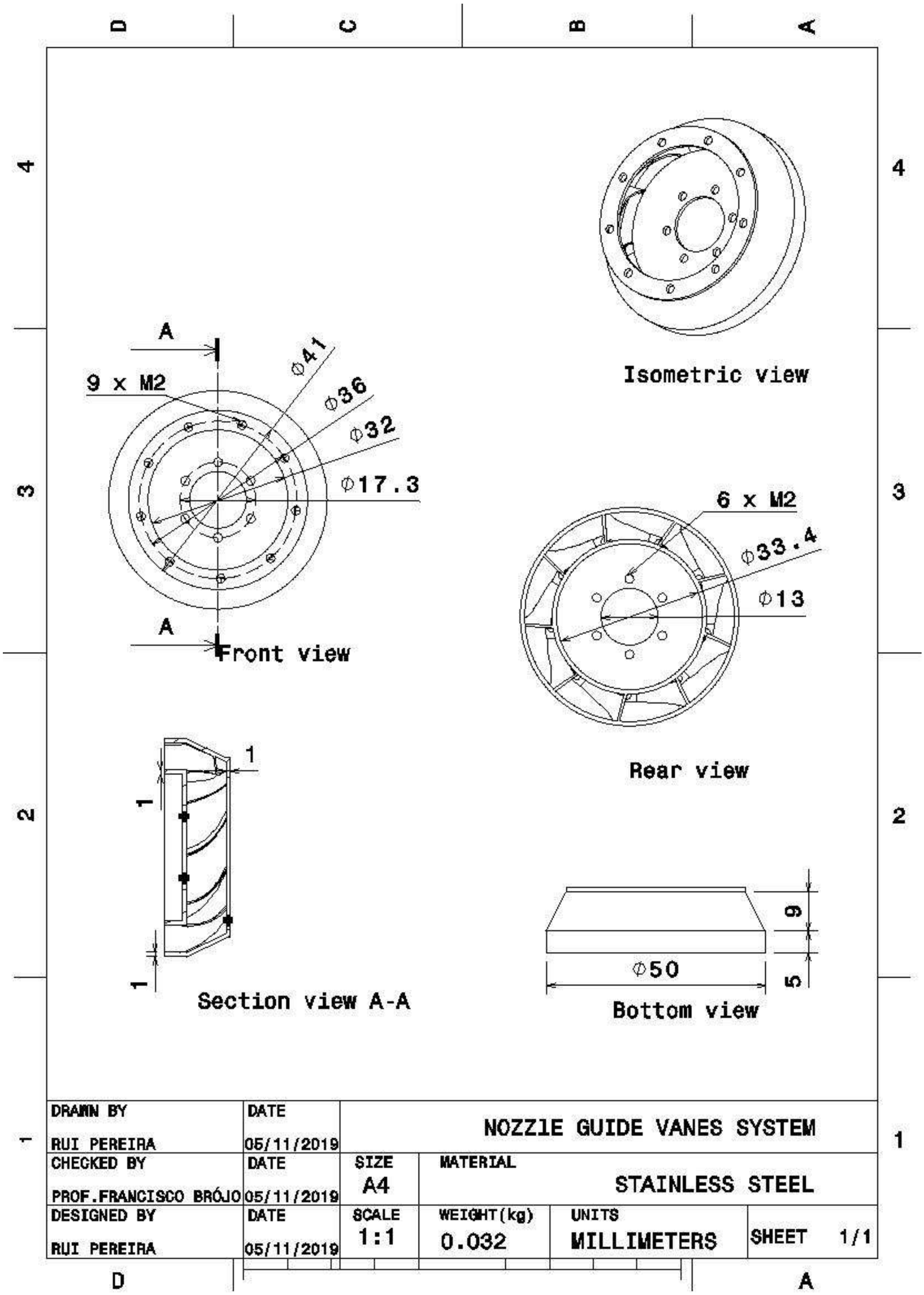

Figure B.9: Nozzle Guide Vane system

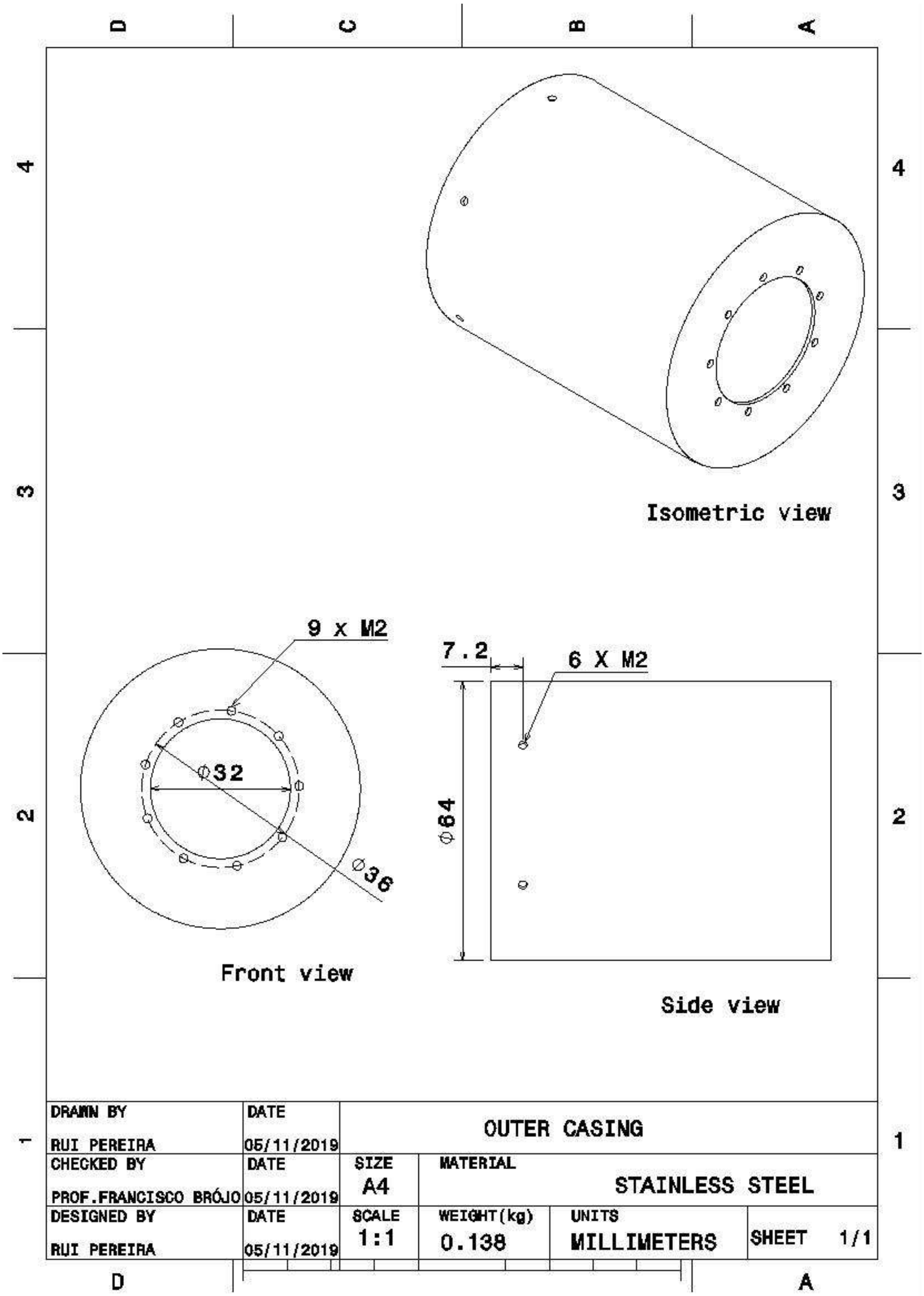

Figure B.10: Outer Casing

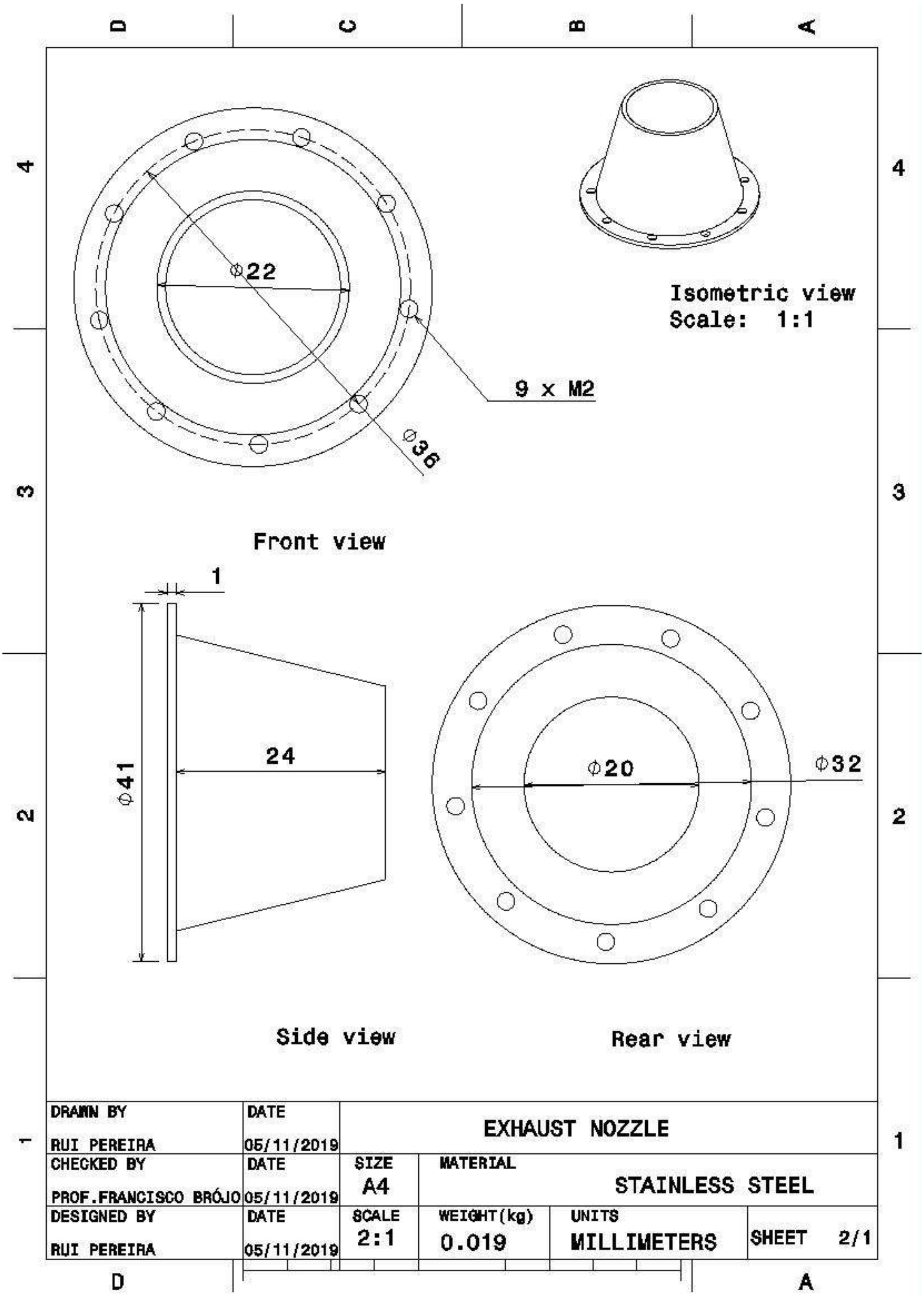

Figure B.11: Exhaust Nozzle

Appendix C - 2D, 3D Views of the turbojet

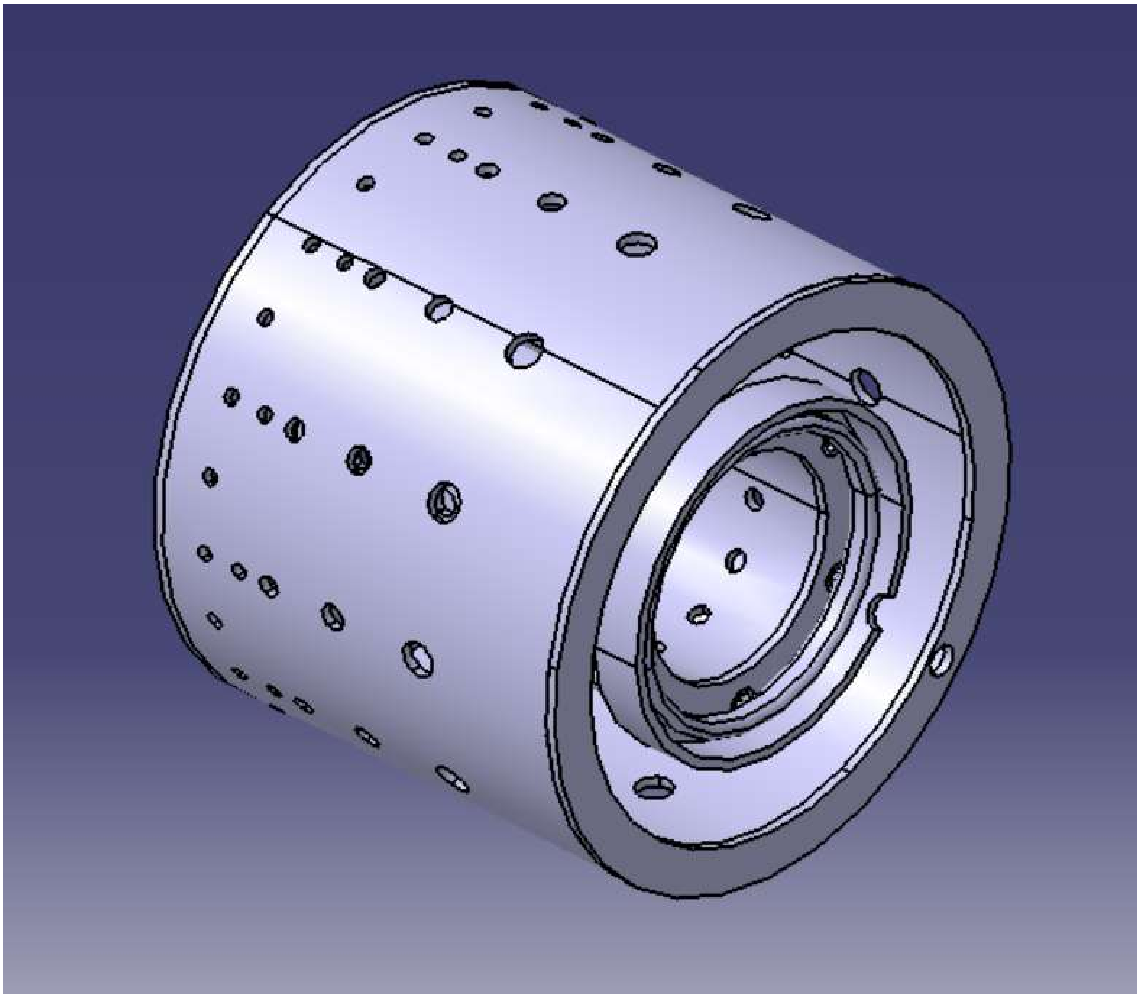

Figure C.1: “Combustion Chamber”

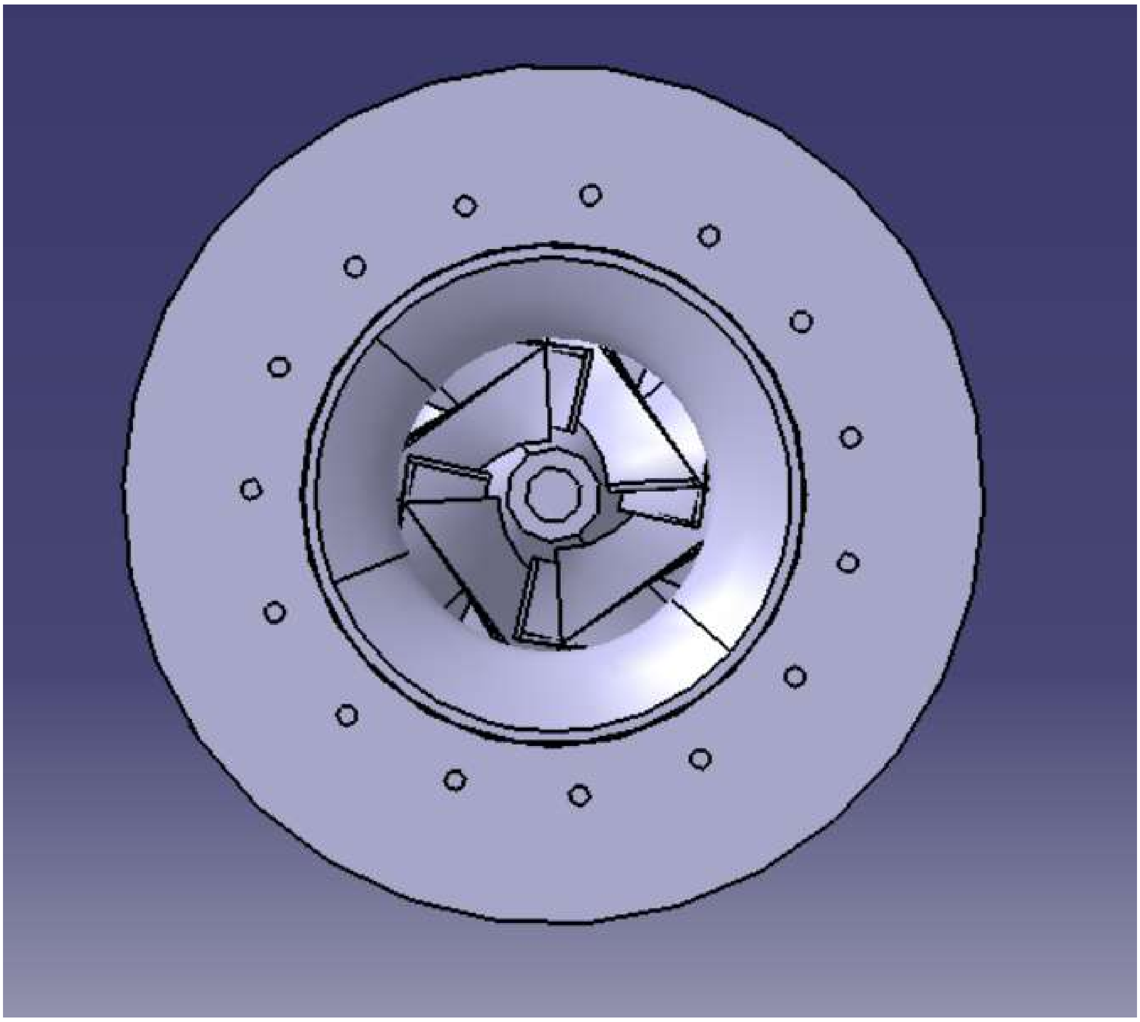

Figure C.2: "Turbojet Front View"

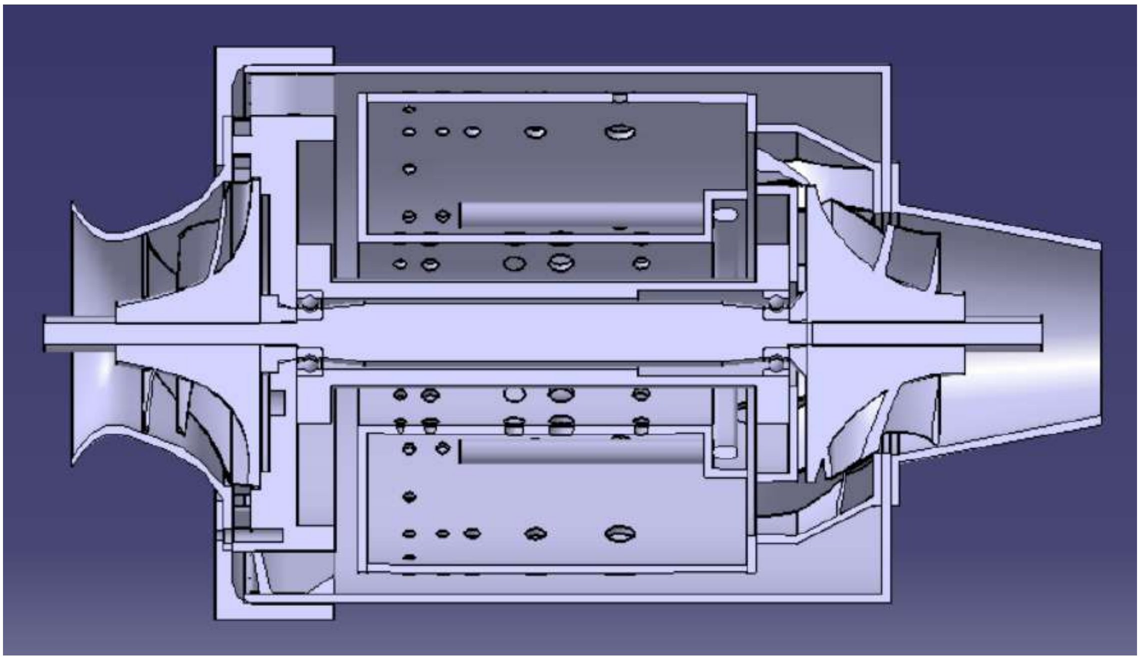

Figure C.3: "Turbojet Midsection View"

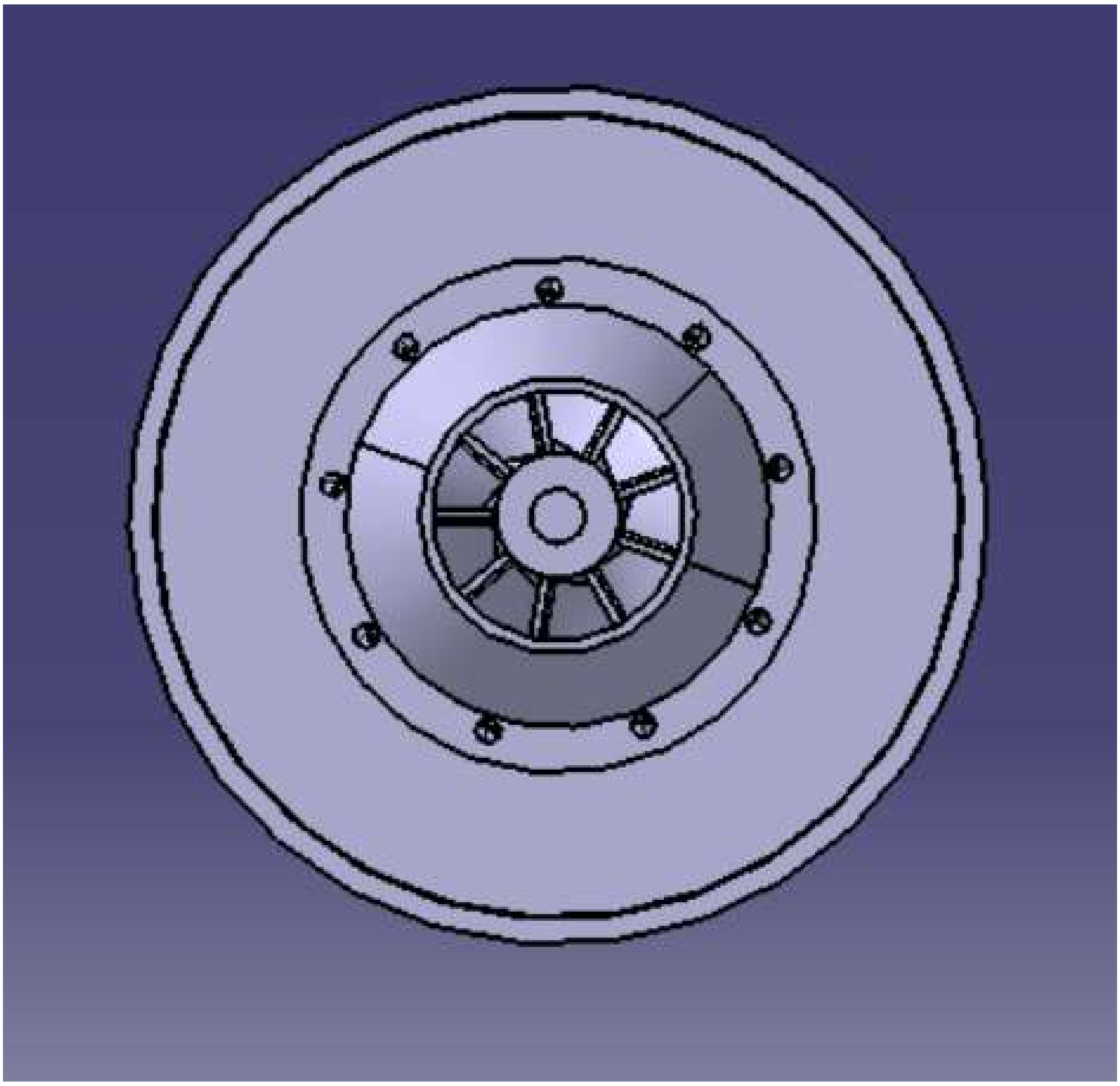

Figure C.4: "Turbojet Back View"

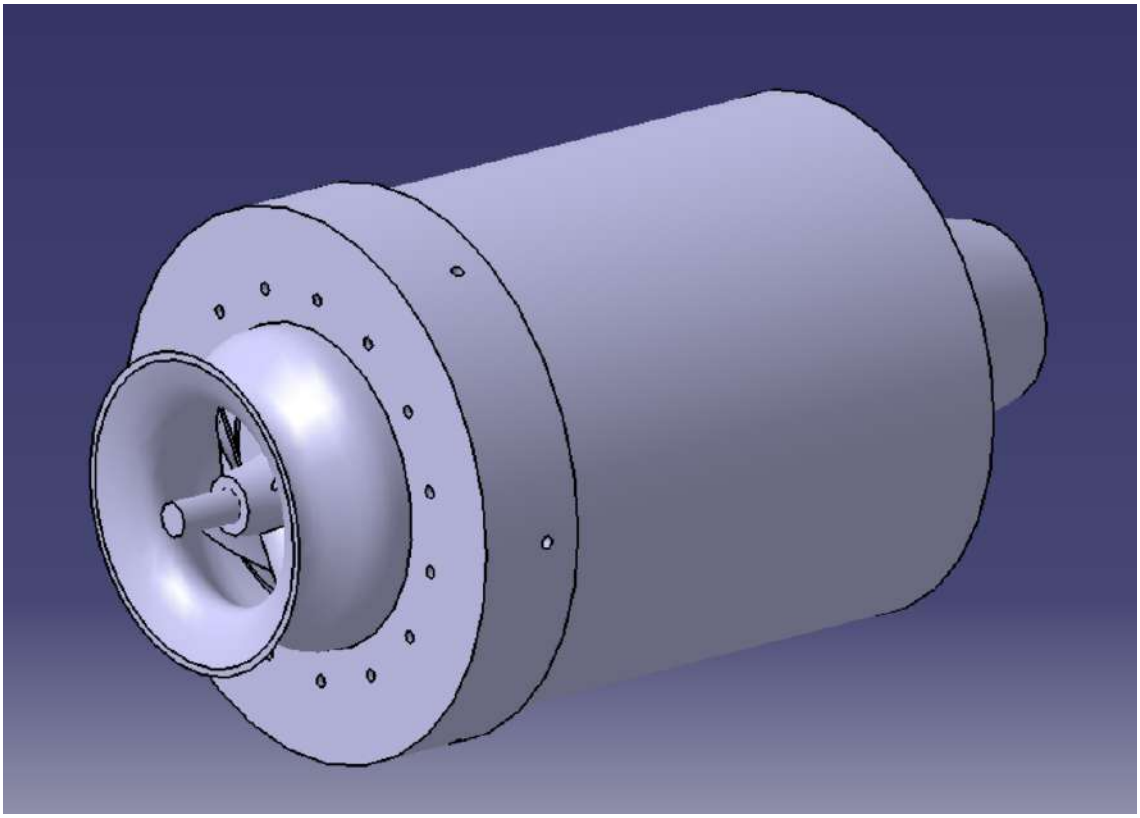

Figure C.5: “Turbojet isometric 3D view 1”

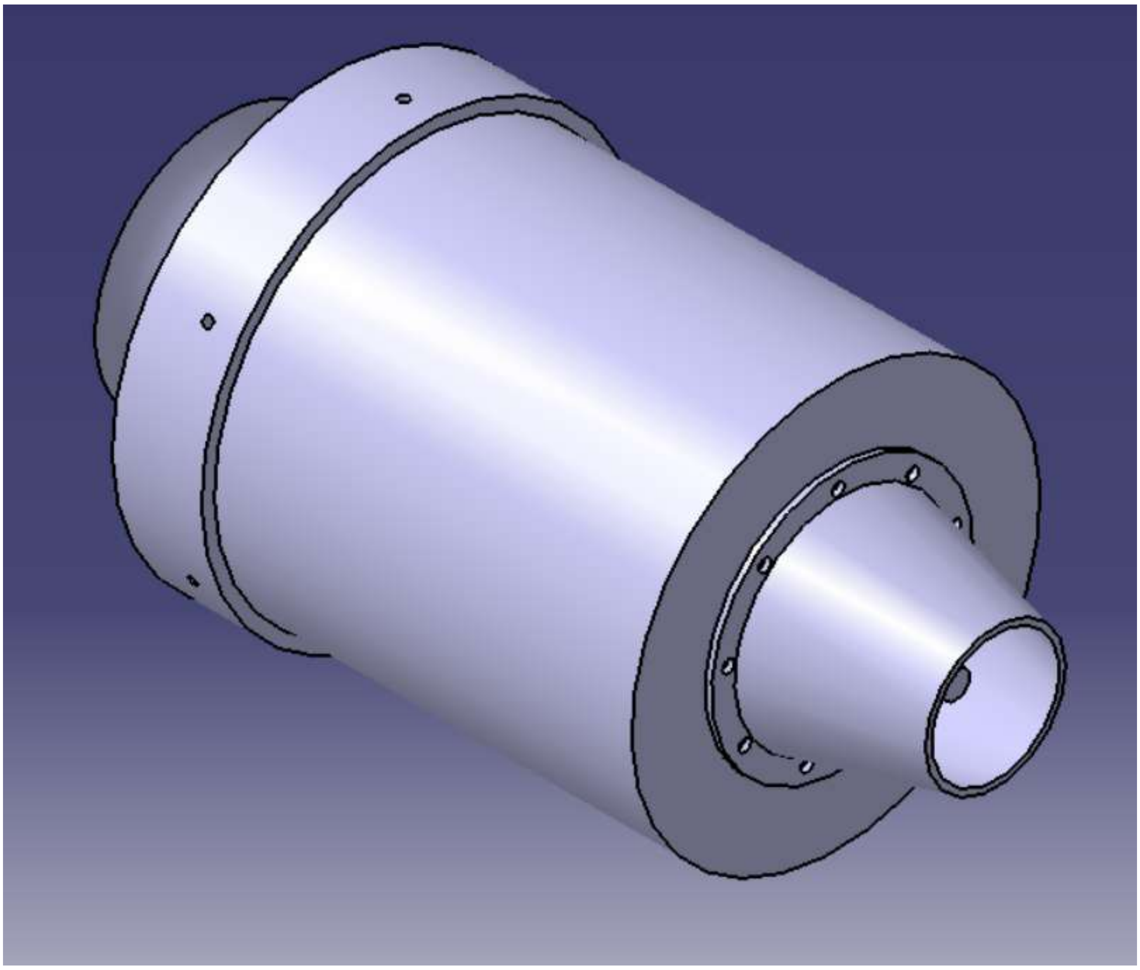

Figure C.6: “Turbojet isometric 3D view 2”

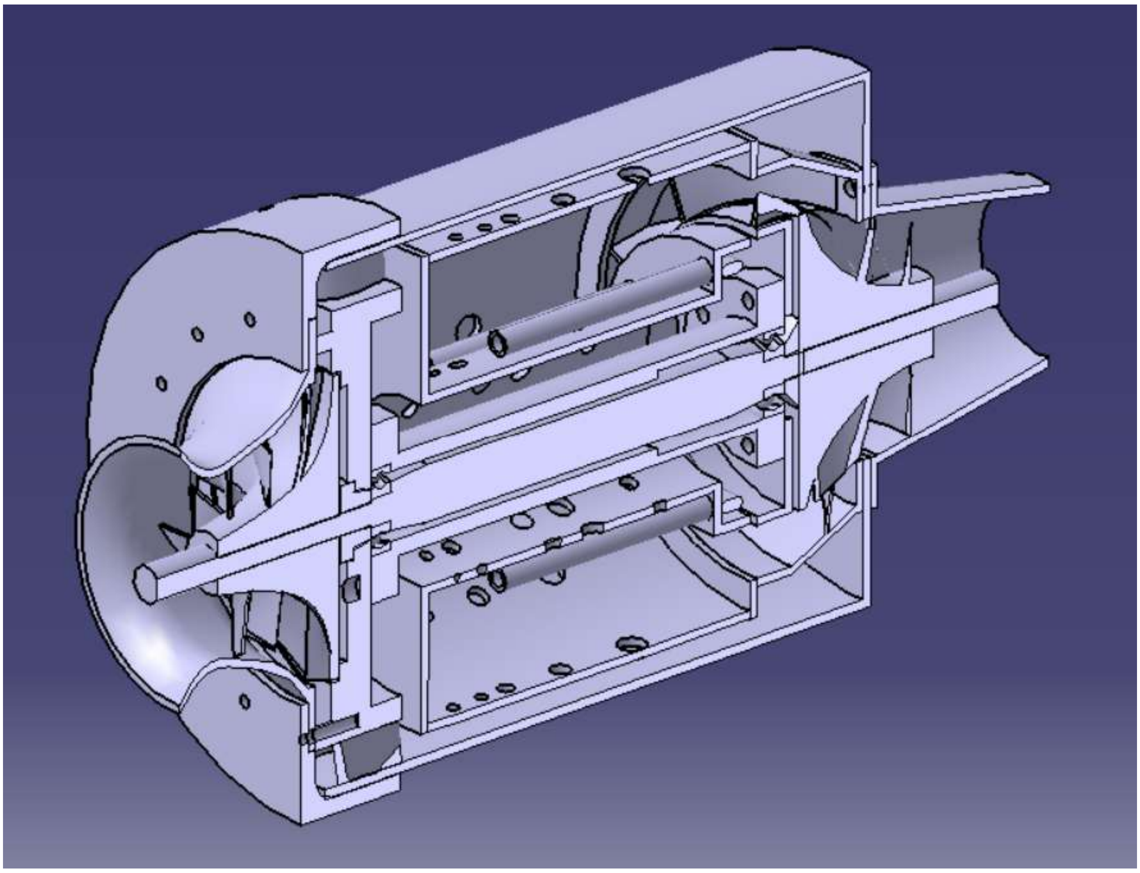

Figure C.7: "Turbojet midsection isometric 3D view"

Appendix D - Turbojet Actual Cycle

Table 2: Turbo VZ21 technical specifications [36]

		Type	RHF3	RHF4	RHF5	RHF55	RHF6	RHE61	RHE62	RHE7	RHE8
Item	Air Flow Rate (at: πc=2.0)	m^3/min	0.75~6.3	1.0~9.4	1.4~10.8	2.4~13.5	3.1~16.5	3.3~17.5	4.5~20.0	5.5~24.0	7.0~30.0
		ft^3/min	26.5~222.5	35.3~332.0	49.4~381.4	84.8~476.8	109.5~582.7	116.5~618.0	158.9~706.3	194.2~847.6	247.2~1059.5
	Maximum Pressure Ratio		2.7	27	2.8	3.0	3.0	3.3	3.3	3.3	3.3
	Maximum Speed	X10^3rpm	250	190	180	168	140	140	131	120	107
	Maximum Allowable Gas Temperature	°C	950	950	950	950	950	750	750	750	750
		°F	1742	←	←	←	←	1382	←	←	←
	Weight (without waste-gate valve)	kg	(1.9)	(2.6)	(3.2)	(5.1)	(6.7)	7.8	10.5	(11.4)	(15.0)
		lb	(4.2)	(5.7)	(7.1)	(11.2)	(14.8)	17.2	23.2	(25.1)	(33.1)
	Diesel Engine Application	Ps	20~100	46~130	54-154	85~200	100~40	50.260	70-300	80-360	105~450
	Gasoline Engine Application	Ps	27~135	62~177	73~208	115~270	135~322				
External Dimensions	A	m/m	135	167	170	207	223	238	253	231	251
	B		22	37	27	43	43	47	45	50	52
	C		133	163	167	201	222	234	245	253	270
	D		88	102	110	124	124	136	146	161	175
	E		58	65	70	75	75	78	76	86	95
	F		65	74	80	102	102	100	125	120	130
	G-1 with Waste-Gate Valve		162	180	211	237	237	256	291		
	G-2 without Waste-Gate Valve		(136)	(155)	(167)	(200)	(196)			(246)	(265)
	H-1 with Waste-Gate Valve		135	125	138	156	156	175	186		
	H-2 without Waste-Gate Valve		(127)	(125)	(138)	(156)	(156)			(195)	(215)

An actual cycle analysis is conducted considering the compressor is rotating at 200,000 RPM. From table 2, a compressor ratio π_c of 2.2 was obtained with an air mass flow rate, $\dot{m}_a$, of 0.1047kg/s.

Assumed parameters:

M_0	0.05		
V_r	17.35944 m/s		
R	0.287 kJ/kgK		
P_r	101.325 kPa		
T_r	300 K	γ_c	1.
4γ_t	1.333	c_{pc}	1.
005 kJ/kgK		c_{pt}	1.
148 kJ/kgK		T_{04}	873.
15 K			
FHV	46300 kJ/kg [29]		
η_i	0.7	η_c	0.7
π_c	2.2	λ	0.8
η_b	0.9	$\%\Delta P_c$	2
η_t	0.8	η_n	0.8

- Inlet

P_{02}	101.4492 kPa
T_{02}	300.15 K
π_i	1.001226

Compressor

P_{03}	223.1882 kPa
T_{03}	408.4893 K
Q_c	11.39 kJ/s

- Burner

P_{04}	218.7244 kPa
f	0.01455321

- Turbine

P_{05}	147.534 kPa
T_{05}	791.3519 K
W_t	-9.824 kJ/s

- Nozzle Critical Pressure Check

P_{06}/P_c	2.196106 kPa
P_{06}/P_a	1.456047 K

$P_{06}/P_c > P_{06}/P_a$ (Unchoked)
V_7 22.17492 m/s
T_{07} 577.1850 K

Jet Engine Performance Parameters

$Specific \quad Thust$ $F/\dot{m}$ 5.138204 Ns/kg
$TFSC$ 10.19647 $kg/Nh\eta_{th}$ T
hermal Efficiency 0.1465787η_p
Propulsive Efficiency 0.88348601η_o
Overall Efficiency 0.1319971